IMPLEMENTATION OF CRISPR BASED TECHNOLOGIES FOR GENOME AND GENE EXPRESSION MANIPULATION OF IRF4 IN MELANOMA CELLS

by

Cansu Yerinde

B.S., Molecular Biology and Genetics, Boğaziçi University, 2013

Submitted to the Institute for Graduate Studies in
Science and Engineering in partial fulfillment of
the requirements for the degree of
Master of Science

Graduate Program in Molecular Biology and Genetics

Boğaziçi University

2016

ACKNOWLEDGEMENTS

I would like to express deepest gratitude to my supervisor, Assoc. Prof. Tolga Emre for his endless support and guidance throughout my thesis studies. Along my master studies, he contributed too much on my improvement as a researcher.

I would like to thank Assoc. Prof. İbrahim Yaman for spending time on the evaluation of this thesis.

I would also like to thank my third jury member Prof. Batu Erman for evaluating this thesis.

I appreciate my lab-mates Nalan Yıldız, Mustafa Can Ayhan, Anna Öğmen and Ulduz Sobhi Afshar for their practical contributions and also for their warm friendship and for motivating me during hard times. I would like to emphasize my special thanks to my former lab-mate Erdem Yılmaz for sharing his knowledge and experience in experiments. I am very thankful to Ahmet Buğra Tufan for his endless patience throughout the times I was very stressful and desperate. Besides his moral support, he also guided me scientifically.

I would like to thank kindly the members of Sumo Lab members, especially to Bahriye Erkaya and Harun Öztürk. They supported me in all aspects. Their help in experiments as well as their moral support cannot be denied.

Finally, I would like to emphasize my strongest gratitude to my family. This thesis is dedicated to them for their support throughout my life.

This study was supported by grants from Boğaziçi Bilimsel Araştırma Projeleri (BAP – 6704, BAP – 9120).

ABSTRACT

IMPLEMENTATION OF CRISPR BASED TECHNOLOGIES FOR GENOME AND GENE EXPRESSION MANIPULATION OF IRF4 IN MELANOMA CELLS

Clustered Regularly Interspaced Short Palindromic Repeats, CRISPR/Cas9, which was originally characterized as an adaptive immune system in bacteria, has become the most powerful genome engineering technology in recent years and it can be used as a genome engineering and knockout technology due to its ease of use and flexibility. CRISPR/Cas9 can also be turned into a powerful gene expression manipulation tool by conversion of Cas9 endonuclease into a catalytically inactive form called dead-Cas9 (dCas9). When dCas9 is fused with transcriptional repressor or activator domains, it is able to supress or activate the target gene expression, respectively with the design of proper target sites and guide RNAs (sgRNA).

In this study, we aimed to set up CRISPR based knockout, inhibition (CRISPRi) and activation (CRISPRa) systems and implement them in melanoma cells to characterize the role of Interferon Regulatory Factor 4 (IRF4) in *in vitro* assays that interrogate cancer-related phenotypes. In this study, we successfully set up lentiviral and inducible CRISPR based knockout, knockdown (CRISPRi) and activation (CRISPRa) methods, which were used to manipulate IRF4 expression in melanoma cell lines. After validation of these systems, we used them in GFP competition assays. According to our preliminary data, IRF4 is important for the competitive fitness and/or survival of melanoma cells, which is in line with a model where melanoma cells have non-oncogene addiction to IRF4 expression, similar to several B-cell origin cancers.

ÖZET

CRISPR TEMELLİ TEKNOLOJİLERİN MELANOMA HÜCRELERİNDE IRF4'ÜN GEN VE GENOME İFADESİNİN MANIPULASYONU AMACIYLA UYGULANMASI

Bakterilerde daha önceleri bir uyarlayıcı bağışıklık mekanizması olarak keşfedilen ve "Düzenli aralıklarla bölünmüş palindromik kümeler" anlamına gelen CRISPR/Cas9 sistemi kullanım kolaylığı ve kolay uyarlanabilme özelliğinden dolayı son yıllarda yaygınlaşan bir genom mühendisliği ve gen nakavt teknolojisi haline gelmiştir. CRISPR/Cas9, Cas9 endonükleazının mutasyona uğratılıp dCas9 olarak adlandırılan katalitik olarak inaktif hale getirilmesiyle çok etkili bir gen ifadesi manipülasyon aracı olarak kullanılabilir. dCas9 proteini transkripsiyon baskılayıcı veya aktive edici protein bölgeleriyle birleştirilince hedef genlerin ifade edilmesini daha güçlü bir şekilde baskılayabilir veya ifade edilmesini aktif hale getirebilir. Genom üzerindeki hedef bölgelerin ve rehber RNA'ların düzgün dizayn edilmesiyle çok yüksek seviyede gen ifadesi baskılama ya da aktive etme seviyelerine ulaşılabilir.

Bu çalışmada CRISPR temelli gen nakavtı, gen ifadesi baskılama ve aktive etme yöntemlerini melanoma hücreleri üzerinde uygulayarak Interferon Düzenleyici Faktör 4'ün (IRF4) bu hücrelerdeki rolünü kanser fenotiplerini araştıran deneylerle karakterize etmeyi amaçladık. Sonuçlarımıza göre, CRISPR temelli, lentiviral ve uyarılabilir gen nakavtı, gen ifadesi baskılama ve aktive etme metotlarını başarıyla dizayn ederek uyguladık ve daha sonra bu sistemleri IRF4'ün ifadesini melanoma hücrelerinde manipule etmek için kullandık. Bu sistemleri valide edilmelerinden sonra GFP hücre yarıştırma deneylerinde kullandık. GFP hücre yarıştırma deneylerinin ön sonuçlarına göre IRF4'ün melanoma hücrelerinin rekabete dayanan sağlık durumları ve hayatta kalmaları için kritik olduğunu gözlemledik. Bu sonuçlar melanoma hücrelerinin de çeşitli B hücresi kanser hücrelerine benzer şekilde IRF4'e karşı onkogen olmayan bağımlılıklarının olduğunu göstermektedir.

TABLE OF CONTENTS

LIST OF FIGURES

LIST OF TABLES

LIST OF SYMBOLS

bp	Base Pairs
g	Gravity
gr	Gram
kb	Kilobase
kDa	Kilodalton
L	Liter
M	Molar
mA	Milliamper
mg	Milligram
min	Minute
ml	Milliliter
mm	Millimeter
mM	Millimolar
ng	Nanogram
s	Second
V	Volt
β	Beta
µg	Microgram
µl	Microliter
^{o}C	Centigrade degree

LIST OF ACRONYMS / ABBREVIATIONS

ABC-DLBCL	Activated B-cell like diffuse large B-cell lymphoma
AKT	V-Akt Murine Thymoma Viral Oncogene / Protein Kinase B
APS	Ammonium persulfate
BCL	B-cell lymphoma
BRAF	V-raf murine sarcoma viral oncogene homolog B
BRCA2	Breast cancer 2
BSA	Bovine serum albumin
$CaCl_2$	Calcium chloride
Cas9	CRISPR associated endonuclease 9
CDK4	Cyclin dependent kinase 4
CDKN2A	Cyclin dependent kinase inhibitor 2A
cDNA	Complementary DNA
CRISPR	Clustered Regularly Interspaced Short Palindromic Repeats
CRISPRa	CRISPR-activation
CRISPRi	CRISPR-interference
CO_2	Carbon dioxide
dCas9	dead Cas9
DCT	Dopachrome tautomerase
ddH_2O	Double-distilled water
DMEM	Dubecco's modified eagle medium
DMSO	Dimethyl sulfoxide
DNA	Deoxyribonucleic acid
DTIC	Dacarbazine
E2F1	E2F transcription factor 1
ECL	Enhanced chemiluminescent solution
EDTA	Ethylenediaminetetraacetate
ERK1/2	Mitogen-activated protein kinase 3/1
EST	Expressed sequence tag
EtOH	Ethanol

FBS	Fetal bovine serum
FC	Fold change
FPKM	Fragments per kilobase of transcript per million mapped reads
gDNA	Genomic DNA
GFP	Green fluorescent protein
GDP	Guanosine 5’ -diphosphate
GWAS	Genome-wide association studies
HEK	Human embryonic kidney
HEPES	4-(2-hydroxyethyl)-1-piperazineethanesulfonic acid
HRP	Horseradish peroxidase
IRF4	Interferon regulatory factor 4
Indel	Insertion-deletion mutations
KRAB	Krüppel like associated box
LB	Luria-Bertani broth
MAPK	Mitogen activated protein kinase
MDM2	Mouse double minute 2 homologue
MEK1/2	Dual specificity mitogen-activated protein kinase kinase 1/2
$MgCl_2$	Magnesium chloride
MITF	Microthalmia-associated transcription factor
MM	Multiple myeloma
mRNA	Messenger RNA
mTOR	Mammalian target of rapamycin
MYC	V-Myc Avian Myelocytomatosis Viral Oncogene Homolog
N-terminal	Amino terminal
NF-κB	Nuclear factor kappa B
NGS	Next-generation sequencing
NRAS	Neuroblastoma v-ras oncogene homolog
PAGE	Polyacrylamide gel electrophoresis
PAM	Proto-adjacent motif
PBS	Phosphate buffered saline
PCR	Polymerase chain reaction
PDK1	3-phosphoinositide dependent protein kinase-1
PE	Phycoerythrin

PFA	Paraformaldehyde
PH	Pleckstrin homology
PI3K	Phosphoinositide-3-OH kinase
PS	Polystrol
PTEN	Phosphate and tensin homologue
PVDF	Polyvinylidene fluoride
RB	Retinoblastoma
RGP	Radial growth phase
RNA	Ribonucleic acid
RNA-seq	RNA sequencing
rpm	Revolution per minute
rRNA	Ribosomal RNA
RT	Room temperature
RT-qPCR	Reverse transcriptase - quantitative PCR
SDS	Sodium dodecyl sulfate
sgRNA	Small guide RNA
shRNA	Short hairpin RNA
shLuc	Short hairpin RNA against Luciferase
SNP	Single nucleotide polymorphism
SQ	Subcutaneous
SQLE	Squalene Monooxygenase
TALEN	Trancription Activator Like Effector Nucleases
TBS	Tris-buffered saline
TBS-T	Tris buffered saline with tween
TEMED	Tetramethylethylenediamine
TFAP2A	Activating enhancer binding protein 2 alpha
Th	T helper cell
TLR	Toll-like receptor
TP53	Tumor protein p53
tracRNA	Trans-active crRNA
Tris	Tris (hydroxylmethyl) aminomethane
Tween	Polysorbate
TRYP1	Tyrosinase-related protein 1

TYR	Tyrosinase
Unt	Untransduced
UV	Ultraviolet
UVR	UV radiation
VEGF	Vascular endothelial growth factor
VGP	Vertical growth phase
V600E	Valine to glutamic acid substitituon
VP64	Viral protein of 64 amino acids
ZFN	Zinc Finger Nucleases

1. INTRODUCTION

CRISPR/Cas9 system, which was originally characterized as a bacterial adaptive immune system, is one of the most popular genome editing tools nowadays. Its rapid development, simplicity and adaptivity have made it a valuable molecular biology tool. Several studies have shown that it can be used as a gene knockout, gene regulation tool along with applications where it can be used for imaging genomic loci, to perform genome-wide screens, and to purify genomic loci. Due to these advantages, CRISPR/Cas9 has mostly replaced former genome engineering technologies such as zinc finger nucleases (ZFNs) and transcriptional activator like effector nucleases (TALENs) technologies (Kim *et al.*, 2014).

1.1. CRISPR: A Nucleic Acid Based Adaptive Immune System in Bacteria

In 1980s, it was reported that one liter of marine water contains millions of bacteriophages, which are considered as the most abundant and diverse living mechanisms on the Earth (Sorek *et al.*, 2013). Therefore, it is not surprising that bacteria have evolved different mechanisms to defend themselves against bacteriophages and for many years, it was known that microbial immune systems were restricted to innate immunity systems such as restriction modification and receptor switching (Wiedenheft *et al.*, 2012). However, it was recently discovered that bacteria and some archea have evolved a nucleic acid based adaptive immune system to defend themselves. In this adaptive immunity system, bacteria integrate short fragments of nucleic acids of bacteriophages in their chromosomes at one end of a repetitive element known as Clustered Regularly Interspaced Short Palindromic Repeat (CRISPR) in order to target and degrade nucleic acids of phages leading to suppression of their propogation (Sander *et al.*, 2014). This mechanism provides a long-term adaptive immunity against bacteriophages similar to a molecular vaccination.

1.1.1. Structure and Organization of CRISPR Locus

CRISPRs can be defined as a diverse family of DNA repeats due to the presence of different types of the locus in different bacterial species. Although they are diverse, all CRISPR loci share a common structure. They have short repeat sequences, whose length is generally 20-50 base pairs and these repeat sequences are separated by unique spacer sequences, whose length is similar. Although repeat sequences are conserved in a CRISPR locus, they can be varied in different CRISPR loci in terms of both length and sequence composition. Based on the similarity of their repeat sequences, CRISPR loci can be clustered. Although there exists high diversity of repeat sequences, they all share a conserved GAAA(C/G) motif at 3'end, which can be seen in Figure 1.1, and it can be used as a binding site for Cas proteins. Additionally, the total length and number of CRISPR loci can be diverse and a single prokoryatic chromosome may harbor more than one CRISPR loci. The size and number of CRISPR loci is independent from the genome size. The defining characteristic of a CRISPR locus is the repeat-spacer-repeat pattern (Wiedenheft *et al.*, 2012).

Another important structural feature of a CRISPR locus is the leader sequence. It is an adenine and thymine (AT) rich sequence and it flanks the CRISPR loci. According to some comparative analysis data, spacer sequences, which are closest to the leader sequence, are the most diverse ones. It was found that the polarity of the CRISPR loci is determined by the presence of the leader sequence. Another function of the leader sequence is that it consists of promoters and binding sites for regulatory proteins and is important for crRNA biogenesis and new spacer integration (Stern *et al.*, 2010).

Apart from the leader sequence, another cassette of genes, *cas* genes, later found to be involved in crRNA biogenesis, target identification and destruction, were identified at CRISPR loci. So far, around 45 *cas* gene families were characterized. Six of these families, *cas1-cas6*, are mostly conserved between different CRISPR loci. However, *cas1* gene is universally conserved and it is considered as the hallmark of this nucleic acid based adaptive immune system of microorganisms (Wilkinson *et al.*, 2014).

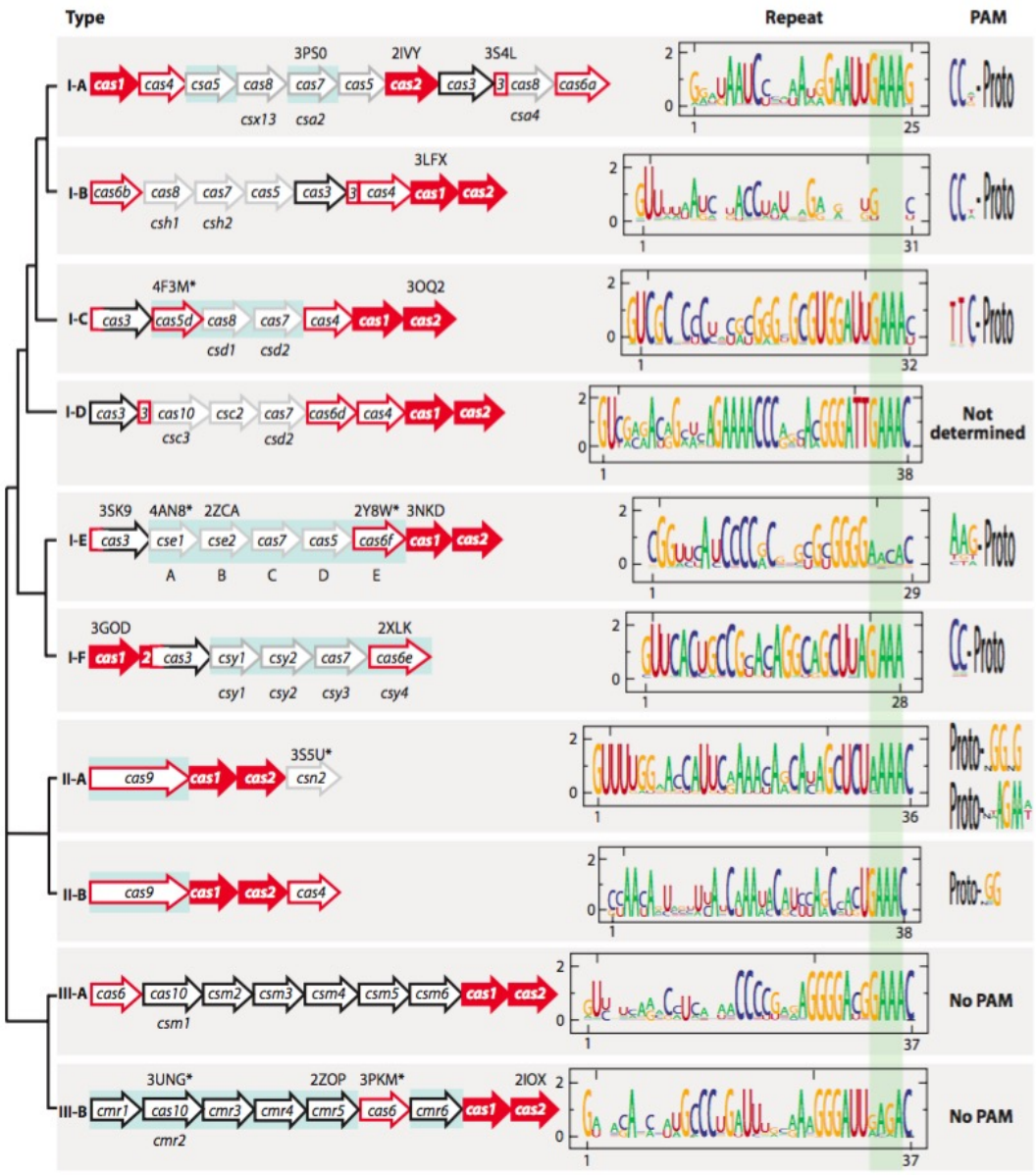

Figure 1.1. Structure and organization of different CRISPR loci and their clustering (Adapted from Sorek *et al.,* 2013)

1.1.2. Stages of CRISPR Mediated Adaptive Immunity

The mechanism of CRISPR-mediated adaptive immunity can be divided into three basic steps as acquisition of foreign DNA into CRISPR locus, generation of short CRISPR derived RNAs (crRNAs) and target interference.

The first step of CRISPR-mediated adaptive immunity is the acquisition of viral DNA into CRISPR locus. A small part of invading viral DNA (protospacer) is integrated into the CRISPR locus at the upstream leader due to its recognition via proto adjacent motif (PAM). After the integration of foreign DNA, conserved CRISPR repeat sequences are duplicated in order to conserve repeat-spacer-repeat architecture of the locus. It was demonstrated via genetic studies that, Cas1 and Cas2 proteins take role in the integration of viral DNA into the CRISPR locus (Wiedenheft *et al.*, 2012). Another critical point for the acquisition of foreign DNA is that integration mechanism must be capable of distinguishing foreign and host DNA from each other. This is mediated by short three-nucleotide sequence motif proximal to the protospacer, which is called protospacer adjacent motif (PAM), serves as the recognition site for foreign DNA parts which will be integrated into CRISPR (Wang *et al.*,2014).

The second step of CRISPR-mediated adaptive immunity is crRNA biogenesis. This step is very critical for all type of CRISPR systems. It consists of two different steps. As the first step, CRISPR locus is transcribed as long precursor CRISPR RNA from the leader sequence, which serves as a promoter. Then, depending on the CRISPR subtype, specific enzymes process this long precursor RNA into small crRNA pieces (Sorek *et al.*, 2013).

The last step of CRISPR-mediated adaptive immunity is the target interference part. In this stage, large CRISPR associated ribonucleoprotein complexes are formed by association of small crRNAs and Cas proteins and these complexes are able to recognize invading foreign nucleic acids. Since foreign nucleic acid protospacers are complementary to small crRNAs, they can be identified via base-pairing interactions. Both complementary

and non-complementary strands of the invading viral DNA can be target of immunity (Wiedenheft *et al.*, 2012). Two strands of viral DNA are targeted and cleaved by ribonucleoprotein complexes so that it can be eliminated efficiently. Here, PAM sequence provides the information for discriminating self and non-self DNA so that it protects the host chromosome from degradation (Kim, 2014). Cas proteins have a direct role in target recognition. CRISPR- associated complexes take role in target recognition by enhancing hybridization between crRNA and complementary target DNA. The presence of a short high- affinity-binding site, which is located at one end of crRNA, determines the binding affinity. This high-affinity-binding site is similar to seed sequence of eukaryotic microRNAs (miRNAs) (Hsu *et al.*, 2014). The mechanism of CRISPR based adaptive immunity is summarized in Figure 1.2.

Depending on the gene conservation and locus organization, CRISPRs can be categorized into three major classes as Type I, Type II and Type III. Type II is the most well characterized CRISPR system and it is widely used for genome engineering applications.

Type II CRISPR system, which is only found in bacteria; harbor four different *cas* genes as *cas9, cas1, cas2* and *cas4*. *Cas9* can be considered the hallmark of Type II CRISPR system. Cas9 protein is a large multi-domain protein and has both RuvC- like nuclease domain and HNH-like nuclease domain. Cas9 takes role in both crRNA biogenesis and the destruction of the target invading viral DNA. While HNH nuclease domain cleaves the DNA strand that is complementary to crRNA, RuvC domain cleaves the anti-sense strand of the target DNA. Another unique feature of Type-II CRISPR systems is the presence of a trans-activating crRNA (tracrRNA), which is encoded at the upstream and on the anti-sense strand of CRISPR locus. When crRNA and tracrRNA hybridize, it leads to the formation of double stranded RNA that is later recognized and cleaved by a non-cas enzyme RNAseIII. It was shown that cleavage of target phage DNA by Cas9 requires both the mature crRNA and tracrRNA (Sorek *et al.*, 2013)

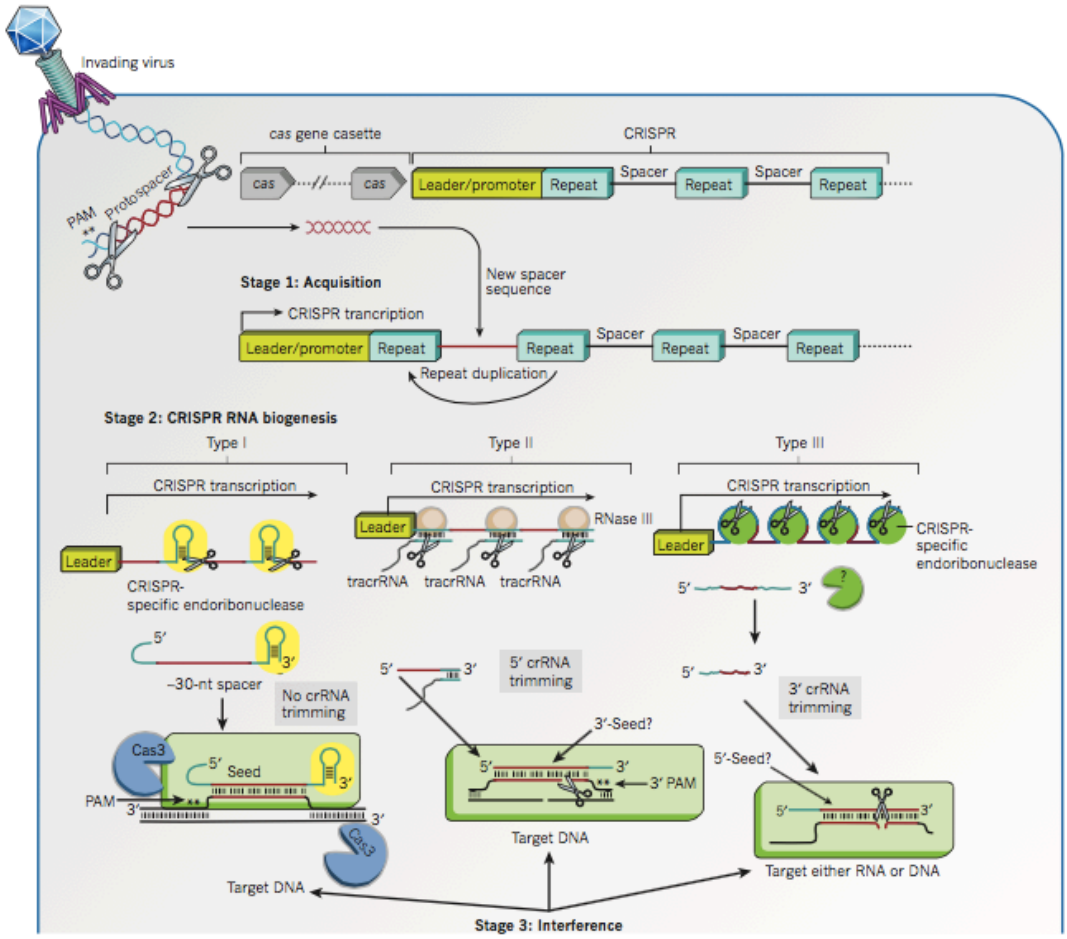

Figure 1.2. Schematic view of stages of CRISPR mediated adaptive immune in Type I, Type II and Type III systems (Adapted from Wiedenheft *et al.*, 2012)

1.2. CRISPR as a Genome Engineering Method

After the discovery of CRISPR mediated adaptive immunity in bacteria, in 2011 tracrRNA and RNase III were shown to be necessary for the processing of long precursor CRISPR RNA (Charpentier *et al.,* 2011). After this crucial finding, in 2013 Jinek *et al*., purified Cas9 protein and showed that Cas9 mediated cleavage of double stranded DNA is dependent on both crRNA and tracrRNA. In order to simplify these two systems, he generated a chimeric RNA and fused 3' end of the crRNA with 5' end of tracrRNA and this chimeric RNA is capable of directing Cas9 protein to any DNA sequence depending on the design, which can be seen in Figure 1.3. (Ran *et al.*, 2013) These were the very first

studies, which demonstrated that CRISPR system might be used as RNA guided genome-editing method. After these studies, two articles by Cong et al., and Mali et al., showed that this RNA guided Cas9 system can be used to edit mouse and human genes (Mali *et al.*, 2013). They used a system in which human codon optimized and nuclear localization signals coupled Cas9 protein is co-expressed with plasmids encoding for tracrRNA and crRNA-guide or a single chimeric guide RNA (sgRNA) which combines the functions of the first two. According to these critical studies, the efficiency of this novel RNA guided genome editing tool was comparable to former technologies like Zinc Finger Nucleases and TALENs and it was even cheaper and easier in terms of design and application. These findings have led to the rapid development and popularity of CRISPR mediated genome-engineering technologies (Sander *et al.*, 2014)

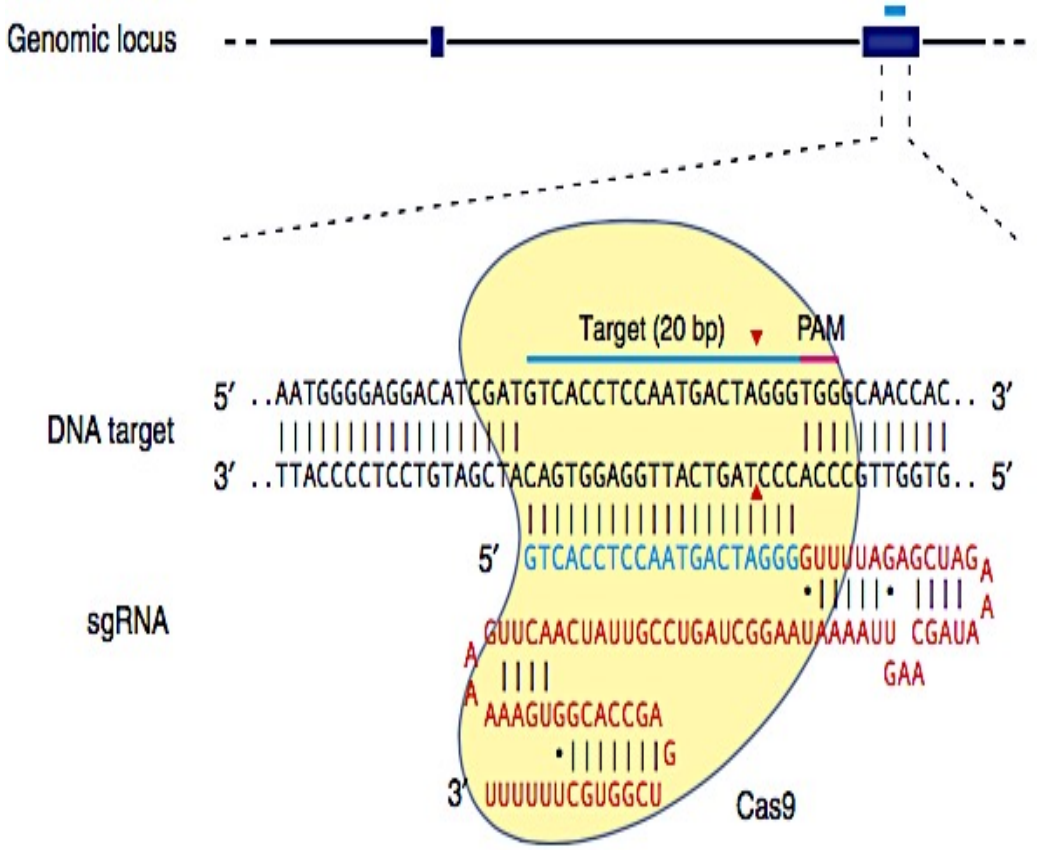

Figure 1.3. Schematic of the RNA-guided Cas9 nuclease and sgRNA (Adapted from Ran *et al.*, 2013)

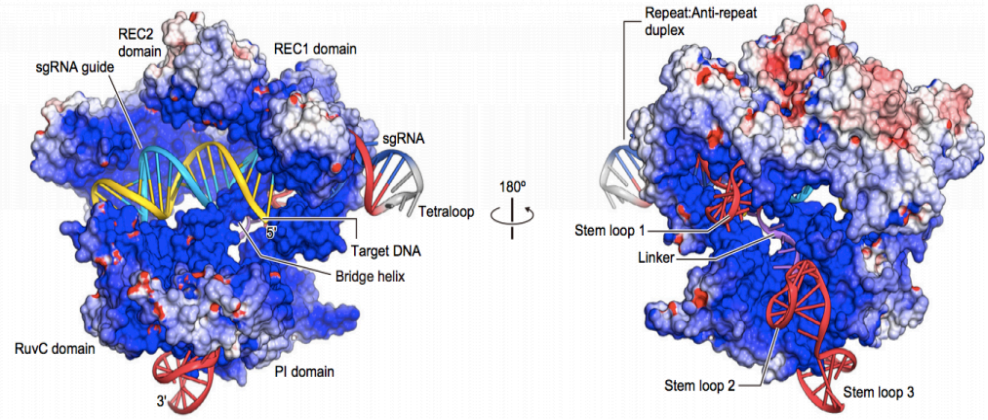

Figure 1.4. Crystal structure of Cas9 protein in complex with sgRNA and target DNA (Adapted from Nureki *et al.,* 2014).

Cas9 endonuclease promotes genome editing via introducing a double stranded break at the target site, which is determined by the design of guide RNA. After cleavage by Cas9 protein, cell intrinsic DNA repair pathways come into play and generated double stranded break undergoes either one of the two major repair mechanisms. If there is no repair template, breaks are repaired by non-homologous end joining pathway (NHEJ), which is error-prone and leaves scars in the form of small insertions or deletions (indel mutations). This mechanism can be used to generate knockouts since indel mutations often results in frameshift mutations and premature stop codons in coding exons. The other cell intrinsic DNA repair pathway is homology dependent repair pathway (HDR). Here, a donor template should be provided in order to make precise gene editing. Via this method, small edits can be introduced in the genome such as single nucleotide mutations as shown in Figure 1.5 (Ran *et al.*, 2013).

Type II CRISPR system, which is the best-characterized one, has a crRNA unit that contains a 20-nucleotide guide sequence and this part should be complementary to the target site. Each target site should be followed by proto adjacent motif (PAM) at 5' end, which is a three-nucleotide motif. PAM sequence is NGG for Type II CRISPR system (Haurwitz *et al.*, 2010). By using chimeric guide RNA, which is the combination of crRNA and tracrRNA, and expressing human codon optimized Cas9 protein; any target of

interest that has PAM can be targeted by the design of 20-nucleotide guide sequence (Sander *et al.*, 2014).

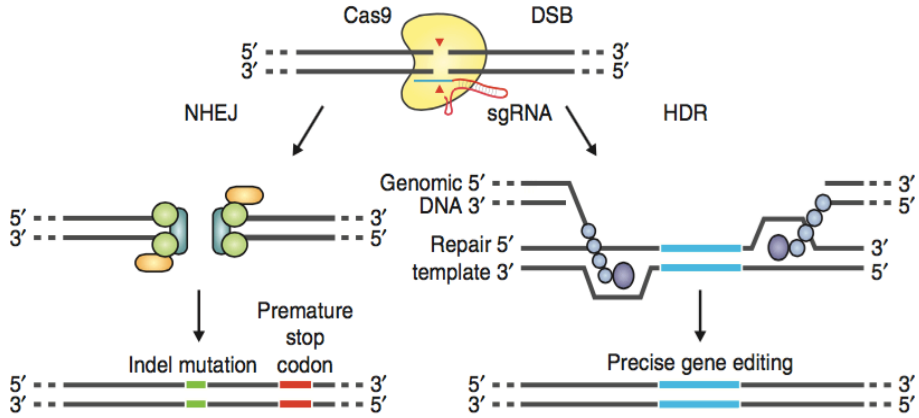

Figure 1.5. DNA repair mechanisms, which becomes active after the formation of double stranded breaks by Cas9 protein (Adapted from Ran *et al.*, 2013)

RNA-guided Cas9 has multiple advantages over the other genome engineering technologies. Firstly, it can be directed to new DNA sequences by the re-design of 20-nucleotide complementary part of sgRNA due to its ease for customization. Cas9 protein can be turned into a nickase, which generates single stranded breaks if one of its catalytic domains is mutated (Tsai *et al.*, 2014). Hence, it can be said that its cleavage pattern can be manipulated. In addition, Cas9 can be directed to multiple regions in the genome by designing and introducing combinations of guide RNAs (Gilbert *et al.*, 2012).

1.3. CRISPR as a Transcriptional Regulation Tool

One of the most powerful strategies for interrogating, perturbing and engineering of cells is the targeted gene regulation. Technologies based on engineered DNA binding proteins such as Zinc Finger Nucleases (ZFNs) and transcription-activator-like (TALE) proteins have been used as powerful methods for genome editing, and in recent years, CRISPR systems mostly replaced these technologies due to its ease of design and

effectiveness (Gaj *et al.*, 2013). However, it was shown that CRISPR/Cas system can be repurposed to use as a powerful genome regulation tool instead of genome editing purposes and it can be either used as a gene repression and activation method. Similar to the situation of former genome engineering technologies, CRISPR has been shown to have potential to replace widely used RNAi and overexpression tools to manipulate gene expression.

1.3.1. CRISPR Interference for Gene Expression Repression

In 2013, Qi *et al.* (2013) performed the first study in which CRISPR/Cas9 system was used as a gene regulation tool. In this novel method, catalytically inactive form of Cas9 endonuclease, which is called dead Cas9 (dCas9), was generated by inserting mutations in HNH and RuvC catalytic domains of the protein. By the insertion of these mutations, dCas9 protein was still capable of binding its target site by the provided sgRNA, however it lost its function of generating double stranded breaks since it is catalytically inactive. When dCas9 protein was co-expressed with sgRNA targeting coding region, it yielded a dramatic and specific silencing of target gene without any observable off-target effects, which was assessed by RNA-seq method. In addition, the same group showed by native elongating transcript sequencing that dCas9-sgRNA complex repressed the target gene expression by blocking transcription elongation. Additionally, depending on the design of sgRNAs and target sites, they showed that dCas9/sgRNA complex could also block transcription initiation in both bacterial and mammalian cells. This method of gene repression by dCas9/sgRNA complex was called as CRISPR-interference (CRISPRi) (Larson *et al.*, 2013)

The same group observed that gene silencing efficiencies achieved by CRISPRi system in mammalian cells was not high as bacterial cells (Larson *et al.*, 2013). Mammalian genomes and transcriptional regulation in mammalian cells are more complex and different activating and repressing transcription factors co-act on DNA regulatory elements. In addition, chromatin regulation and DNA methylation have further role in gene regulation. Therefore, more specific and effective tools were needed to study gene and genome regulation. Again in 2013, Qi *et al.*, in another study demonstrated that CRISPRi

method could be further modified to meet this need of novel tools. In this novel tool, they fused catalytically inactive dCas9 protein to different transcriptional repressor domains, which recruits repressive chromatin modifying complexes, which can be seen in Figure 1.1.4. They showed that fusion of dCas9 protein to Krüppel associated box (KRAB) led to improved and significant repression levels of the target genes in mammalian cells. They also demonstrated that target genes could be repressed when dCas9-KRAB fusion protein was directed to promoter regions, which are close to transcription start sites of the target genes *(*Qi *et al.*, 2013)

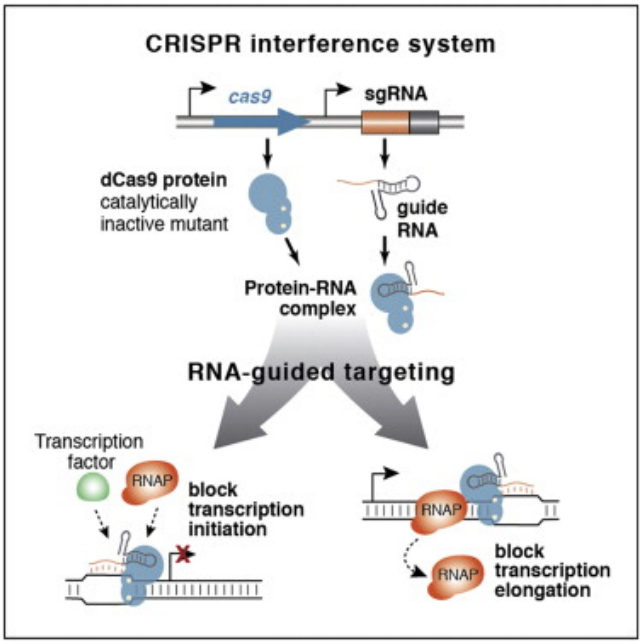

Figure 1.6. Mechanism of CRISPRi system where dCas9 protein blocks either transcription initiation or transcription elongation (Adapted from Qi *et al.*, 2013).

CRISPRi method has multiple advantages over RNAi technology, which has been the most widely used method for gene silencing so far. While CRISPRi method has comparable repression levels with RNAi method, it has less off-target effects, i.e. it minimally impact on the transcription of other non-targeted genes. Similar to RNAi libraries for gene knockdown, multiple sgRNA libraries were generated by many groups (Wang *et al.*, 2014). In addition, design of sgRNAs is more flexible and it does not have restricted use in

different organisms like RNAi. Additionally, in CRISPRi method multiple genes can be targeted by introducing different sgRNAs simultaneously *(*Bikard *et al.*, 2013)

1.3.2. CRISPR Based Gene Expression Activation

In addition to a gene expression silencing method, Qi *et al*. (2013) also showed that CRISPR/Cas9 system can also be used as an gene activation method, which they called CRISPR-activation (CRISPRa). Similar to CRISPRi approach, catalytically inactive dCas9 protein was used in CRISPRa method. Different transcriptional activator domains were fused to dCas9 protein and they were co-expressed with sgRNAs, which target promoter regions of target genes. It was found that fusion of dCas9 protein with four tandem repeats of well characterized transcriptional activator domain VP16 (VP64) led to the significant activation of target gene by recruitment of RNA polymerase II to the target site (Cheng *et al.*, 2013). However, this study was restricted to the activation of reporter genes and data for endogenous mammalian genes were not included. The mechanism of CRISPRa system is summarized in Figure 1.7.

Later, Jaenesch *et al*. (2013) showed that CRISPRa method was also effective for the activation of endogenous mammalian genes. However, co-expression of dCas9-VP64 with single sgRNA did not lead to activation more than 2-fold. They tried combinations of different sgRNAs spanning the promoter of their gene of interest and they observed that using more than one sgRNA was more effective and resulted in 10-12-fold activation. The same group also demonstrated that multiple genes could be activated simultaneously by the co-expression of different sgRNAs for different genes *(*Bikard *et al.*, 2013)

In summary, both CRISPRi and CRISPRa systems have great potential since they offer to control the expression of any gene or combinations of genes simultaneously. Hence, they can become powerful tools to study genetic networks and to manipulate the genes and genomes of different organisms.

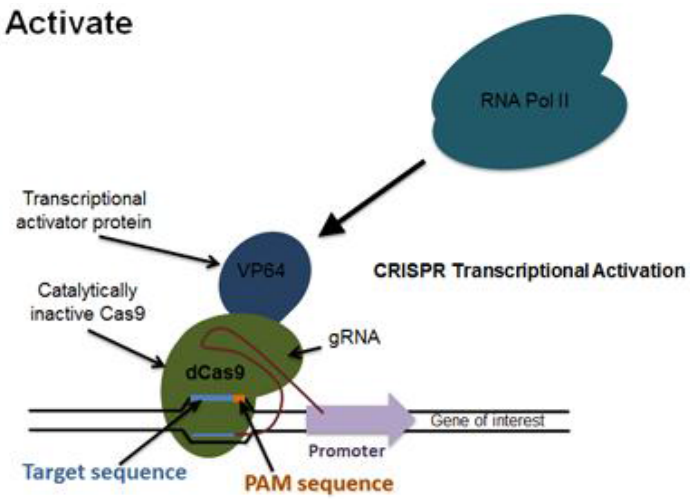

Figure 1.7. dCas9-VP64 mediated CRISPRa based gene activation mechanism Adapted from Addgene CRISPR Resource, 2014)

1.4. Cancer Overview

Cancer can be defined as a neoplastic disease, which results from limitless and uncontrolled growth and proliferation of cancerous cells. By acquiring different genetic and epigenetic changes, normal cells are transformed into cancer cells which are capable of escaping from cellular limits and checkpoints which normally restricts growth and proliferation mechanisms via cell death and senescence (Vogelstein *et al.*, 2013). By time, cancer cells can acquire additional capabilities to migrate, invade and localize to distant regions of the body, via a mechanism called metastasis. Metastasis generally results in functional loss in related organs and eventually leads to death of the patients (Cheon and Orsulic, 2011). In 2011, Hanahan and Weinberg suggested that all cancers share common features that alter cell physiology leading to malignant growth (Hanahan *et al.*, 2011). They summarize these features under six different categories as shown in Figure 1.8.

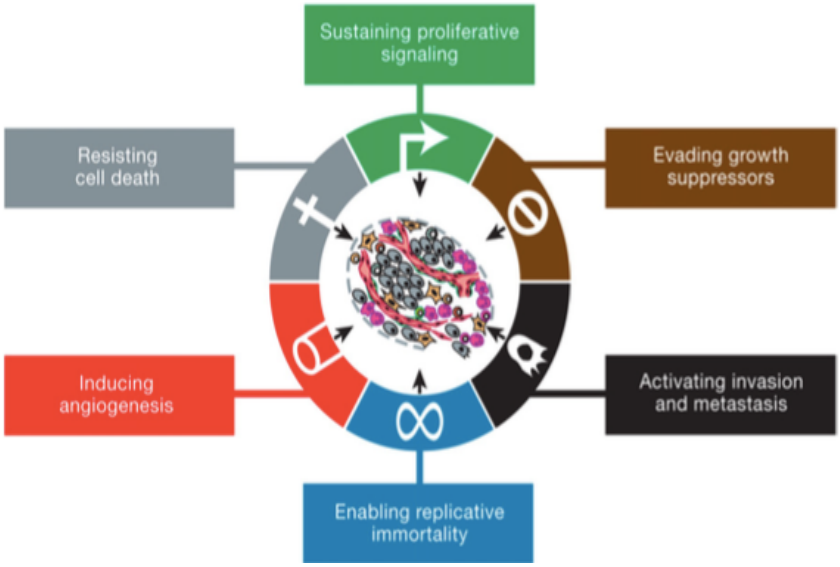

Figure 1.8. Schematic view of the hallmarks of cancer (Hanahan *et al.*, 2011)

1.5. Melanoma Overview

Melanoma, which is considered as the most deadly form of skin cancers, results from the transformation of pigment-producing cells, melanocytes. Due to its high metastatic potential, it is the most aggressive form of skin cancers compared to basal cell carcinoma and squamous cell carcinoma that are found more frequently. According to American Cancer Society estimates, about 76,380 individuals will be diagnosed with melanoma and 10,130 of them are expected to die due to the disease in 2016. If melanoma can be diagnosed at Stage I, the typical 10-year survival rate is around 90%, however for Stage IV it is less than 15 % (Siegel *et al.*, 2016).

Although skin is the primary part of the body where melanocytes reside and melanoma is formed, melanocytes are not confined there. Melanocytes exist in uveal tract of the eye and in other tissues such as meninges and anogenital tract in considerable numbers (Lin *et al.*, 2007). Melanocytes that are present in these sites may also be transformed and give rise to uveal melanoma, vulval melanoma and vaginal melanoma. However, cutaneous melanoma, which originates from skin melanocytes, is the most

common form of the disease (Beaumont *et al.*, 2014). Melanocytes are a minority group of cells within basilar epidermis and they divide infrequently, generally twice a year. The main function of melanocytes is to provide melanin pigment to keratinocytes. When keratinocytes are exposed to UV radiation, they secrete α-melanocyte stimulating hormone (α-MSH) and this factor binds to its receptor expressed on melanocytes leading to melanin synthesis, which is later delivered to keratinocytes. Melanin pigments protect the skin against the harmful effects of UV radiation resulting DNA damage. Since melanocytes along with keratinocytes act as barriers to UV radiation, they are affected from its harmful effects and therefore, UV radiation is considered as the major risk for melanoma. Additionally, genetic background and pigmentation status of individuals are other factors contributing to the development of melanoma (Shain *et al.*, 2016).

The first step in malignant transformation of melanocytes is generally deregulation of cellular hemostasis. At this step, melanocytes start to proliferate and spread leading to the formation of nevi, which are benign neoplasms. After this step, melanocytes acquire the capability of grow horizontally and pass to radial growth phase and starting from this step they are considered as malignant. In the next step, they can grow vertically and invade basement membrane located between epidermis and dermis so that cells acquire the capacity to metastasize as shown in Figure 1.9. (Kit *et al.*, 2013)

1.5.1. Common Genetic Alterations in Melanoma

In melanoma, signaling pathways, which have important roles for the proliferation and survival of cells, are mainly deregulated. BRAF and NRAS, which are the most common genetic targets in melanoma, are mutated around 60% of melanoma and these mutations leads to the hyper activation of MAPK pathway, which is a key pathway for cell proliferation and survival (Tsao *et al.*, 2012). Amplification of AKT3 and loss of PTEN by epigenetic silencing or deletion are among the other common alterations in melanoma, which result in constitutive PI3K signaling (Mitra *et al.*, 2009). The other reasons for deregulation of MAPK and PI3K pathways include overexpression or hyper-activation of growth factor receptors like c–KIT, MET and epidermal growth factor receptor (EGFR). In addition, NF1, which is the negative regulator of Ras may be deleted (Lo *et al.*, 2014).

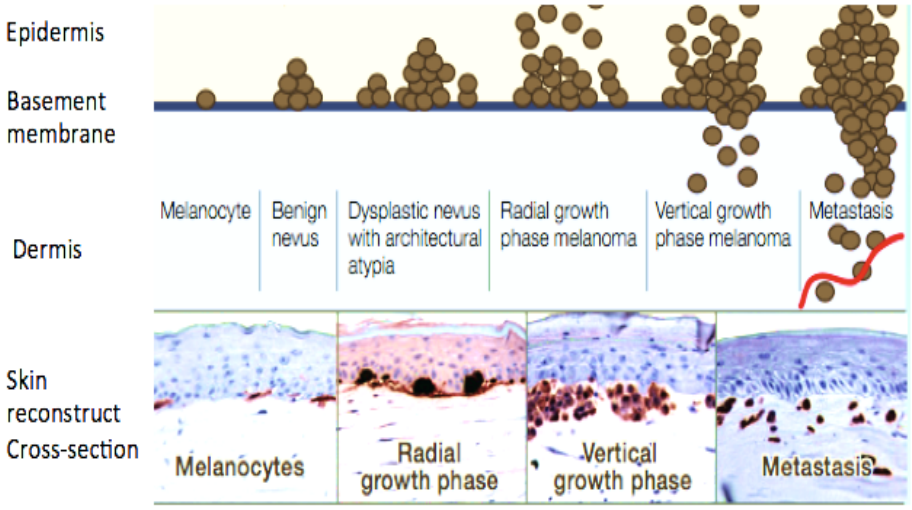

Figure 1.9. Steps of melanocyte transformation. Melanocytes that form the benign nevi proceed to radial growth phase followed by vertical growth phase where transformed cells become capable of metastasizing (Adapted from Kit *et al.*, 2013)

Apart from these key-signaling pathways, cell cycle and proliferation regulators are affected in melanoma. For instance, $p14^{ARF}$and $p16^{INK4A}$, which are encoded from CDKN2A locus and tumor suppressors, regulate p53 and RB (retinoblastoma) pathways. In melanoma, p53 cell cycle checkpoint and apoptotic pathway is lost due to deletions in $p14^{ARF}$or TP53, or amplifications of MDM2 rarely and MDM4 more commonly. CDK4 point mutations or amplifications, RB1 mutations, CCDN1 amplifications, $p16^{INK4A}$ lesions may lead to loss of RB pathway in melanoma *(*Shain *et al.*, 2016)

In melanoma progression, some transcription factors and epigenetic regulators also have important roles. For instance, MITF, which is the master regulator of melanocyte function and development, can act as a lineage-specific oncogene via upregulation of target genes, which are important for cell cycle progression and survival. Additionally, MITF amplification is observed in many sporadic melanomas and a gain of function mutation in MITF is associated with familial melanoma. (Yokoyama *et al.*, 2011). In one third of melanomas, nuclear β-catenin, which is the mediator of canonical Wnt pathway, is activated although its nuclear activation mechanism is not understood completely. In

addition, loss of function mutations of ARID1a and ARID2a, which belong to the SWI/SNF chromatin remodeling complex, were observed in cutaneous melanomas (Lo *et al.*, 2014). The pathways and transcription factors, which are mostly deregulated in melanoma, are summarized in Figure 1.10.

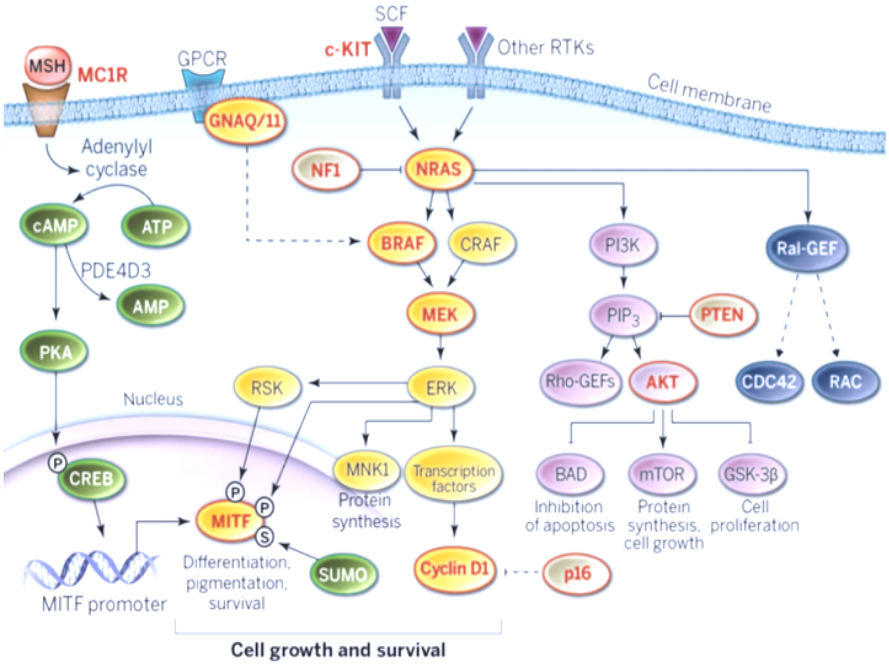

Figure 1.10. Commonly deregulated pathways in melanoma (Adapted from Lo *et al.*, 2014)

1.6. Interferon Regulatory Factor 4 (IRF4) Overview

Interferon Regulatory Factor 4 (IRF4) is a transcription factor, which belongs to the interferon family of transcription factors. In most immune cells, IRF4 is expressed. For instance, IRF4 is expressed in B-cell lineage in all developmental steps of this cell type except germinal center (GC) reaction. IRF4 has critical roles for the development and function of B cells and T cells. In previous studies, it was observed that GC B cells lack IRF4 expression, however during differentiation of these cells into plasma cells, IRF4 expression increases (De Silva *et al.*, 2012). It was also demonstrated that mice in which IRF4 is deleted does not have plasma cells and germinal centers, where B cells normally

proliferate and develop. Another observation for IRF4 role in immune cells was that its deficiency was linked to reduced immunoglobulin levels and defective B and T cell proliferative responses upon mitogenic stimuli (De Silva *et al.*, 2012). IRF4 was also shown to be important for immunoglobulin class switch mechanisms in B cells. The role of IRF4 is not restricted to B and T cells. IRF4 is also critical for dendritic cells and macrophages, which belong to the myeloid lineage. For instance, IRF4 is expressed higher during monocyte differentiation into macrophages and dendritic cells. It is also critical for the expression of major histocompatibility complex class II and antigen presentation to T cells and IRF4 also takes role in TLR signaling in macrophages (Klein *et al.*, 2008).

Although IRF4 belongs to IRF family, it is not induced by interferons, but it is induced by mitogenic stimuli. These mitogenic stimuli includes antigen-receptor engagement, lipopolysaccharide binding and CD40 signaling, all of which feed into NF-kB pathway at the downstream level. Depending on the tissue type in which it is expressed and the presence of different cofactors, IRF4 can acts as either as an activator or repressor as shown in Figure 1.11. IRF4 protein, which is a single polypeptide chain, can be divided into three major parts as N-terminal DNA binding domain, a functional regulatory domain comprising two transactivation domains and auto inhibitory domains and an intermediate linker domain needed for conformational change. If cofactors of IRF4 are not present, DNA binding domain of IRF4 is masked by its association domain and IRF4 is no longer binds to DNA and cannot form ternary complex that is needed for its functions (De Silva *et al.*, 2012).

1.7. IRF4 In Immune Cell Cancers

Since IRF4 is very critical for immune cell development and function, it is not surprising that its deregulation is linked to malignant transformation lymphomas. Firstly, IRF4 was shown to be translocated (t(6;14)(p25;q32)) in multiple myeloma cells, leading to juxtaposition of immunoglobulin heavy chain locus to IRF4 gene, but this translocation and genetic aberrations are very rare in Multiple Myeloma (Shaffer *et al.*, 2009).

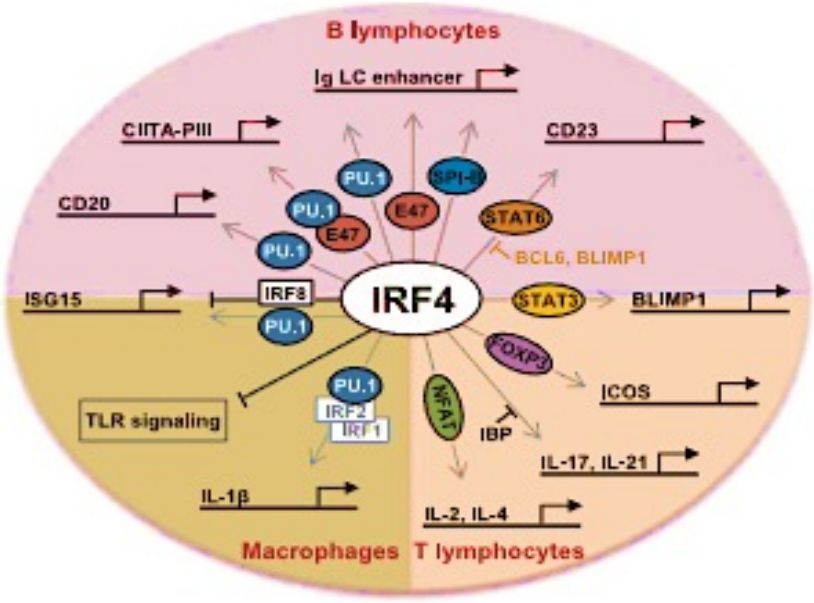

Figure 1.11. Role of IRF4 in immune cells depending on its cofactor (Adapted from De Silva *et al.*, 2012)

Another finding, which shows critical role of IRF4 in Multiple Myeloma, was that IRF4 levels are linked to outcome of the disease and its high expression is related with poor survival rates. Additionally, Multiple Myeloma cells were shown to have non-oncogene addiction to IRF4 expression since their knockdown results in reduced survival of these cells without any genetic alteration like translocations or mutations (Shaffer *et al.*, 2008).

The role of IRF4 in immune cell cancers is not restricted to Multiple Myeloma. IRF4 was shown to be overexpressed in Activated B cell like diffuse large B cell lymphoma (ABC-DLBCL), which is an aggressive type of DLBCL, due to NF-kB pathway that is constitutively active in these cells. Knockdown of IRF4 in ABC-DLBCL cells resulted in a similar effect as Multiple Myeloma and it was demonstrated that ABC-DLBCL cells have non-oncogene addiction to IRF4 expression. However, survival of germinal center DLBCL (GC-DLBCL) cells were not dependent on IRF4 expression and

this observation was consistent with low NF-kB activity leading to low IRF4 expression in germinal center. These results are summarized in Figure 1.12 (Yang *et al.*, 2012).

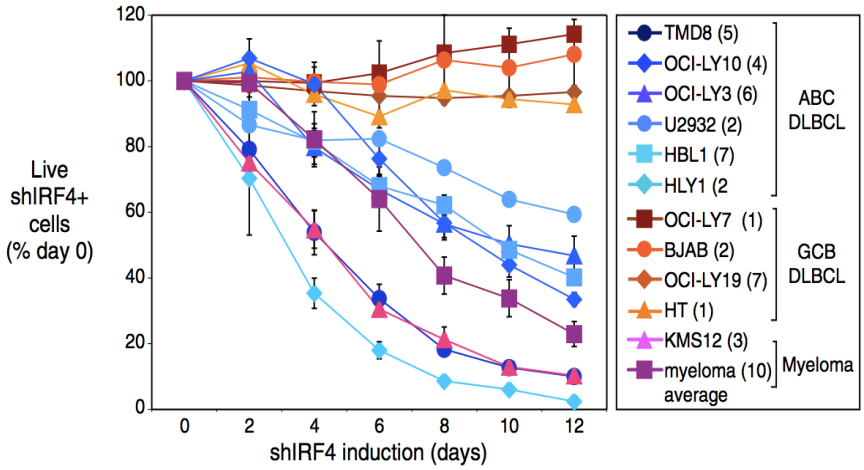

Figure 1.12. GFP competition assay results for ABC-DLBCL, GCB-DLBCL and Multiple Myeloma cells. IRF4 knockdown results in reduced competitive fitness of ABC-DLBCL and Multiple Myeloma cells, but does not affect GCB-DLBCL cells (Adapted from Yang *et al.*, 2012).

1.8. IRF4 in Melanocytes and Other Non-Immune Cells

Apart from lymphocytes, IRF4 expression has recently been observed in cardiac tissue and central nervous system neurons. In these recent studies, the role of IRF4 expression in cardiac hypertrophy, its protective role in ischemia and reperfusion and its role in fat metabolism in adipocytes were demonstrated (Lin *et al.*, 2012).

According to multiple studies, IRF4 expression is not restricted to only immune cells, adipocytes and cardiac cells. One of the cell types that have IRF4 expression is melanocyte and until recent years, the functional role of IRF4 in this cell type was not clear. Some genome wide association studies pointed out that a SNP in IRF4 locus (rs12203592-T) was linked to some pigmentation phenotypes such as sensitivity of skin

against sun exposure, increased rate of freckles and blue eyes and brown hair color. (Duffy *et al.*, 2010)

Apart from these GWAS studies, a recent study demonstrated that the same SNP, rs12203592, is located at the 4th intron of IRF4 and an enhancer region of IRF4 at the same time. It was shown that MITF, which is the master regulator of melanocyte development and function, binds to this region along with AP2∝ transcription factor in a cooperative manner leading to the activation of IRF4 expression. However, the presence of the variant form of the SNP in this region impairs the cooperative binding activity of MITF and AP2∝ and results in a decrease in IRF4 expression. Importantly, in the same study IRF4 was shown to bind to Tyrosinase (TYR) promoter, which is the key enzyme for melanin synthesis in melanocytes, along with MITF cooperatively. Therefore, authors suggested that the presence of rs12203592-T SNP decreases IRF4 expression leading to less human pigmentation due to the low IRF4 binding to TYR, which results in decreased human pigmentation in normal melanocytes (Praetorius *et al.*, 2013). The cooperative activities of IRF4, MITF and AP2∝ are shown in Figure 1.13.

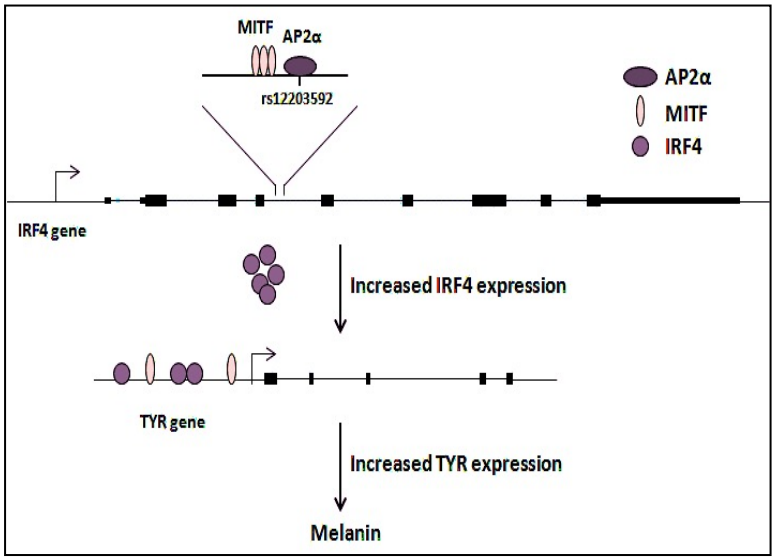

Figure 1.13. The mechanisms of melanin synthesis by TYR, which is regulated by the cooperative activities of IRF4, MITF and AP2∝ (Adapted from Praetorius *et al.*, 2013)

1.9. IRF4 in Melanoma

There are several evidences for the potential role of IRF4 in melanoma. Firstly, IRF4 expression was observed in different skin-related tissues and G361 melanoma cell line was shown to express IRF4 at protein level. In the same study, it was also observed that melanocytes of mouse foreskin have IRF4 expression. These studies were the first clues, which proved that IRF4 was not specific for lymphocytes (Grossman *et al.*, 1996). In additional studies, IRF4 expression was detected in melanoma patient samples by immunohistochemistry staining (Natkunam *et al.*, 2001). Metastatic melanoma samples staining positive for IRF4 even led to the proposal that IRF4 could be a diagnostic marker in melanoma. (Sundram *et al.*, 2003).

In addition to these studies, the germline SNP in IRF4 locus (rs12203592) was associated with skin related diseases and some melanoma-related predispositions. Individuals which harbor this SNP in their *IRF4* locus were shown to have higher nevi counts, variations in skin color, blue eyes and brown hair color and more tanning tendency, all of which are known risk factors for melanoma. (Nan *et al.*, 2009). As discussed above, the same SNP was shown to affect human pigmentation through cooperative activity of MITF and AP2∝ in normal melanocytes (Praetorius *et al.*, 2013).

According to these findings, IRF4 does not only have important roles in immune cells, but rather it has critical functions in melanocytes, and likely in melanoma which need to be fully characterized. Previously, in our research group it was demonstrated that IRF4 is highly expressed in melanoma cells compared to other solid tumors based on cancer database analysis. IRF4 expression was validated in several melanoma cell lines at mRNA and protein levels. In addition, we found that shRNA-based knockdown of IRF4 in several melanoma cell lines resulted in a decrease in competitive fitness and/or survival of these cells, which are shown via GFP competition assays. Therefore, we decided that these findings are encouraging for further studies on the role of IRF4 in melanoma.

2. PURPOSE

The aim of this study is to set up CRISPR based knockout, knockdown (CRISPRi) and activation (CRISPRa) systems and implement them in melanoma cells to characterize the role of Interferon Regulatory Factor 4 (IRF4) in *in vitro* assays that interrogate cancer-related phenotypes.

3. MATERIALS

3.1. General Kits, Enzymes and Reagents

Table 3.1 List of general kits, enzymes and reagents.

BCA Protein Assay Kit	Life Technologies, USA
DMEM	Gibco, LifeTechnologies, USA
FBS	Gibco, LifeTechnologies, USA
Non Essential Amino Acids	Gibco, LifeTechnologies, USA
Penicillin / Streptomycin	Gibco, LifeTechnologies, USA
Trypsin	Gibco, LifeTechnologies, USA
Plasmid Miniprep Kit	Roche, Switzerland
EndoFree Plasmid Maxi Kit	Macherey Nagel, Germany
PCR Purification and Gel Extraction Kit	Macherey Nagel, Germany
Q5 High Fidelity DNA Polymerase	New England Biolabs, USA
Deoxynucleotide (dNTP) Solution Mix	New England Biolabs, USA
Quick-Load 1 kb DNA ladder	New England Biolabs, USA
Quick-Load 100 bp DNA ladder	New England Biolabs, USA
Quick-Load 50 bp DNA ladder	New England Biolabs, USA
BsmBI	Thermo Scientific, USA
FastAP	Thermo Scientific, USA
T4 PNK	New England Biolabs, USA
T4 DNA Ligase	New England Biolabs, USA
Protease Inhibitor Cocktail Tablets	Roche, Switzerland

3.2. Biological Materials

3.2.1. Bacterial Strains

For storage, expansion and transformation of all plasmids, *Escherichia Coli* STBL3 bacterial strain was used since it has low recombinase activity and prevents recombination of lentiviral vectors.

3.2.2. Cell Lines

SKMEL-28 (human melanoma cell lines, kindly provided by Marisol Soengas), MALME-3M (human melanoma cell line, kindly provided by Dr. Ali Osmay Güre), A2058 (human melanoma cell line, kindly provided by Yetiş Gültekin and Dr. David M. Sabatini), HEK293FT (human embryonic kidney cell line, kindly provided by Dr. Nesrin Özören) were mainly used in the experiments.

3.2.3. Plasmids

pCW-Cas9 (Addgene plasmid # 50661, a gift from Eric Lander & David Sabatini), pHAGE-TRE-dCas9-KRAB (Addgene plasmid #50917, a gift from Rene Maehr & Scot Wolfe) and pHAGE-TRE-dCas9-VP64 (Addgene plasmid # 50916, a gift from Rene Maehr & Scot Wolfe) were used for the generation of stable cell lines. pLKO5.sgRNA.EFS.GFP backbone (Addgene plasmid #57822, a gift from Benjamin Ebert) was used for the expression of all sgRNAs used in this study.

3.2.4. Primers

Table 3.2 Primers used in this study.

Primer ID	Sequence	Application
IRF4	Primer1: 5'-GGGACATTGGTACGGGATT-3' Primer2: 5'-CTACACCATGACAACGCCTTA-3'	qRT-PCR
GAPDH	Primer1: 5'-TGTAGTTGAGGTCAATGAAGGG-3' Primer2: 5'-TGTTCCAATATGATTCCACCCA-3'	qRT-PCR
IRF4-KO-1	Primer1: 5'-GAGAGAGGGTGCAAGACGAG-3' Primer2: 5'-CACCTGATGCCTCCGCC-3'	Sanger Sequencing
IRF4-KO-2	Primer1: 5'-GAGAGAGGGTGCAAGACGAG-3' Primer2: 5'-CACCTGATGCCTCCGCC-3'	Sanger Sequencing
IRF4-KO-3	Primer1: 5'- TTGGCAGTGATAGGGTCCAAG-3' Primer2: 5'- TCAAGGATCTGGCTGCCTCT-3'	Sanger Sequencing
pLKO_U6_SEQ_fw	5'-TTTGCTGTACTTTCTATAGTG-3'	Sanger Sequencing

3.3. Chemicals

Table 3.3 List of chemicals used in this study.

Ethidium Bromide	Merck, USA
EDTA	Merck, USA
Hydrochloric Acid	Merck, USA
Sodium Chloride	Merck, USA
Bromophenol Blue Indicator	Merck, USA
Tween 20	Merck, USA
Methanol	Merck, USA
Acetic Acid	Merck, USA
LB Broth	Merck, USA SigmaAldrich, USA
Glycine	Merck, USA
DMSO	Merck, USA
Ethanol	Merck, USA
Nonidet P40	Fluka, USA
Hexadimethrine bromide	Sigma Aldrich, USA
Chloroquine diphosphate	Applichem, Germany
Ammonium persulfate	Applichem, Germany
SDS	Applichem, Germany
Ampicilllin	Applichem, Germany
Acrylamide	Sigma Aldrich, USA
Sodium Deoxycholate	Sigma Aldrich, USA
N,N'-Methylenbisacrylamide	Sigma Aldrich, USA
DEPC-treated water	Fisher Scientific, USA
Agarose	Sigma Aldrich, USA
Glycerol	Merck, USA
Chloroquin	Merck, USA
TEMED	Merck, USA
Tris-Cl	Merck, USA
Calcium Chloride	Merck, USA

3.4. Buffers and Solutions

Table 3.4 List of buffers and solutions used in this study.

10X SDS Running Buffer	1% SDS 1.92M Glycine 250 mM Tris-Base
10X Transfer Buffer	1.92M Glycine
	250 mM Tris-Base
1X Transfer Buffer	10% 10X Transfer Buffer
	20% Methanol
4X Protein Loading Dye	200 mM Tris-Cl (pH: 6.8)
	8% SDS
	40% Glycerol
	4% β-mercaptoethanol
	50 mM EDTA
	0.8% Bromophenol Blue
Cell Lysis Buffer	150 mM NaCl
	50 mM Tris (pH: 8.0) 0.1% SDS
	0.5% Sodium deoxycholate
	1.0% NP-40
10% SDS-PAGE Gel, Resolving Part (20ml)	8 ml ddH2O 6.66 ml 30% Acrylamide/Bisacrylamide mix 5ml 1.5M Tris, pH: 8.8 200 µl 10% SDS 120 µl 10% APS 20 µl TEMED
4% SDS-PAGE Gel, Stacking Part (8ml)	7788 µl ddH2O 1072 µl 30% Acrylamide/Bisacrylamide mix 1ml 1 M Tris, pH: 6.8 200 µl 10% SDS 50 µl 10% APS 10 µl TEMED
10X TBS	200 mM Tris-Cl (pH: 7.6)
	1.5 M NaCl
1X TBS-T	50 mM Tris-Base (pH: 7.4)
	150 mM NaCl
	0.1% Tween 20
Paraformaldehyde (4%)	1 g Paraformaldehyde
	25 ml distelled water
5% Blocking Solution	5% BSA (w/v) in 1X TBS-T

3.5. Antibodies

Table 3.5 List of antibodies used in this study.

Name	**Species**	**Dilution**	**Source**
Anti-HA	Rabbit	1:1000	Ab18181, Abcam
Anti-IRF4 X (M-17)	Goat	1:2000	Sc-6059, Santa Cruz
Anti-FLAG	Mouse	1:2000	F1804, Sigma Aldrich
Anti-GAPDH	Rabbit	1:2000	4695S, Cell Signaling

3.6. Disposable Labware

Table 3.6 List of disposable labwares used in this study.

Western Blotting Paper	Whatman, UK
Parafilm	Brand, Germany
Scalpel	Swann-Morton, UK
Centrifuge Tubes, 15 ml	Vwr, USA
Centrifuge Tubes, 50 ml	Vwr, USA
Serological pipette, 5ml	Tpp, Switzerland
Serological pipette, 10ml	Tpp, Switzerland
Serological pipette, 25ml	Tpp, Switzerland
Pipette Tips, filtered	Biopointe, USA
Pipette Tips, bulk	Biopointe, USA
Microcentrifuge tubes	Axygen, USA
PCR Tubes, 0.2 ml	Axygen, USA
Medical Gloves	Vwr, USA
Syringe Filters	Sartorius, Germany
Cryovial	Tpp, Switzerland
Cell Culture Flasks, 75cm2	Tpp, Switzerland
Cell Culture Plates, 6-well	Tpp, Switzerland
Insulin Syringes, 1 ml	Vwr, USA
Syringe, 10ml	Becton Dickinson, USA
PS Test Tubes, 5 ml	Becton Dickinson, USA Isolab, Germany
Glass Pasteur Pipette, 230 mm	Witeg, Germany
Chemiluminescent Detection Film	Roche, Switzerland

3.7. Equipment

Table 3.7 List of equipment used in this study.

Micropipettes	Axygen, USA
Heat Block	Cleaver Scientific EL-01, UK
Pipettor	Greiner Labopet 240, Germany
Vortex	Vwr, USA
Vertical Electrophoresis	Cleaver Scientific Omni-page Mini, UK
Centrifuges	J2-21, Beckman Coulter, USA Allegra X-22, Beckman Coulter, USA 5415R, Eppendorf, USA
Rotor	Beckman Coulter JA-14, USA
Cell Culture Incubator	Binder C-150, Germany
Documentation System	GelDoc XR System, Bio-Doc, Italy
Flow Cytometer	FACSCalibur , Becton Dickinson, USA
Freezers	-20°C, Ugur UFR 370 SD, Turkey -80°C, Thermo Scientific TS368, USA -150°C, Sanyo MDF1156, Japan
Microplate Reader	680, Biorad, USA
Microscopes	Inverted Microscope, Nikon Eclipse TS100, Japan Fluoroscence Microscope, Observer Z1, Zeiss, Germany
Thermal Cycler	Antarus MyCube ANT101, USA
Power Supply	Vwr, USA
Shaker	VIB Orbital Shaker, InterMed, Denmark Vwr Mini Orbital Shaker, USA
Spectrophotometer	NanoDrop 1000, USA
Stirrer - Heater	Dragonlab MS-H-S, China
Rotator	Grant Bio Multifunctional Rotator PTR-35, UK
Refrigerator	4°C, Ugur USS 374 DTKY, Turkey
Refrigerated Vapor Trap	Thermo Scientific SPD111V, USA
Oil-free Gel Pump	Thermo Scientific Savant VLP110, USA
Vacuum Pump Oil Filter	Thermo Scientific VPOF110, USA
Carbon dioxide Tank	Genc Karbon, Turkey
Ice Maker	Brema, Italy Scotsman Inc. AF20, Italy
Autoclave	Model ASB260T, Astell, UK
Dishwasher	Miele Mielabor G7783, Germany
Stella	Raytest, Germany
Freezing Container	Nalgene, USA
Oven	Nüve KD200, Turkey

4. METHODS

4.1. Cell Culture

4.1.1. Maintenance of Cell Lines

SKMEL-28, SKMEL-5, Mewo, A2058, Malme-3M and HEK293FT cell lines were grown in DMEM-high glucose media that contain 10% FBS, 1% penicillin/streptomycin antibiotics and 1% non-essential amino acid solution. Cells were maintained in a 37^{o} incubator with 5% CO_2. For the growth maintenance of the cells, they were passaged twice a week. For cell passage, firstly old media of the cells were aspirated and cells were washed with 1X PBS. After PBS is aspirated, 0.05% trypsin-EDTA was added onto the cells and they were incubated at 37^{o}C for 3 minutes. After incubation, DMEM was added to the cells at least at equal amounts to trypsin in order to inactivate it. Cells were mixed well and passaged. Additional DMEM was added to the remaining cells depending on the surface area of the plates/flasks.

For long-term storage of the cells, they were centrifuged at 500 g for 2 minutes and old medium was discarded. Cell pellet was resuspended in cell freezing DMEM medium, which contains 10% DMSO and 20% FBS. This cell suspension was aliquotted into 1 ml cryovials and put into Nalgene Freezing Container that is filled with isopropanol and stored at -80^{o}C for 2-3 days. Then, cryovials were transferred into -150^{o}C freezer for long-term storage. In order to make these stock cells, 10-cm plates at full confluency were divided into 3 cryovials.

In order to open a cell stock from -150^{o}C, cryovials were quickly transferred to 37^{o}C water bath. After cell suspension was defrozen completely, it was transferred to 15 ml falcon tubes and centrifuged at 500 g for 2 minutes. Freezing medium was discarded and cell pellet was resuspended in regular DMEM medium that is used for the maintenance

of the cells. Cell suspensions were transferred to 10-cm plates and additional medium was added to the cells for the maintenance.

4.1.2. Transfection of HEK293FT Cells via Calcium Phosphate Method

In order to produce lentivirus of sgRNA constructs, pCW-Cas9, PHAGE-TRE-dCas9-KRAB and PHAGE-TRE-dCas9-VP64 vectors, HEK293FT cells were transfected. For transfection, cells were seeded into 10-cm plates at 80% confluency 1 day prior to the transfection. Next day, medium of the cells were aspirated and replaced with fresh medium that contains 1X chloroquine at a final concentration of 25 μM and incubated at 37^{o}C. In eppendorf tubes, 10μg of the corresponding plasmid was mixed with 7,5 μg psPAX2 and 5 μg p-VSV-G helper plasmids. 62,5 μl of 2M $CaCl_2$ (125 mM) was added and the volume of the solution was completed to 500 μl by the addition of autoclaved double distilled water. The solution was vortexed and spinned down and added into eppendorf tubes that contains 1X HBS solution very slowly and drop wise. This mixture was mixed very well until bubbles were observed and incubated at room temperature for 5 minutes. After incubation, DNA mixture was added onto the cells dropwise and cells were incubated at 37^{o}C. After 6 hours, the medium of the cells was aspirated and 9 ml medium was added onto the cells.

4.1.3. Lentivirus Harvest from Cell Media

Lentivirus containing media of HEK293FT cells were harvested 72 hours later from the transfection. Firstly, the success of the calcium phosphate transfection was analyzed by fluorescence microscopy for PLKO-5-EFS-sgRNA-GFP vector based sgRNA constructs. For pCW-Cas9, PHAGE-TRE-dCas9-KRAB and PHAGE-TRE-dCas9-VP64 plasmids, lentivirus containing media was directly harvested since they do not have any fluorescence marker. Lentivirus containing media was filtered through a 0.45 μm filter into a 15 ml falcon tube. Filtered media were divided into eppendorf tubes as 1 or 2 ml aliquottes and used directly for lentiviral transduction or stored at -80^{o}C for later use.

4.1.4. Lentiviral Transduction

For lentiviral transduction, 150.000 cells were seeded into 6-well plates one day before the transduction. Next day, lentivirus aliquottes were thawn from -80^{o}C and mixed with polybrene at a final concentration of 4 μg/ml. The media of the cells were aspirated and lentivirus-containing medium was added onto the cells. After 6-8 hours, lentivirus-containing medium was removed and regular medium was added onto then cells.

4.1.5. Analysis of Transduction Efficiency by Flow Cytometry

In order to analyze the transduction efficiency of sgRNA constructs, which have GFP marker, the cell media and death cells were collected into FACS tubes. Cells were tyripsinized and one third of the cells were transferred into FACS tubes. Cells were centrifuged at 500 g for 2 minutes and supernatant was discarded. Cell pellet was washed with 1X PBS and centrifuged again. Supernatant was discarded and cell pellet was resuspended in 1 ml 1X PBS. Cells were vortexed well to obtain single cells. For FACS analysis, BD FACS Calibur machine and CellQuestPro software was used. Firstly, untransduced cells were analyzed by FL-1 channel to determine their self-fluorescence. Then, transduced cells were analyzed to determine the percentage of GFP positive cells based on the threshold that was adjusted by using untransduced cells.

4.1.6. Generation of Stable Cell Lines by Antibiotic Selection

For the generation of pCW-Cas9, PHAGE-TRE-dCas9-KRAB and PHAGE-TRE-dCas9-VP64 stable melanoma cells, cells were transduced with the corresponding lentiviruses. After 72 hours, transduced cells were transferred into 10-cm plates from 6-well plates. For pCW-Cas9 lentivirus transduced cells were added 2 μg/ml puromycin and PHAGE-TRE-dCas9-KRAB and PHAGE-TRE-dCas9-VP64 lentivirus transduced cells were added 1000 μg/ml G418 antibiotics. Selection was continued until all untransduced cells were dead.

4.1.7. Doxycycline Treatment of Inducible Stable Cell Lines

For the induction of Cas9, dCas9-KRAB and dCas9-VP64 proteins, stable cell lines were treated with 2 μg/ml doxycycline. Cells were seeded one day before the treatment at 60% confluency. Next day, doxycycline solution was thawed from -20^{o}C and mixed with medium of the cells. Doxycycline was refreshed every 24 hours since its half-life is short. Doxycycline treatment was performed in dark since it is light sensitive.

4.2. Molecular Cloning

4.2.1. Plasmid Preparation

pLKO-5-sgRNA-EFS-GFP plasmid was received as a bacterial stab culture from Addgene. Stab culture was streaked onto an ampicillin containing LB-Agar plate and incubated at 37^{o}C overnight. Next day, single bacterial colonies were obtained and one colony was inoculated into 10 ml LB-Ampicillin solution and grown overnight at 37^{o}C. Later, plasmid DNA isolation was performed by using Roche High Pure Mini Plasmid Isolation Kit according to the manufacturer's instructions. For transfections, plasmid DNA was isolated with Macherey Nagel Nucleobond Xtra Plus EF Plasmid Isolation Kit in order to obtain endotoxin free plasmids. All plasmid DNAs were stored at -20^{o}C.

4.2.2. Restriction Enzyme Digestion of Plasmids

PLKO.5.sgRNA.EFS.GFP plasmid was digested with BsmBI FD (Fermentas) restriction enzyme for the cloning of sgRNA oligos. 2 μg of plasmid DNA that was prepared via mini prep plasmid isolation protocol was digested with the enzyme according to the manufacturer's instructions. Plasmid DNA was mixed with BsmBI restriction enzyme and Fast AP (Fermentas) thermo sensitive alkaline phosphatase in 10X FD Buffer (Fermentas) and the total volume of the reaction was completed to 60 μl by using nuclease free double distilled water. Restriction enzyme reaction was performed for 30 minutes at

37°C by using a thermal cycler. Restriction digestion reaction was followed with incubation at 65°C for 10 minutes in order to heat-inactivate the enzyme.

4.2.3. Preparation, Annealing and Phosphorylation of sgRNA Oligos

sgRNA oligos were ordered and received from Macrogen (S. Korea) oligo synthesis services. They were suspended in appropriate volumes of nuclease free distilled water to obtain 100 μM oligo suspensions. Oligo solutions were kept at -20°C for long-term storage. For oligo annealing and phosphorylation reaction, 1 μl of forward and reverse oligos were mixed with 0,5 μl T4 polynucleotide kinase enzyme (NEB) and 1 μl of 10X T4 DNA ligase buffer (NEB). The total volume of the reaction was completed to 10 μl with nuclease free distilled water. For phosphorylation reaction, the mixture was incubated at 37°C for 45 minutes in a thermal cycler. After phosphorylation, samples were incubated at 95°C for 5 minutes and the temperature was decreased to 25°C with a 1°C/min rate. After incubation at 25°C for 5 min, oligo phosphorylation and annealing reaction was completed and samples were stored at -20°C.

4.2.4. Agarose Gel Electrophoresis of Digested Plasmid

In order to determine whether the restriction digestion reaction of the plasmid was successful, all of digestion sample and undigested plasmid as the control that was mixed with ethidium bromide was loaded into 1% agarose gel and electrophoresis was performed at 120 V for 30 minutes. The gel was visualized under UV light by using Biorad Geldoc. If the digestion is successful, digested band was cut from the gel on a UV box and it was extracted from the gel by using Nucleospin Gel and PCR Clean –up kit (Macherey Nagel) according to manufacturer's instructions. Extracted digested plasmid DNA was stored at -20°C. Similarly, annealed oligos were run in 2,5% agarose gel to see the success of the annealing reaction. They were not gel extracted.

4.2.5. Ligation Reaction of Digested Plasmid and Annealed Oligos

In the ligation reaction, 50 μg digested plasmid DNA and 1 μl of 1:500 diluted annealed oligos were used. Oligos were diluted with double distilled water. For the reaction, T4 DNA ligase enzyme (NEB) was used. Plasmid DNA and diluted oligo was mixed with T4 DNA ligase buffer (NEB) and 0,5 μl T4 DNA ligase was added. The total volume of the reaction was completed to 5 μl with double distilled water. The mixture was incubated at 24^{o}C for 90 minutes in a thermal cycler and heat inactivation was performed at 65^{o}C for 10 minutes. Ligation products were stored at -20^{o}C or used in the transformation directly.

4.2.6. Transformation of Ligation Products into Competent Bacteria

After digested sgRNA vector and oligo duplexes were ligated, total amount of ligation product was transformed into recombinase deficient Stbl3 E. coli strain which were previously made competent by $CaCl_2$ method. For the transformation part, 5 μl of ligation product was added into the competent bacterial cells and this mixture was incubated on ice for 20 minutes. Then, competent cells were incubated at 37^{o}C for 45 seconds followed by another incubation on ice for 5 minutes. For the recovery of heat shocked competent bacterial cells, 1 ml of LB without any antibiotics was added to the cells and incubated at 37^{o}C for 1 hour on an orbital shaker. After this incubation, this mixture was spinned down and bacterial pellet was resuspended in 150 μl LB solution and then plated on ampicillin containing LB-agar plates. Plates were incubated at 37^{o}C overnight. Next day, the success and the efficiency of the cloning was analyzed by comparing the numbers of bacterial colonies on the ligation plates to the negative control plate, in which there was no insert.

4.2.7. Validation of sgRNA Oligo Cloning via Sanger Sequencing

All Sanger sequencing reactions were performed by Macrogen Europe Incorporation. Briefly, some bacterial colonies were picked from the ligation plates and put

into ampicillin containing LB liquid followed by an overnight incubation at 37°C on an orbital shaker. Next day, plasmid DNA was isolated from these bacterial cultures and around 20 μg plasmid DNA was sent to Macrogen for Sanger sequencing. For the sequencing reaction, pLKO_U6_SEQ_fw primer was used.

4.3. Western Blotting

4.3.1. Preparation of Protein Samples

Medium of the cells, whose total protein will be isolated, was aspirated and cells were washed with 1X PBS. Cells were tyripsinized and detached from the monolayer. Tyripsinized cells were collected in 15 ml falcon tubes and centrifuged at 500 g for 2 minutes. Supernatant was discarded and cell pellet was washed with cold 1X PBS and centrifuged again. Supernatant was discarded and cell pellet was resuspended in 150 μl cold RIPA buffer (for $1x10^6$ cells) which contains protease inhibitor to preserve protein integrity. Resuspended cell pellet was vortexed 10 times for 1 second vigorously and incubated on ice for 30 minutes. Vortexing was repeated for each 10 minutes. After 30 min incubation, cells were centrifuged at 14000 g for 15 minutes. After centrifugation, supernatant was transferred into new 1,5 ml eppendorf tubes. Total protein samples were stored at -20°C. For long-term storage, they were kept at -80°C.

4.3.2. BCA Assay for Protein Concentration Determination

Pierce BCA Protein Assay Kit (Thermoscientific) was used for protein concentration determination. Standard BSA samples were prepared in the range of 2000 ng/μl- 25 ng/μl range according to manufacturer's instructions. For each sample, 150 μl of Reagent A and 3 μl of Reagent B were mixed and 150 μl of this mixture was put into one well of 96-well plate. Then, all wells are added with 5 μl of protein sample whose concentration will be measured. RIPA buffer was used as the blank solution for protein samples and 1X PBS was used as the blank solution for standard solutions. After this step, 96-well plate was incubated at 37°C for 30 minutes at dark. After incubation, absorbance

of each well was measured at 562 nm by using a plate reader. Absorbance of the blank solutions were subtracted from the samples and a standard curve by using values of the standard solutions were drawn by using Microsoft Office Excel and a formula for the calculation of the protein concentrations was obtained. By putting absorbance of protein samples into this formula, protein concentrations were calculated.

4.3.3. Protein Sample Preparation and SDS-PAGE Electrophoresis

Protein samples, which were going to be analyzed, were mixed with 4X Laemlie loading dye buffer and boiled at 95^{o}C for 5 minutes. After boiling, they were loaded into the wells of SDS-PAGE gel. For the preparation of the gel, 10 % resolving gel was prepared and loaded into Biorad gel cassette and 1 ml 100% isopraponal was added onto the resolving gel. After the solidification of the resolcing gel, 4% stacking gel was prepared and loaded onto the resolving gel after isopropanol was discarded and the comb was put to make the wells. After solidification, the gel was ready to be loaded with protein samples. After sample loading, samples were run at 80V for 15 minutes and when they passed to resolving part, they were run at 100 V for about 1,5 hours in 1X running buffer.

4.3.4. Blotting and Transfer of Proteins

After protein samples were run on SDS-PAGE gel, they were transferred to PVDF membrane. For this purpose, Whatmann papers whose sizes are equal to the gel were cut and soaked in 1X Transfer Buffer. SDS-PAGE gel was detached from the glasses and put onto the soaked Whatmann paper. Then PVDF membrane whose size is equal to the gel was incubated in 100% methanol for 10 seconds, followed by incubation in distilled water for 1 minute to remove excess methanol. After this washing step, membrane was incubated in 1X Transfer Buffer at least for 1 minute. Then, activated PVDF membrane was put onto the gel and covered with another soaked Whatmann paper. After transfer sandwich was prepared, transfer tank was filled with cold 1X Transfer Buffer. Transfer of proteins was performed at constant 250 mA for 1 hour 45 minutes in cold room. Following the transfer part, membrane was washed with 1X TBS-T three times for 5 minutes and blocked in 5%

BSA solution, which is prepared by using 1X TBS-T, for 1 hour at room temperature. Blocking part was followed by a wash step with 1X TBS-T three times for 5 minutes.

4.3.5. Primary and Secondary Antibody Incubations

After the washing step, membrane was cut according to the sizes of the proteins to be analyzed by using the protein ladder as the reference. Primary antibodies were diluted in 5% BSA solution depending on the antibody type and manufacturer's instructions. Membranes were incubated in primary antibody solutions overnight at $4^{o}C$ on an orbital shaker. After primary antibody incubation was completed, membranes were washed with 1X TBS-T three times for 5 minutes. Secondary antibody solutions were prepared either in 1X TBS-T or 5% BSA solution according to antibody type and manufacturer's instructions. Secondary antibody incubation was performed at room temperature for 1 hour and 30 minutes on an orbital shaker. After secondary antibody incubation was completes, membranes were again washed with 1X TBS-T three times for 5 minutes.

4.3.6. Chemiluminescence Detection of Protein Bands

In order to visualize protein bands, SuperSignal West Pico chemilumiscent substrate was prepared according to the manufacturer's instructions. Membranes were incubated in this solution for a short time at dark and then visualized by using imaging device, which are either Stella or SynGene and their softwares.

4.4. Real Time Quantitative PCR (q-RT-PCR)

4.4.1. Isolation of Total RNA

For the isolation of total RNA, Direct-zol RNA Miniprep Kit (Zymoresearch) was used according to the manufacturer's instructions. Briefly, cells were detached from the plates by treating them with appropriate volume of Trizol and then remaining steps were

applied as described in the manual of the kit. Optional DNase treatment was performed to remove possible DNA contamination. RNA samples were eluted in sterile nuclease free water supplied by kit. Concentrations and the purities of samples were measured by using nanodrop. Isolated RNAs were stored at -80^{o}C.

4.4.2. cDNA Synthesis

In order to convert isolated RNAs into cDNAs, RevertAid First Strand cDNA synthesis kit was used according to the manufacturer's instructions. Briefly, 500 ng RNA was mixed with 1 μl of oligo-dT primers and the total volume was completed to 12 μl with nuclease free water. This mixture was incubated at 65^{o}C for 5 minutes to eliminate the secondary structures. After this incubation, reaction buffer, dNTP solution, reverse transcriptase enzyme and RNase inhibitor were added to the same tube. cDNA synthesis reaction was performed at 42^{o}C for 1 hour, followed by incubation at 72^{o}C for 5 minutes. cDNAs were stored at -20^{o}C for further use.

4.4.3. q-RT-PCR

In RT-qPCR method, 1:30 diluted cDNAs were used as the templates of the reactions. cDNAs were diluted by using nuclease free distilled water. For RT-qPCR reaction, Maxima SYBR Green Kit (Thermo Scientific) was used according to manufacturer's instructions. Briefly, 2,5 μl of diluted cDNAs were distributed to the wells of the 96-well plate. Master mix that includes the primer pair, Maxima SYBR Green and sterile water was prepared and 7,5 μl distributed to all wells of 96-well plate. After vortex and spindown steps, PCR reaction was performed in PikoReal 96 PCR machine and by using its software software. Cq values that are detected with automatic threshold were used to calculate the relative expression of *IRF4*, which is normalized to the internal control *GAPDH*. For each sample, at least three replicates were used and the median of these samples was used for the calculation of relative expression. Standard errors were calculated for each sample by using the replicates.

4.5. GFP Competition Assay

Stable and inducible melanoma cell lines were transduced with sgRNA-expressing GFP-marked lentiviruses. On the 3rd day of transduction, GFP-positive cells, which are expressing corresponding sgRNAs, were mixed with untransduced cells, which do not express any sgRNA. Final GFP percentage for each sample was adjusted to 50-60%. Next day, cells were treated with doxycycline and GFP percentages for each sample were detected via FACS with 3-4 day intervals. Each time point was normalized to the first day GFP percentage or the percentage of empty vector control for each day. During the experiment, doxycycline-containing media was refreshed since the half-life of doxycycline is 24 hours.

5. RESULTS

5.1. Generation of Stable and Inducible Melanoma Cell Lines

For the implementation of CRISPR based knockout, dCas9-KRAB-mediated knockdown (CRISPRi) and dCas9-VP64-mediated activation (CRISPRa) technologies, we decided to use a lentiviral and doxyxcycline inducible system. We also chose a two-vector system, where Cas9, dCas9-KRAB, dCas9-VP64 proteins and sgRNAs are expressed from separate vectors. For this purpose, we firstly generated either Cas9, dCas9-KRAB or dCas9-VP64 expressing doxycycline inducible and stable melanoma cell lines. In order to generate either Cas9, dCas9-KRAB and dCas9-VP64 expressing melanoma cell lines, pCW-Cas9, PHAGE-TRE-dCas9-KRAB and PHAGE-TRE-dCas9-VP64 lentiviral vectors were used, respectively (Kearns et al., 2014). Plasmids were transfected into HEK293FT cells along with P-VSV-G and PSPAX2 helper vectors for lentiviral production. After lentivirus harvest, melanoma cells were transduced lentiviral supernatant and transduction was followed by antibiotic selection. For the generation of Cas9 expressing stable cell lines, cells were selected with puromycin and for dCas9-KRAB and dCas9-VP64 expressing cell lines, cells were selected with G418 until all untransduced cells died (Figure 5.2 and Figure 5.3). We generated SKMEL-28-Cas9, A2058-Cas9, A2058-dCas9-KRAB, Malme3M-dCas9-KRAB and Mewo-dCas9-VP64 stable cell lines.

Since all these lentiviral vectors are doxycycline inducible, stable cell lines were tested for their inducibility. In order to determine the optimal concentration of doxyxcycline needed for Cas9, dCas9-KRAB and dCas9-VP64 proteins in stable cell lines, cells were treated with its different concentrations for 24 hours. Total protein lysates were prepared, and Western blotting was performed to determine flag-tagged Cas9 protein levels. As can be seen in Figure 5.4, increasing doxycycline concentrations led to higher Cas9 expression after 24 hours and we chose 2 μg/ml as optimal concentration for further doxycycline treatments.

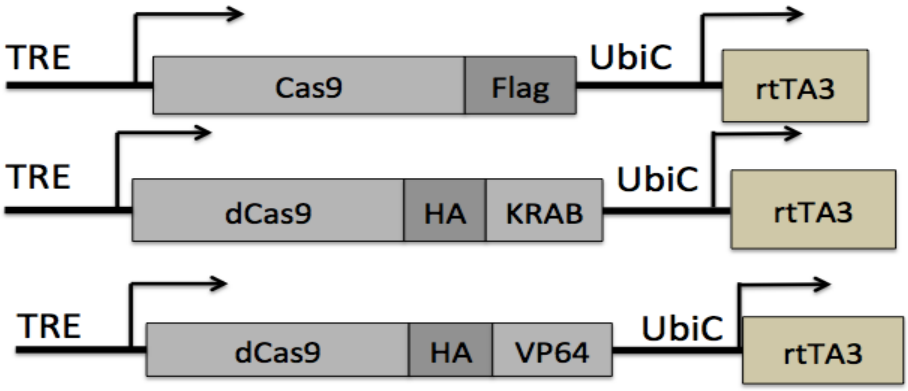

Figure 5.1. Schematic views of pCW-Cas9, PHAGE-TRE-dCas9-KRAB and PHAGE-TRE-dCas9-VP64 vectors

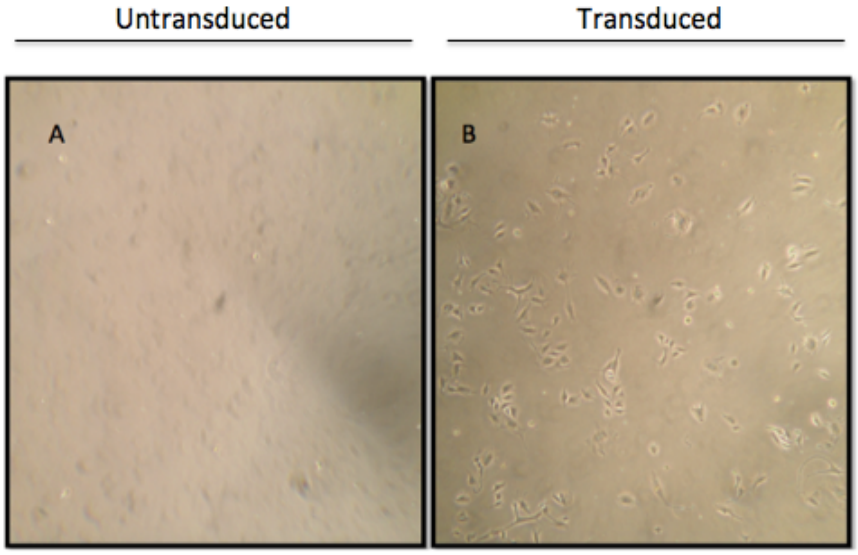

Figure 5.2. Bright field microscope images of puromycin selection of pCW-Cas9 transduced SKMEL28 cells. Skmel28 photographs are representative, similar results were observed in other cell lines. A) Untransduced cells. B) pCW-Cas9 transduced cells.

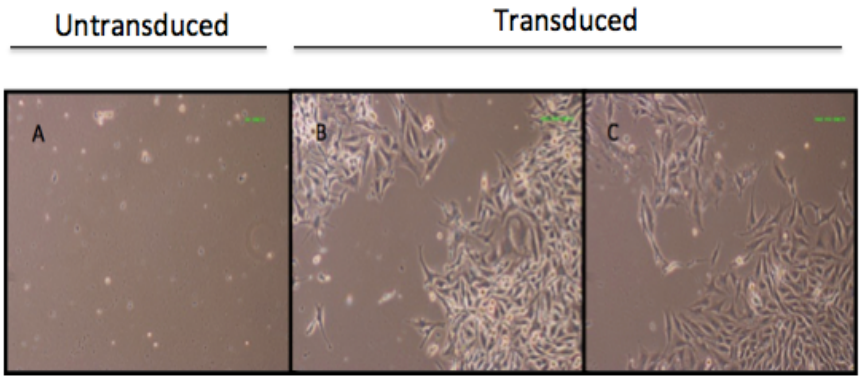

Figure 5.3. Bright field microscope images of G418 selection of PHAGE-TRE-dCas9-KRAB and PHAGE-TRE-dCas9-VP64 transduced SKMEL28 cells. These images are representative. A) Untransduced cells. B) PHAGE-TRE-dCas9-KRAB transduced cells C) PHAGE-TRE-dCas9-VP64 transduced cells.

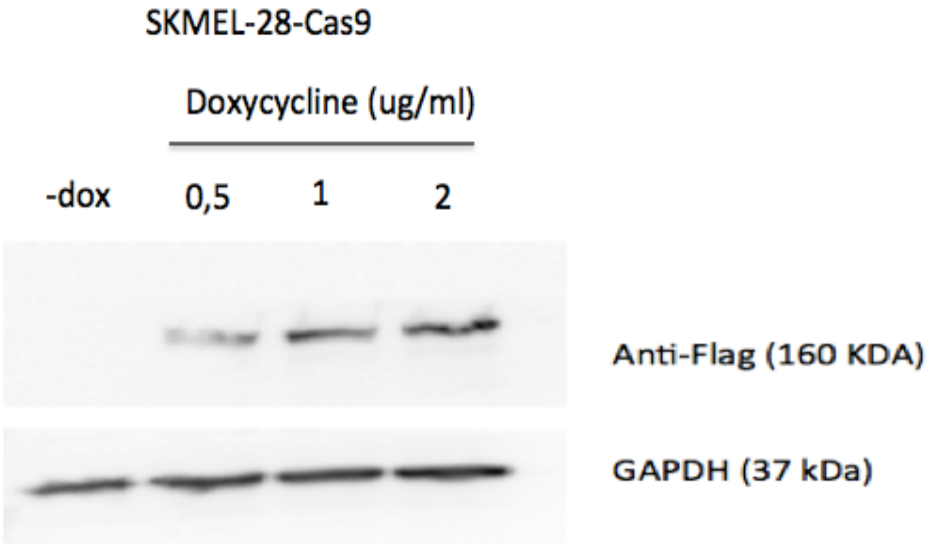

Figure 5.4. Western blot results for 24-hour doxycycline induction of SKMEL-28-Cas9 stable cell line. Cells were treated with indicated doxycycline concentrations. GAPDH is used as loading control. For Cas9 detection, anti-Flag antibody was used.

Next, the inducibility of Cas9, dCas9-KRAB and dCas9-VP64 in stable cell lines were also validated, similarly as shown in Figure 5.5 and Figure 5.6.

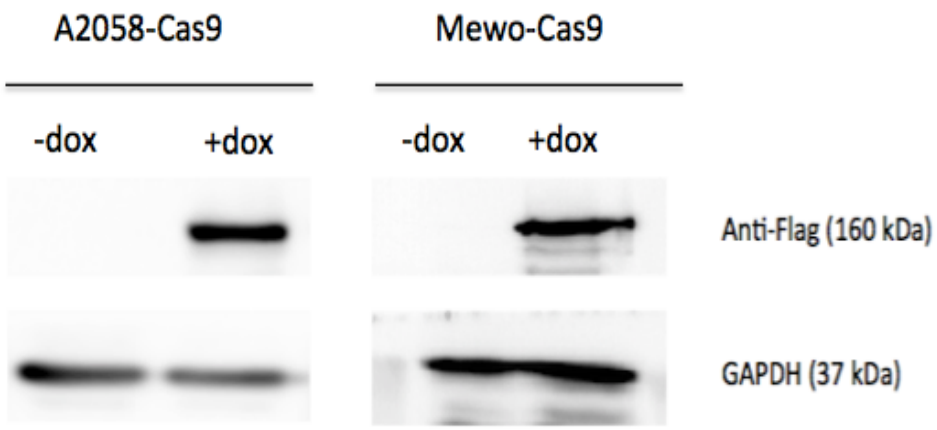

Figure 5.5. Western blot results for 24-hour doxycycline induction of A2058-Cas9 and Mewo-Cas9 stable cell lines. Cells were treated 2 μg/ml doxcycline. For Cas9 detection, anti-Flag antibody was used.

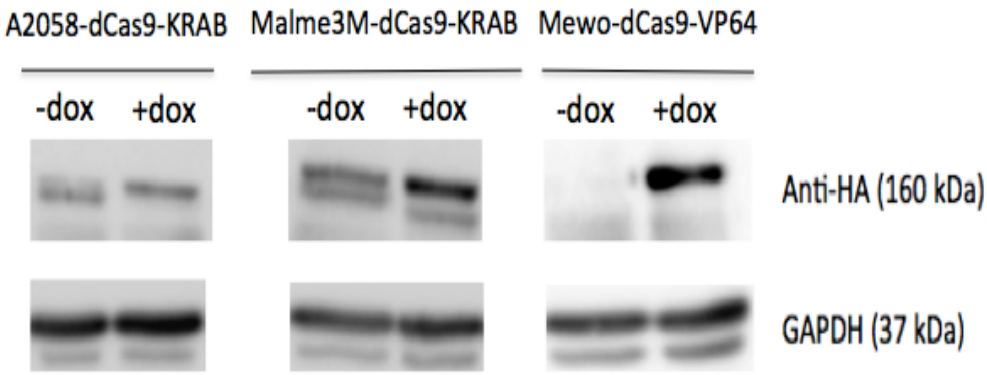

Figure 5.6. Western blot results for 24-hour doxycycline induction of A2058-dCas9-KRAB, Malme3M-dCas9-KRAB and Mewo-dCas9-VP64 stable cell lines. Cells were treated with 2 μg/ml doxycycline. For dCas9-KRAB and dCas9-VP64 detection, anti-HA antibody was used.

5.2. Design and Expression of sgRNAs in Stable Cell Lines

Target sites and sgRNAs for knockout, CRISPRi and CRISPRa methods were designed by using online Optimized CRISPR Design Tool (Zhang *et al*., 2014). For knockout, target sites were designed to be in the first and second exon of *IRF4* since it was previously reported that first and second constitutive exons of genes are optimal targets for CRISPR based knockout approach (Wang *et al*., 2014) . For CRISPRi, target sites were chosen close to transcription start site, and for CRISPRa, promoter of *IRF4* was targeted based on the knowledge obtained from previous studies which showed that these regions are optimal target sites for these applications (Qi *et al*., 2013). Optimal CRISPR Design Tool ranked candidate target sites with respect to their possible off-target regions and gave scores based on the number of off-target regions. We chose target sites with the lowest number of off-target regions and highest scores for our further experiments. All target sites used in this study and their scores are listed in Table A.1. in Appendix section.

PLKO.5.sgRNA.EFS.GFP plasmid is a lentiviral vector. sgRNAs which are cloned into this vector are expressed from hU6 promoter constitutively. GFP fluorescent marker is also expressed from a separate promoter in a constitutive manner. In order to express sgRNAs in stable Cas9/dCas9-KRAB/dCas9-VP64 expressing cell lines, sense and anti-sense sgRNA oligos, which have BsmBI restriction site overhangs, were annealed and cloned into PLKO.5.EFS.sgRNA.GFP vector, which was digested with BsmbI restriction enzyme. The verification of PLKO.5.sgRNA.EFS.GFP plasmid digestion and sgRNA oligo annealing are shown in Figure 5.8.

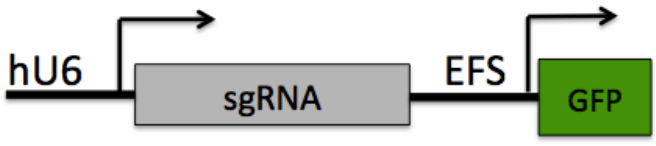

Figure 5.7. Schematic view of PLKO5.sgRNA.EFS.GFP vector

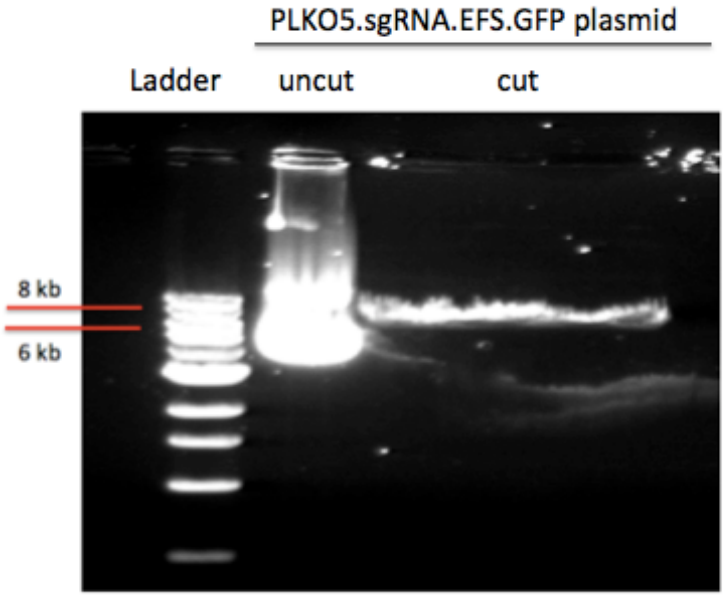

Figure 5.8. Agarose gel electrophoresis image of BsmBI-digested PLKO5.sgRNA.EFS.GFP plasmid along with undigested plasmid control. 1 kb DNA ladder was used as size marker.

Sense and anti-sense sgRNA oligos that have BsmBI restriction overhangs at their ends were annealed to form oligo duplexes, which would be later cloned into BsmBI digested PLKO.5.EFS.sgRNA.GFP plasmid. Successful oligo annealing was confirmed by agarose gel electrophoresis and DNA bands that have the expected size (25 bp) were observed as shown in Figure 5.9.

After confirmation of oligo annealing of sgRNAs, they were diluted and ligated with BsmBI digested PLKO.5.EFS.sgRNA.GFP plasmid followed by transformation into competent bacterial cells and plating. Later, plasmid DNAs were isolated from bacterial colonies and sgRNA cloning was confirmed by Sanger sequencing (Figure 5.10).

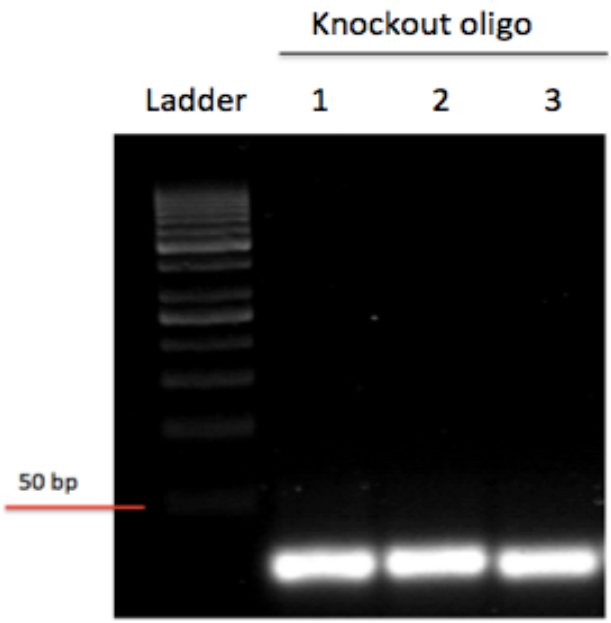

Figure 5.9. Agarose gel electrophoresis of oligo annealing for IRF4 knockout sgRNAs.

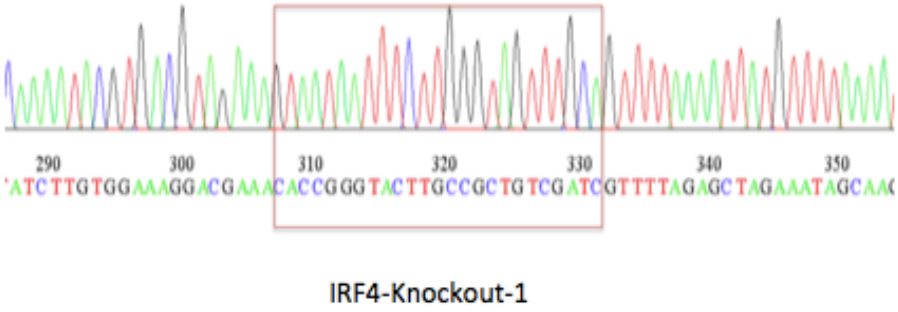

Figure 5.10. Sanger sequencing result of sgIRF4-Knockout-1 cloning into PLKO.5.EFS.sgRNA.GFP plasmid. This result is representative.

In order to express sgRNAs in stable cell lines, lentiviruses of PLKO.5.EFS.sgRNA.GFP sgRNA constructs were produced by transfecting them into HEK293FT cells along with helper plasmids. Transfection efficiencies of HEK293FT cells were analyzed by fluorescence microscopy as shown in Figure C.4 in Appendix section.

Next, lentiviruses were harvested and stable Cas9, dCas9-KRAB or dCas9-VP64 expressing melanoma cells were transduced with these lentiviruses followed by fluorescence microscope and flow cytometry analysis. According the results of these experiments, lentivirus production was successful and transduction efficiencies of all lentiviruses were higher than 90%. Therefore, sgRNAs are expected to be expressed in transduced stable melanoma cells.

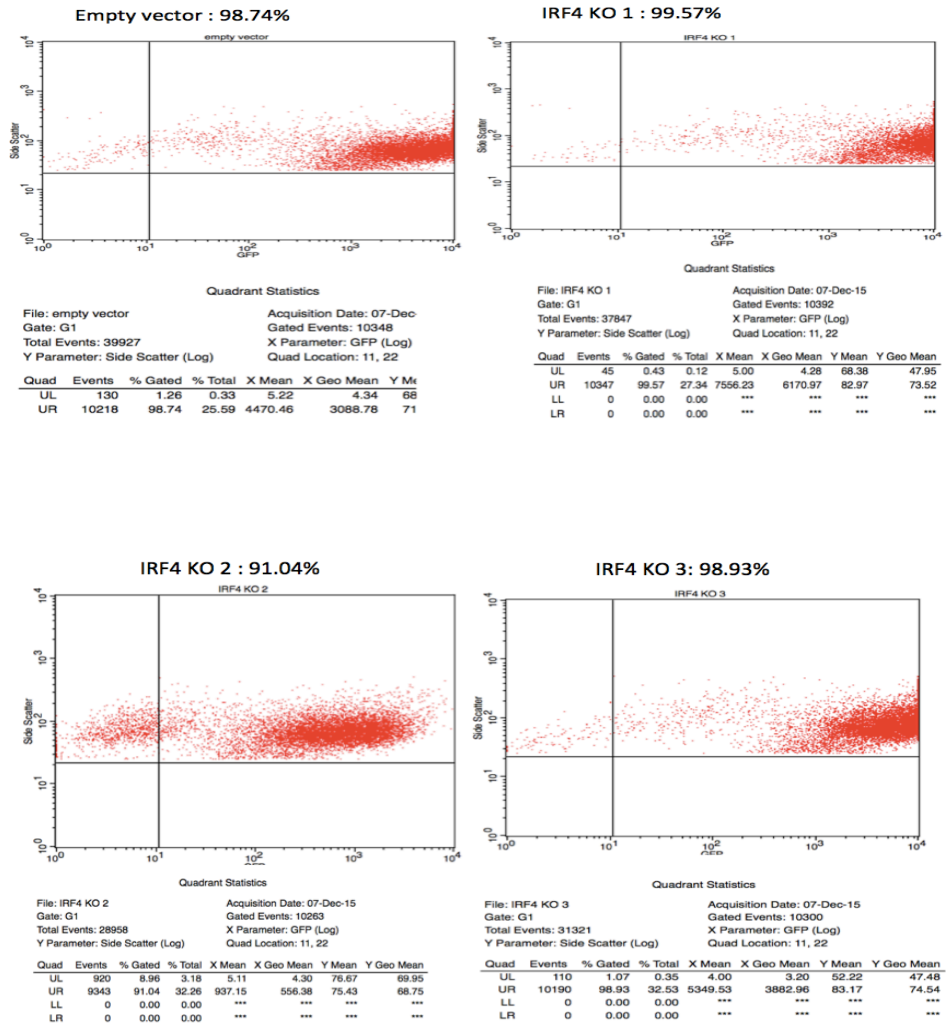

Figure 5.11. Lentiviral transduction efficiencies of empty vector control, IRF4-Knockout-1, IRF4-Knockout-2 and IRF4-Knockout-3 sgRNA constructs determined via flow cytometer. These results are representative.

5.3. IRF4 Knockout in Melanoma Cells by CRISPR/Cas9

After generation of stable Cas9 expressing inducible stable cell lines and construction of sgRNA vectors, we wanted to knockout IRF4 in melanoma cell lines. In order to knockout IRF4 in melanoma cells, doxycycline inducible Cas9 expressing stable SKMEL-28 and A2058 cells were transduced with IRF4 knockout sgRNA lentiviruses. As negative control, cells were transduced with empty control lentiviruses, which do not express any sgRNAs. Cells were treated with 2 μg/ml doxycycline on the third day of transduction and this treatment continued for 12 days. On the 12th day, total protein lysates were collected and western blotting was performed to analyze IRF4 expression at protein levels as shown in Figure 5.13.

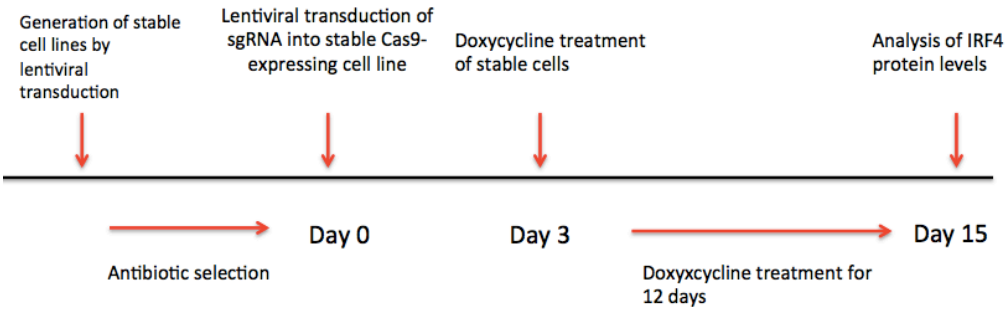

Figure 5.12. Timeline for CRISPR-based knockout of IRF4 in melanoma cells.

According to western blotting results, IRF4 expression was dramatically reduced at protein levels compared to empty vector control as shown in Figure 5.11.

After 12 days of doxycycline treatment, genomic DNA was isolated from pooled IRF4 knockout cells and sequenced to validate the formation of indel mutations at target sites. According to Sanger sequencing results, indels were formed starting from the target site as can be seen in Figure 5.14.

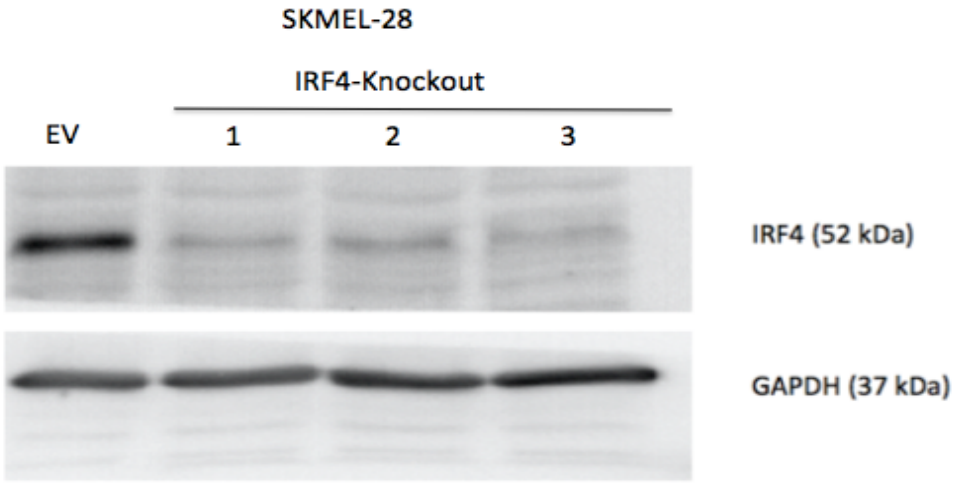

Figure 5.13. Western blotting analysis of IRF4 protein levels for SKMEL-28-pCW-Cas9 stable cell line transduced with corresponding sgRNA IRF4 knockout constructs and treated with doxycycline for 12 days.

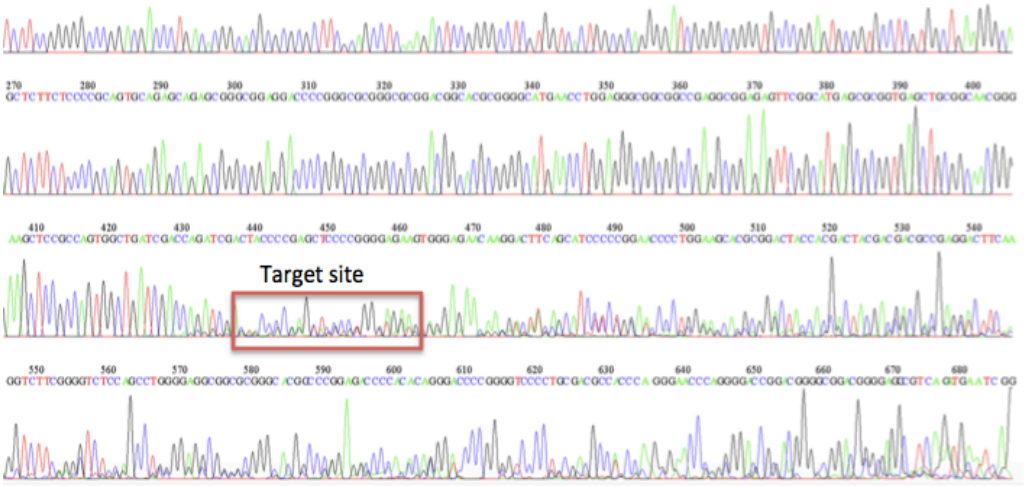

Figure 5.14. Sanger sequencing validation of indel formation in SKMEL-28 cells at IRF4 knockout target site for IRF4-Knockout-1 sgRNA. This result is representative.

We also tested our experimental set up for knockout in another IRF4-expressing melanoma cell line and we analyzed IRF4 protein levels in earlier time points, 3th and 7th

day, of doxycycline treatment to figure out the time needed to knockout IRF4. The results are demonstrated in Figure 5.15 and Figure 5.16.

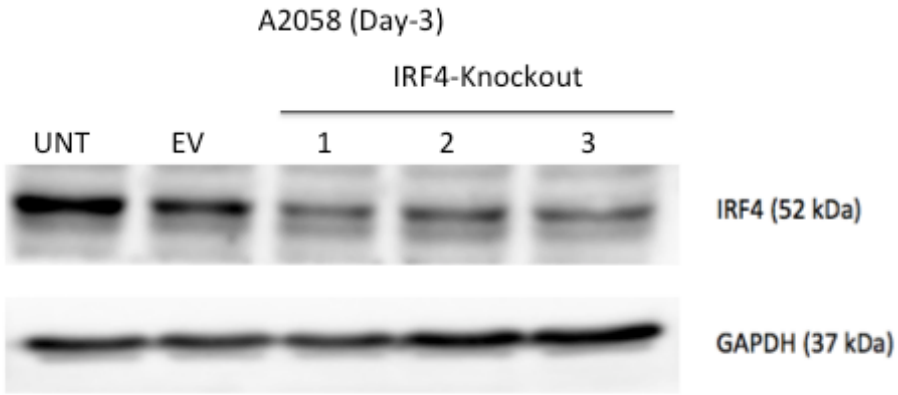

Figure 5.15. Western blot result for IRF4 knockout in A2058 cells after 4 days of doxycycline treatment.

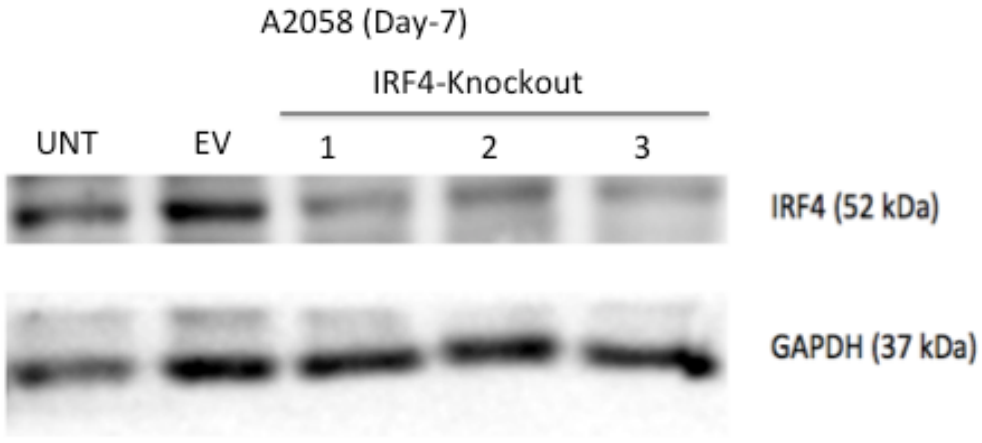

Figure 5.16. Western blot result for IRF4 knockout in A2058 cells after 7 days of doxycycline treatment.

According to these western blot results, on the 3th day of doxycycline treatment, IRF4 protein levels decreases significantly for all three sgRNAs. On the 7th day, IRF4 protein levels decrease even more compared to 3th day for all three sgRNAs.

5.3.1. GFP Competition Assay with IRF4 Knockout Cells

In order to determine whether IRF4 is important for the competitive fitness and/or survival of melanoma cells, GFP competition assay was performed for SKMEL-28-pCW-Cas9 and Mewo-pCW-Cas9 stable cells, which were transduced with IRF4 knockout lentiviruses. In GFP competition assay, a cell population which is a mixture of GFP-positive sgRNA-expressing cells and GFP-negative untransduced cells, are treated with doxyxcycline and the changes in GFP percentages are followed by flow cytometry. We observed that in GFP competition assays, the percentages of GFP positive SKMEL-28 cells in which IRF4 is knocked out, decreases over time, while, as a control, the percentages of IRF4-expression-negative Mewo cells does not change significantly over time. According to these preliminary data, IRF4 is important for the competitive fitness of SKMEL-28 cells.

5.4. IRF4 Knockdown by CRISPRi Method

After generation of dCas9-KRAB stable and inducible melanoma cell lines and preparation of sgRNA constructs for IRF4 repression (Section 5.2), we wanted to knockdown IRF4 expression levels in melanoma cells. For this purpose, corresponding stable cell lines were transduced with 5 different sgIRF4 knockdown constructs and treated with doxycycline. In this experiment, we also combined two different sgRNAs, IRF4-Knockdown-2 and IRF4-Knockdown-5, to see whether co-expression of two sgRNAs can lead to higher knockdown levels. On different timepoints, RNA and protein lysates were collected and IRF4 expression was analyzed at mRNA and protein levels by using RT-q-PCR and Western blotting techniques, respectively.

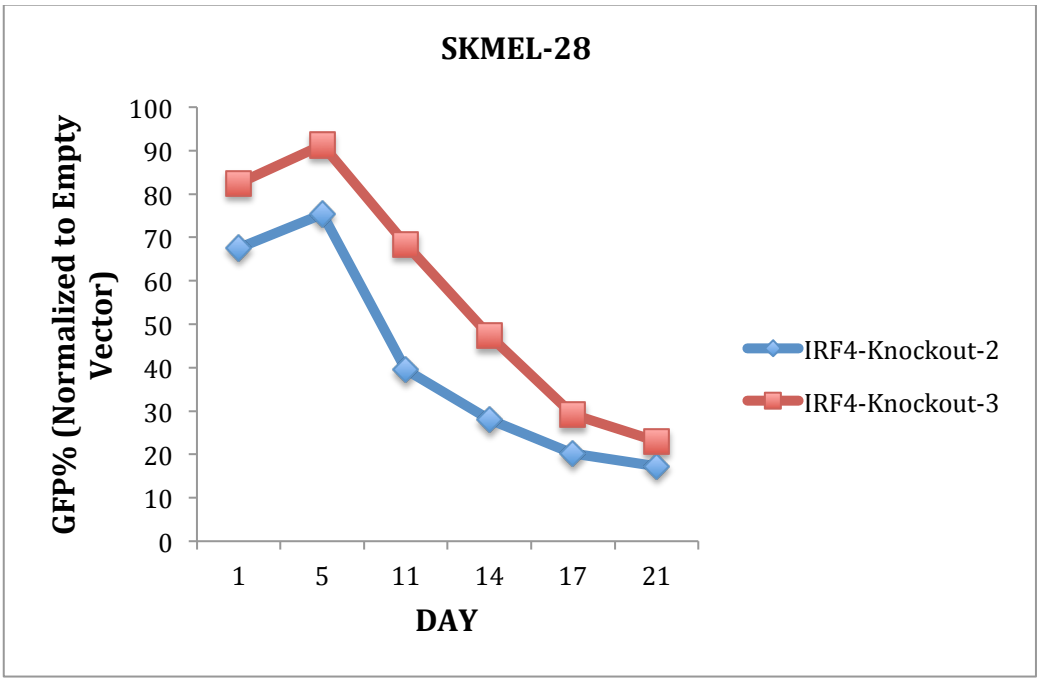

Figure 5.17. GFP competition assay results for IRF4 knockout in SKMEL 28 stable cell line. GFP percentages were normalized to empty vector control for each day.

According to the results of these experiments, in A2058 cells, IRF4 was repressed significantly by IRF4-Knockdown-2, IRF4-Knockdown-4 and IRF4-Knockdown-5 sgRNA constructs at both mRNA and protein levels on the third day of doxycycline treatment (Figure 5.20 and Figure 5.22). For 6 days doxycycline treatment, IRF4 mRNA was dramatically repressed in A2058 cells, which were transduced with IRF4-Knockdown-4 construct where the knockdown level is 92% (Figure 5.18). These results are consistent with Western blot results where IRF4 is also dramatically repressed at protein levels as can be seen in Figure 5.20. We also observed significant IRF4 knockdown at protein levels when we co-expressed IRF4-Knockdown-2 and IRF4-Knockdown-5 constructs as can be seen in Figure 5.21 and Figure 5.23.

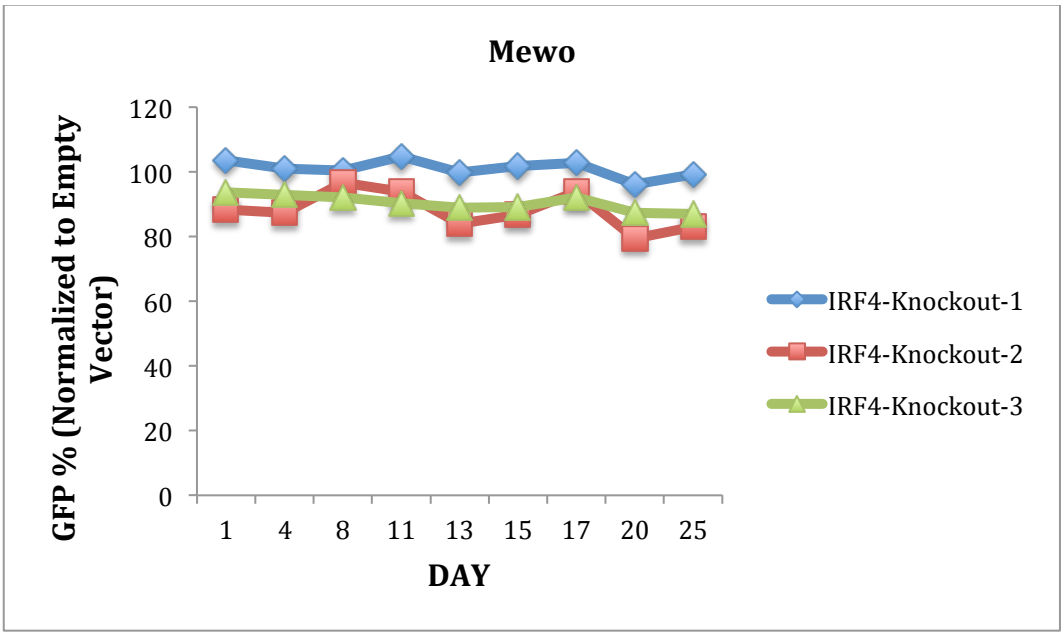

Figure 5.18. GFP competition assay results for IRF4 knockout in Mewo stable cell line. GFP percentages were normalized to empty vector control for each day.

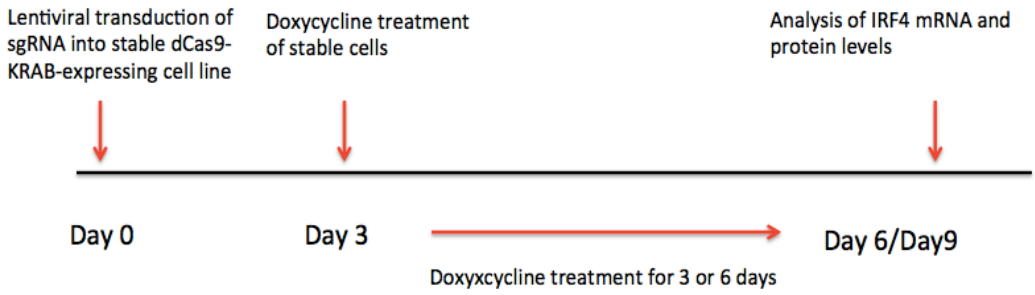

Figure 5.19. Timeline for IRF4 knockdown by CRISPRi method.

We also tested our CRISPRi method in Malme-3M cells, which is another IRF4-expressing melanoma cell line. Similar to A2058 cells, IRF4 mRNA and protein levels were analyzed by RT-qPCR and Western blot, respectively, at 3rd and 6th day of doxycycline treatment. In Malme3M cells, knockdown levels were not as high as A2058 cells. However, we still observed a significant knockdown of IRF4 in Malme3M cells for IRF4-Knockdown-4 and IRF4-Knockdown-5 sgRNA constructs as can be seen in Figure 5.26 and Figure 5.27.

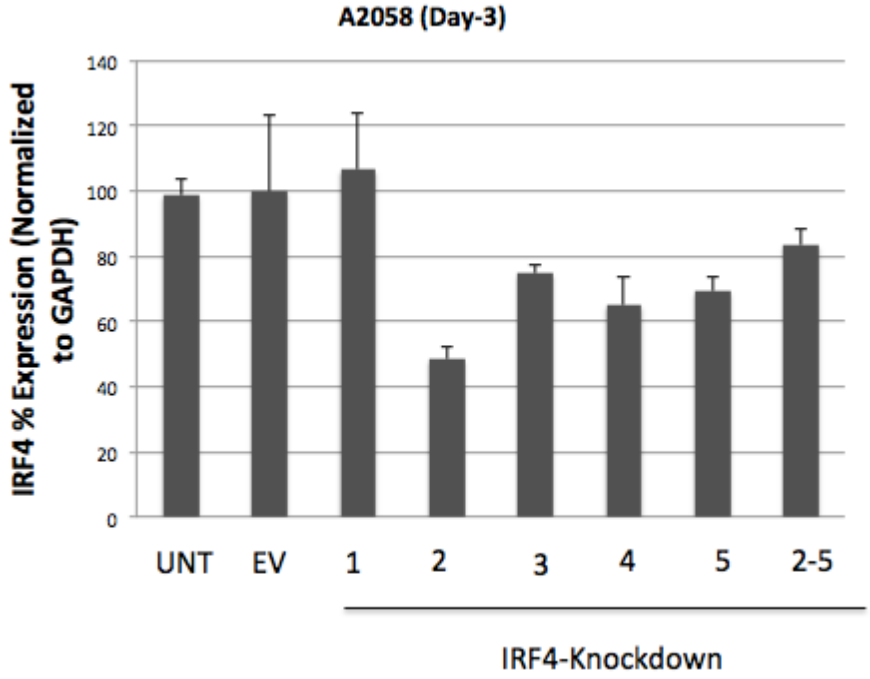

Figure 5.20. RT-q-PCR results for analysis of IRF4 expression in A2058 cells after knockdown by CRISPRi method upon 3 days of doxycycline treatment.

5.4.1. GFP Competition Assay with CRISPRi

After validation of successful knockdown of IRF4 expression by CRISPRi method, we performed a GFP competition assay with A2058 cells by using the most efficient sgRNAs, IRF4-KD-4 and IRF4-KD-5 along with empty vector control. We observed that the percentages of GFP positive cells, in which IRF4 expression was repressed, decreased over time as shown in Figure 5.28. According to preliminary GFP competition assay results performed with CRISPRi method, IRF4 is important for the competitive fitness of A2058 cells.

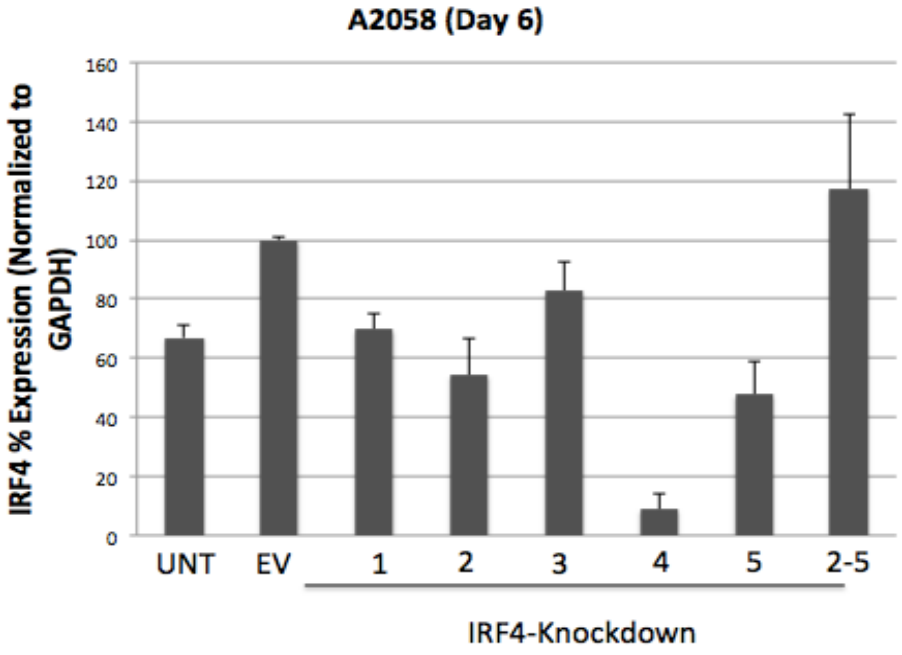

Figure 5.21. RT-q-PCR results for analysis of IRF4 expression at mRNA levels in A2058 cells after knockdown by CRISPRi method upon 6 days of doxycycline treatment.

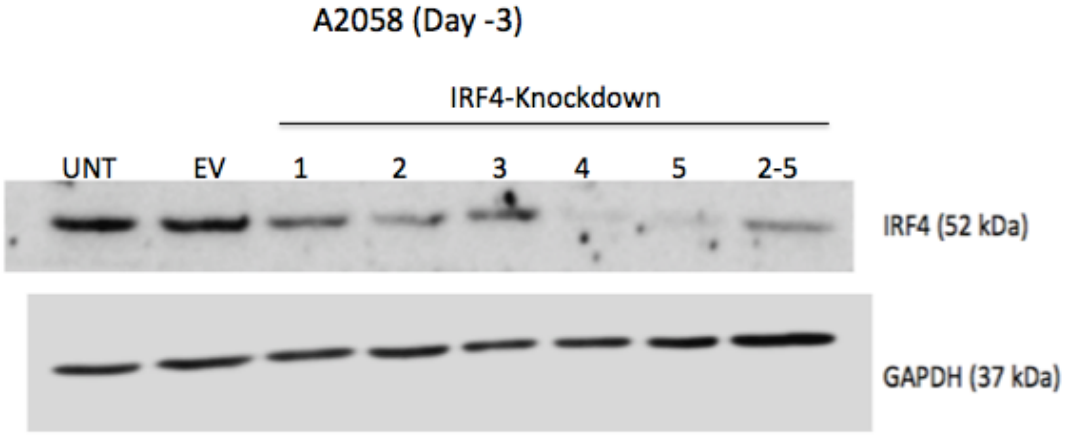

Figure 5.22. Western blotting results for analysis of IRF4 expression at protein levels in A2058 cells after knockdown by CRISPRi method upon 3 days of doxycycline treatment.

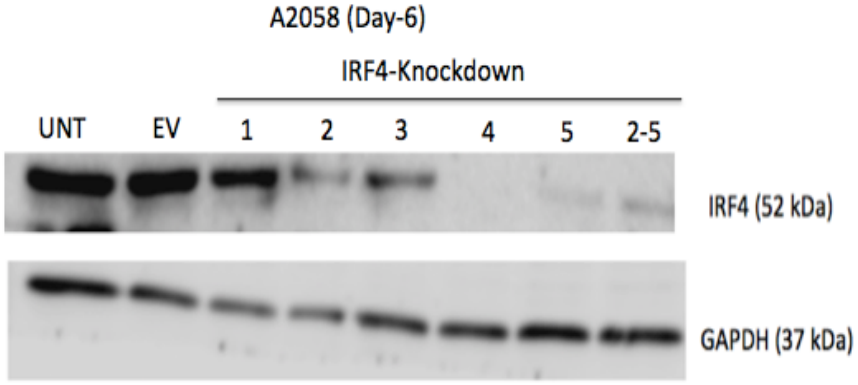

Figure 5.23. Western blot results for analysis of IRF4 expression at protein levels in A2058 cells after knockdown by CRISPRi method upon 6 days of doxycycline treatment.

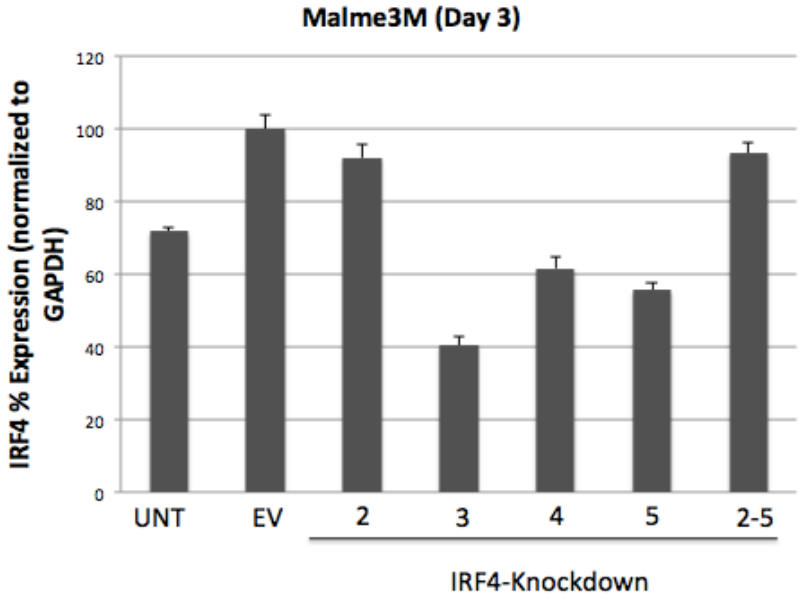

Figure 5.24. RT-q-PCR results for analysis of IRF4 expression at mRNA levels in Malme-3M cells after knockdown by CRISPRi method upon 3 days of doxycycline treatment.

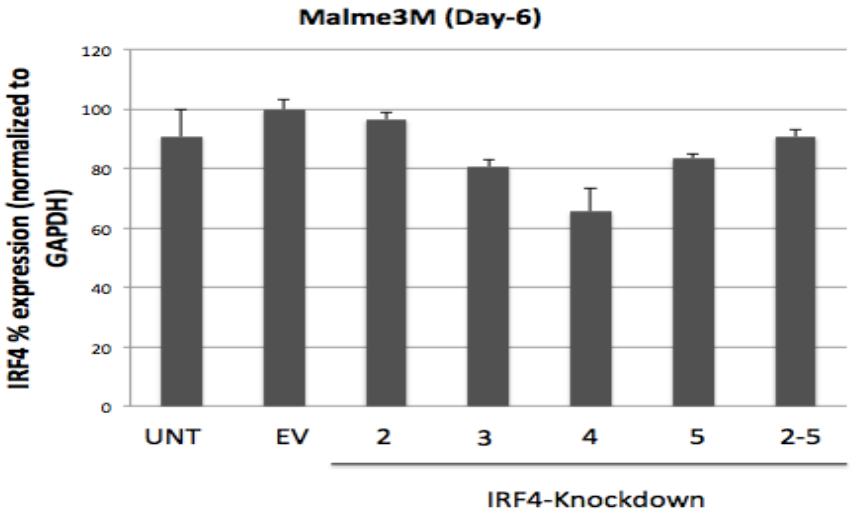

Figure 5.25. RT-q-PCR results for analysis of IRF4 expression at mRNA levels in Malme-3M cells after knockdown by CRISPRi method upon 6 days of doxycycline treatment.

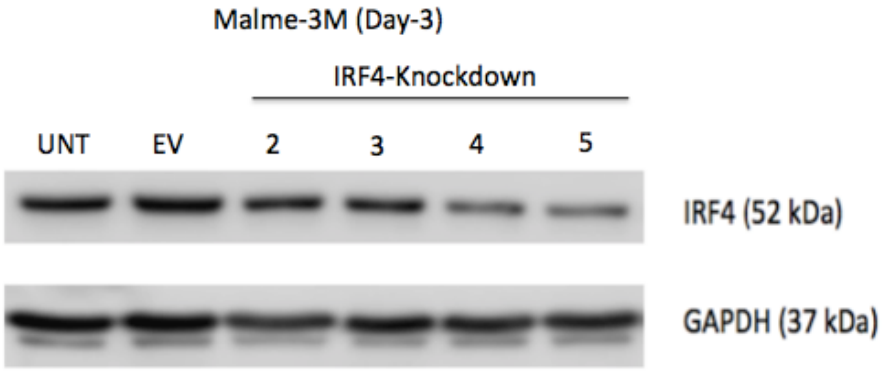

Figure 5.26. Western blot results for analysis of IRF4 expression at protein levels in Malme-3M cells after knockdown by CRISPRi method upon 3 days of doxycycline treatment.

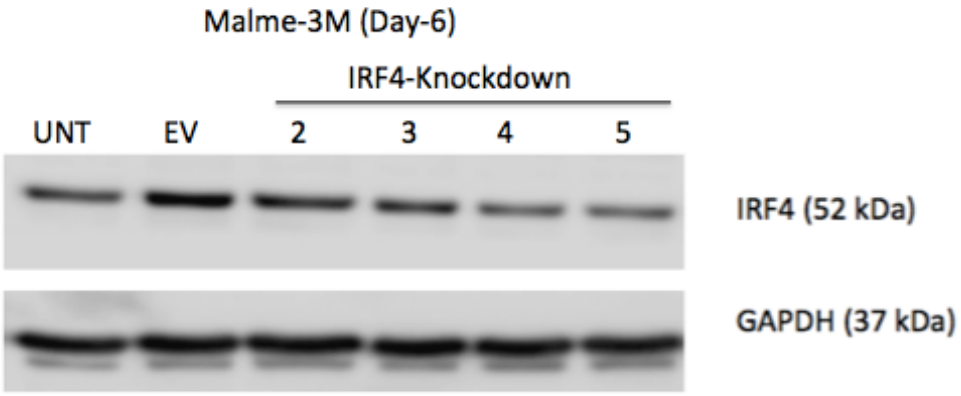

Figure 5.27. Western blot results for analysis of IRF4 expression at protein levels in Malme-3M cells after knockdown by CRISPRi method upon 6 days of doxycycline treatment.

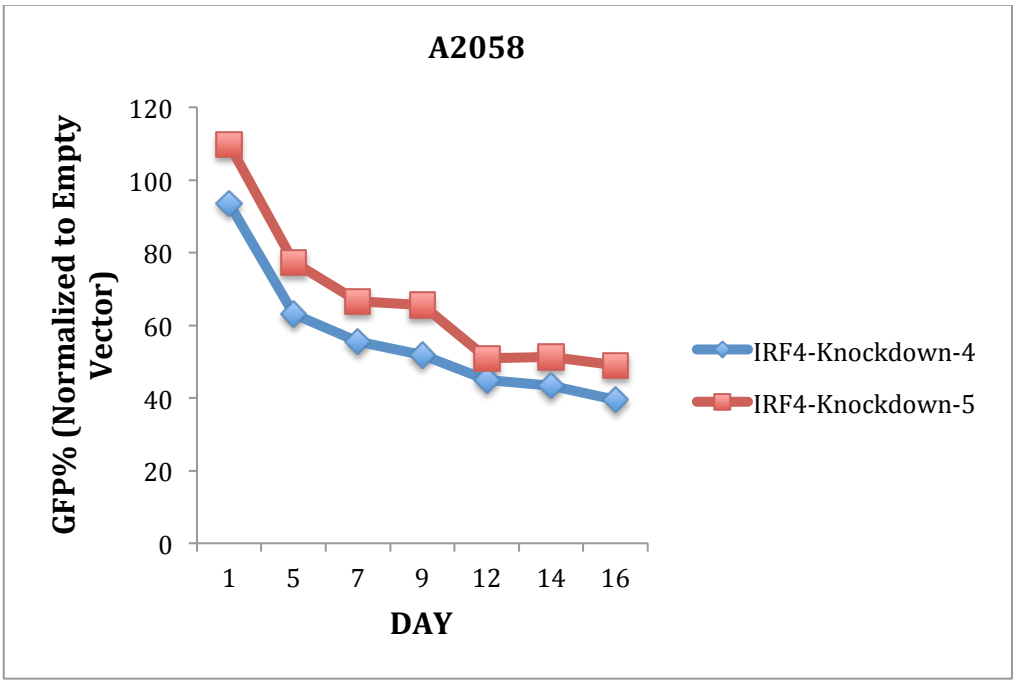

Figure 5.28. GFP competition assay results for A2058 cells performed with CRISPRi method. IRF4-Knockdown-4 and IRF4-Knockdown-5 were used to knockdown IRF4 expression along with empty vector control. GFP percentages for each day were normalized to the percentages of their empty vector controls.

5.5. IRF4 Expression Activation in IRF4-Negative Cell Lines by CRISPRa Method

In parallel with IRF4 expression repression, we tried to activate IRF4 in IRF4-expression-negative cell lines. Similar to CRISPRi method, dCas9-VP64 expressing stable and doxycycline inducible cells were transduced with different sgRNA lentiviruses, which target the promoter of IRF4 and treated with doxycycline. On different timepoints, RNA and protein lysates were collected and IRF4 expression induction was analyzed at mRNA and protein levels by using RT-q-PCR and Western blotting techniques, respectively.

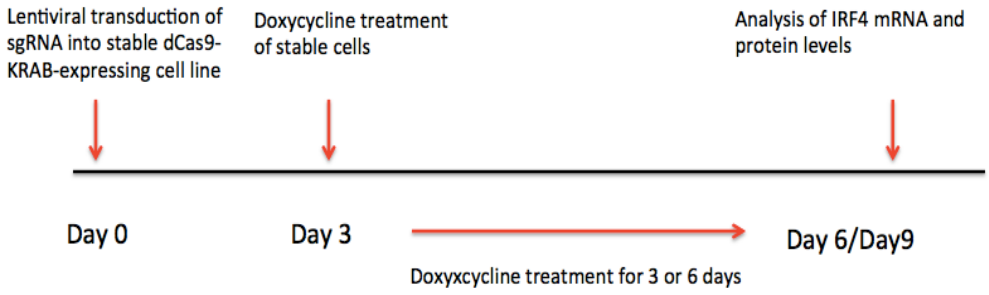

Figure 5.29. Timeline for IRF4 knockdown by CRISPRa method.

In Mewo cells, which are transduced with IRF4-a-1 and IRF4-a-4 lentiviruses simultaneously, IRF4 was activated successfully. IRF4 induction in these cells was confirmed both at mRNA and protein levels as can be seen in Figure 5.30, Figure 5.31 and Figure 5.32.

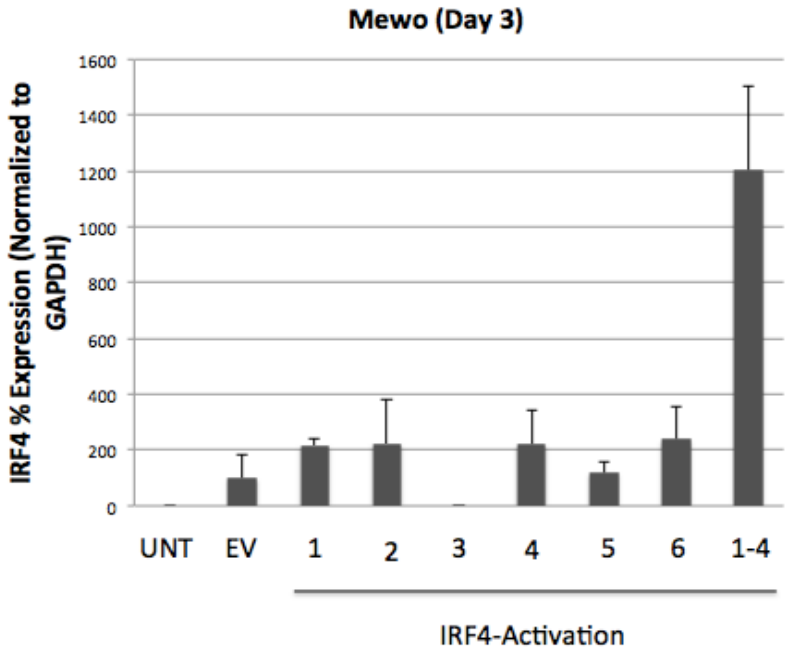

Figure 5.30. RT-q-PCR results for analysis of IRF4 expression at mRNA levels after activation by CRISPRi method upon 3 days of doxycycline treatment.

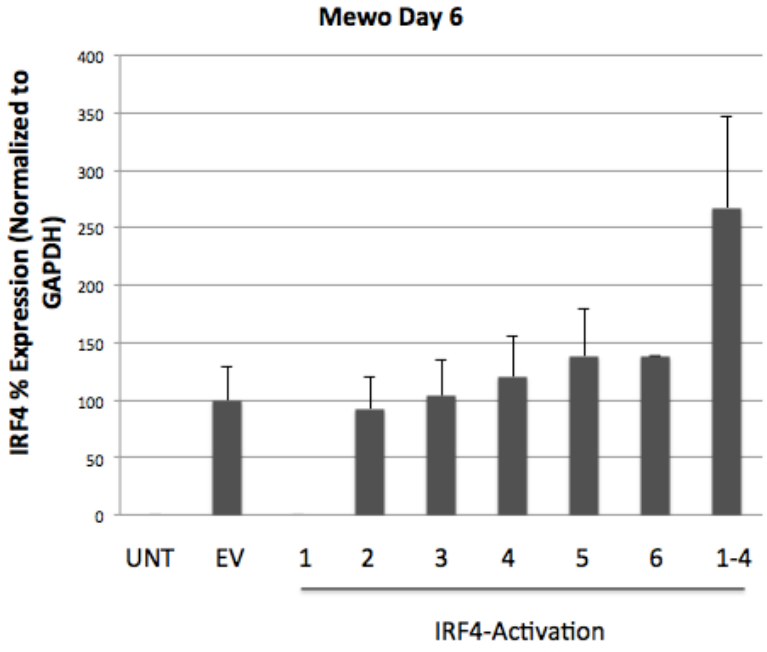

Figure 5.31. RT-q-PCR results for analysis of IRF4 expression at mRNA levels after activation by CRISPRi method upon 6 days of doxycycline treatment.

According to this experiment, combination of sgRNA 1 and 4 led to significant activation of IRF4 expression in Mewo cells and other sgRNAs do not lead to observable activation at protein levels, which is demonstrated in Figure 5.33.

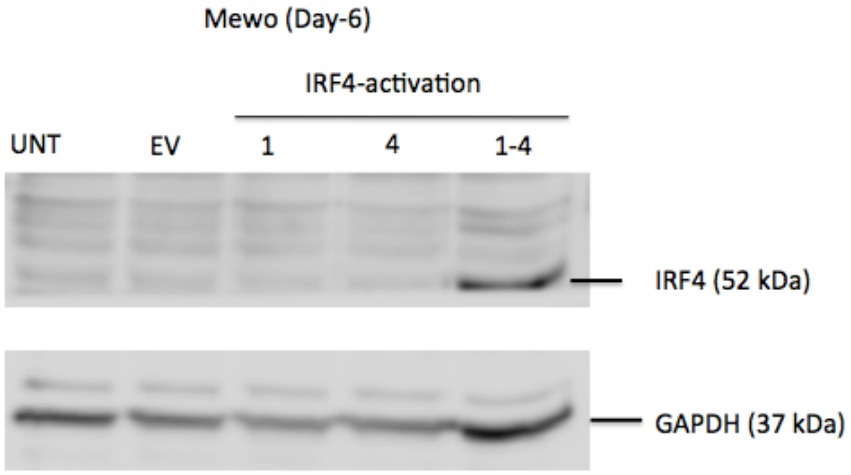

Figure 5.32. Western blot result for IRF4 activation in Mewo-dCas9-VP64 cells after 6 days of doxyxcycline treatment.

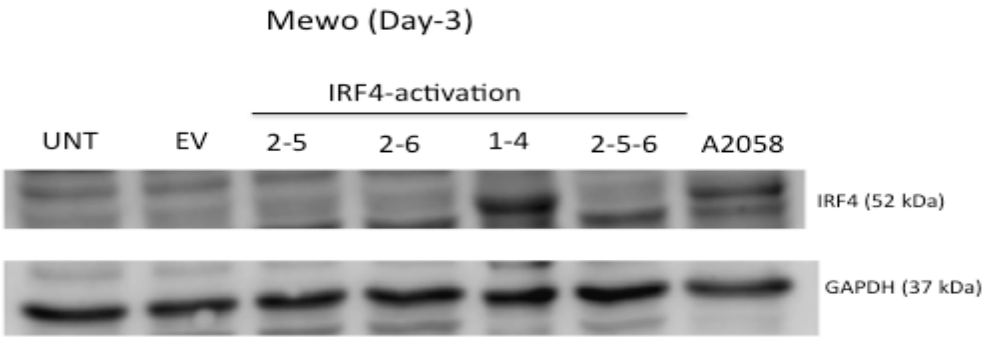

Figure 5.33. Western blot results for analysis of IRF4 expression at protein levels after activation by CRISPRi method upon 3 days of doxycycline treatment.

6. DISCUSSION

IRF4 is a transcription factor whose roles and functions have been well studied and characterized in lymphocytes in previous studies (De Silva *et al.*, 2012) Since IRF4 is very critical for lymphocyte development and function, it was not surprising that its deregulation is linked to malignant transformation in B-cell origin cancers (Shaffer *et al.*, 2009). In one major study, multiple myeloma cells were shown to have non-oncogene addiction to IRF4 expression, and even 50% knockdown of IRF4 expression was sufficient to kill these cells in *in-vitro* assays. In addition, Activated B-cell like Diffuse Large B Cell Lymphoma (ABC-DLBCL) cells were also shown to have non-oncogene addiction to IRF4 expression (Yang *et al.*, 2012). Previously, by using publicly available databases our group observed that IRF4 is highly expressed in melanoma cells compared to other solid tumors although its expression is not as high as in lymphomas. Expressions of IRF4 at mRNA and protein levels in several melanoma cell lines were also validated in our lab (Ayhan, unpublished). The presence of a SNP in IRF4 locus that predisposes individuals to melanoma (Nan *et al.*, 2009; Han *et al.*, 2009), and the finding that shows its role in human pigmentation were also encouraging to perform further studies to characterize the role of IRF4 in melanoma *(*Praetorius *et al.*, 2013).

One of the most powerful ways to study the role of a transcription factor in cell lines is to manipulate its expression. In our group, we previously used shRNA based knockdown and other overexpression technologies to manipulate IRF4 expression in melanoma cells. However, as commonly observed with RNAi-based gene silencing, we have not achieved a complete knockdown. Later, we decided to use alternative ways to manipulate IRF4 expression, so that we could achieve more consistent results with larger effect sizes. One alternative way to siRNA and shRNA techniques are CRISPR based technologies, which have become very popular in recent years. CRISPR/Cas system, which is originally characterized as a nucleic acid based adaptive immunity system in bacteria, has been turned into a powerful genome editing tool which has relatively easier design and application compared to other former genome engineering methods such as ZFNs and TALENs technologies (Kim *et al.*, 2014). Other than being a powerful genome

editing tool, CRISPR/Cas system was also shown to be a powerful and efficient gene expression manipulation tool by conversion of Cas9 endonuclease into catalytically inactive form of Cas9 protein (dCas9) and coupling it to either transcription repressor or activator domains (Sander *et al.*, 2014). Therefore, we thought that implementation of these relatively new technologies to study the role of IRF4 in melanoma cells would be very beneficial since we would be able to manipulate its expression in a more efficient manner and it could be complementary to our shRNA and overexpression systems that have been used in our experiments so far. Another advantage of having this technology in our lab is that it can be applied to the studies of other factors, not restricted to only IRF4, due to the fact that it is easily customizable by the design of sgRNAs that target different target sites. Therefore, we firstly aimed to set up CRISPR based knockout, CRISPR-mediated knockdown and activation technologies in our lab, and use them to manipulate IRF4 expression in melanoma cells.

In order to implement CRISPR based technologies, we decided to use a lentiviral system. Since melanoma cells are relatively difficult to transfect, we thought that we could overcome this problem by using lentiviruses. Another reason for the use of such a system was that phenotypic assays, which would be later used to study IRF4's role in melanoma cells, are long-lasting experiments and stable knockdown or activation of IRF4 are needed in these assays. Hence, we could stably manipulate the expression of IRF4 by using such a lentiviral system in which lentiviruses are able to integrate into the genomes of the cells. Another criterion for our set up was to include a fluorescent marker since we could quantitatively measure transduction efficiencies by using flow cytometer and we could have the chance to trace transduced cells and benefit from the presence of such a marker in phenotypic assays like GFP competition assays. By taking all these criteria into account, we decided to generate melanoma cell lines which express Cas9 endonuclease for knockout, dCas9-KRAB for CRISPRi mediated repression and dCas9-VP64 for CRISPRa mediated activation in a doxycycline inducible manner. Additionally, we decided to use a separate lentiviral vector for sgRNA expression, which has a GFP marker that would allow us to analyze transduction efficiencies and trace cells in our experiments.

For the generation of Cas9, dCas9-KRAB and dCas9-VP64 expressing inducible stable cell lines, we used lentiviral vectors as shown in Appendix A (Kearns *et al.*, 2014). After lentivirus production of these vectors and transduction of corresponding melanoma cell lines with these viruses, we performed antibiotic selection including untransduced cells as controls. Inducible expression of Cas9, dCas9-KRAB and dCas9-VP64 cells were validated by Western blotting. One advantage of having these stable cell lines is that one can be sure that each cell is expressing the corresponding protein since they are selected with antibiotic for days. Additionally, these stable cell lines can be stored for long term and used for other studies in which other factors different than IRF4 can be studied by just introducing sgRNAs targeting them.

In order to express sgRNAs in the generated doxycycline inducible and stable melanoma cell lines, we used the PLKO.5.sgRNA.EFS.GFP vector as can be seen in Appendix A.4 (Heckl *et al.*, 2015). In this lentiviral vector, sgRNAs are under the expression of humanized U6 promoter so that it provides constitutive expression of sgRNAs in cells. Also, the presence of the GFP marker is well suited for our experiments to trace the cells and to know what percentage of cells are expected to express sgRNAs. We transduced our stable cell lines with the lentiviruses produced from this vector and measured the transduction efficiencies by flow cytometry. We observed that we achieved an efficiency which is around 99%. Having such high transduction efficiency is beneficial for us since we can say that each cell is expected to express the sgRNAs and we can also manipulate introduction of sgRNAs to the cells. For instance, more than one sgRNA can be given to the cells by mixing different lentiviruses and cells can be transduced with them successfully since the transduction efficiencies are high.

One of the most critical steps in implementation of CRISPR/Cas technologies is the proper design of sgRNAs and their target sites. For the design of sgRNAs, we used online sgRNA design tools such as Optmized CRISPR Design Tool (Zhang *et al.*, 2014). These tools mostly rank the candidate sgRNAs with respect to their uniqueness in the genome and their possible off-target sites which may result in undesired outcomes in our experiments (Xiao *et al.*, 2014). Therefore, we chose to use sgRNAs that have the highest scores and less possible off-target sites in our experiments (Li *et al.*, 2014). In previous

ChIP-seq studies it was shown that dCas9 protein has a large number of off-target sites in the genome. However, genome editing by Cas9 is relatively specific (Kuscu *et al.*, 2014). Hence, in studies where dCas9-KRAB/VP64 mediated gene expression manipulation methods are used, it is suggested to be better to perform experiments with multiple sgRNAs. If we are capable of obtaining similar results with these multiple sgRNAs to the same target gene, the possibility of off-target activities will be deemed lower. Another critical point in CRISPR based technologies is to choose target sites properly. In previous studies, optimal target sites for gene knockout were shown to be the first and second constitutive exons of the genes (Cho *et al.*, 2014). However, the design of target sites for CRISPRi and CRISPRa methods have not been well established. According to a recent genetic screen study, the most efficient target sites for CRISPRi method are located between -50 bp and +150 bp relative to the transcription start site. For CRISPRa method, this range is approximately between -50 and -400 bp with respect to transcription start sites of the genes (Gilbert *et al.*, 2014). Therefore, we picked our target sites based on this study and designed multiple sgRNAs spanning these regions for CRISPRi and CRISPRa mediated manipulation of IRF4 expression in melanoma cells.

After validating the generation of stable cell lines and optimization of sgRNA transduction successfully, we started to test the success and efficiencies of our CRISPR-based systems. Firstly, we tested our knockout system in melanoma cells. For this purpose, doxyxcycline inducible stable SKMEL-28 cells were transduced with three different sgRNA lentiviruses along with an empty control vector in which no sgRNA is expressed, treated with doxycycline for 12 days and IRF4 protein levels were analyzed. We observed that IRF4 was very efficiently eliminated in these cells compared to our control, as judged by immunoblotting. This observation can be attributed to our set up, in which we ensured that each cell expresses Cas9 endonuclease since they are selected with antibiotics and sgRNAs due to high transduction efficiency of sgRNA vector. We also tried IRF4 knockout in other melanoma cell line, A2058 cells, and in these cells we also checked earlier time points of doxycycline treatment. We observed that decrease in IRF4 protein levels is observed after 3 days of doxycycline treatment and IRF4 is mostly eliminated after 7 days. Hence, it can be said that we can achieve highly efficient and rapid knockout, which will be very beneficial in our further experiments in terms of time. Another important point is that all three sgRNAs that are used for IRF4 knockout resulted in high

knockout efficiencies. These sgRNAs were designed to target first and second constitutive exons of IRF4. Their high efficiencies are consistent with literature where targeting first and second constitutive exons are shown to be optimal for CRISPR based knockout (Wang *et al.*, 2014). In addition to Western blot analysis of knockout efficiencies, generation of insertion or deletion mutations (indel) at target sites should be validated by additional methods. We performed Sanger sequencing based analysis of pooled IRF4-knockout cells and observed that starting from the target sites many insertions, deletions and mismatches were observed compared to wild type cells and empty vector control (See Appendix F). However, surveyor nuclease assay is one of the most widely used methods for this purpose (Li *et al.*, 2014). Therefore, as a future work we suggest that this kind of assay should be performed to validate IRF4 knockout in melanoma cells.

For IRF4 knockdown in melanoma cells by CRISPRi method, five different sgRNAs that target regions close to transcription start site were used. Similar to IRF4 knockout, stable cell lines were transduced with these sgRNA constructs, and treated with doxycycline, and then IRF4 knockdown at mRNA and protein levels were analyzed. In A2058 melanoma cell line, with sgRNA-4 and sgRNA-5, which target +30 and + 50 bp downstream of transcription start site, we achieved a dramatic repression of IRF4 expression at both mRNA and protein levels. For other sgRNAs, we did not observe consistent and efficient IRF4 knockdown. This variations between different target sites are expected since it was previously reported that all sgRNAs do not show an effective knockdown, and the efficiency of this method is very much dependent on the target site and the factors like local chromatin structure and the base composition of target site (Wu *et al.*, 2014). Therefore, we suggest that design and application of multiple sgRNAs are useful for CRISPRi studies because it increases the chances of achieving high knockdown efficiencies. It is also important that IRF4 knockdown is observable at different time points meaning that it is stable over time which is needed for reliable results for further assays. IRF4 knockdown in melanoma cells via CRISPRi method was also validated in additional cell lines. For instance, we knocked down IRF4 in Malme3M cells and analyzed knockdown levels. According to our results, sgRNA-4 and sgRNA-5, which achieved the most dramatic knockdown in A2058 cells, resulted in an efficient knockdown in these cells compared to other sgRNAs. However, knockdown levels were not as dramatic as in A2058 cells. Actually, these results were consistent with our previous observations with shRNA,

in which we mostly achieved higher knockdown levels in A2058 cells compared to other melanoma cell lines. One explanation for this observation is that A2058 cells normally have lower IRF4 expression than Malme-3M cells and knockdown levels in melanoma cells are inversely correlated with IRF4 expression levels. Although in Malme3M cells we did not achieve knockdown levels as dramatic as in A2058 cells, IRF4 knockdown levels in these cells are still significant and comparable to shRNA-based knockdown efficiencies. One advantage of the CRISPRi method that we set up is its inducibility. By using such a doxyxcycline inducible system, we have the chance to perform reversible knockdown since dCas9-KRAB protein should be no more expressed upon doxyxcyline withdrawal, and after degradation of dCas9-KRAB protein that is already present in the cells, IRF4 levels are expected to climb back to normal levels. However, in immunoblotting experiments, we observed dCas9-KRAB band for A2058 cells that were untreated with doxycycline. Although this leakage problem does not interfere with IRF4 knockdown, it probably will affect the rescue experiments in which doxycycline withdrawal is expected to reverse IRF4 knockdown. Therefore, we suggest that reversibility of knockdown should be studied in more detailed way, and timepoint analysis of dCas9-KRAB and IRF4 protein levels should be analyzed. Having this kind of knowledge would be very useful for further phenotypic assays, e.g rescue experiments can be performed by removal of doxycycline from cell media.

Similar to CRISPR based IRF4 knockout and knockdown approach; we tried to activate IRF4 expression in melanoma cells by designing six different sgRNAs. The target sites are mostly in the promoter of IRF4 upstream of transcription start site. As our model, we tried to activate IRF4 expression in Mewo cells, in which we know that there is no observable IRF4 expression at mRNA and protein levels. Similar to CRISPRi method, we transduced dCas9-VP64 expressing Mewo cells with sgRNAs, treated them with doxyxcycline and analyzed IRF4 levels. We observed that IRF4 expression is not significantly induced upon introduction of a single sgRNA. However, we observed that co-expressing sgRNA-1 and sgRNA-4 led to a significant IRF4 expression in these cells, which are observable at mRNA and protein levels. We replicated these results and we observed that the only sgRNA combination, which resulted in significant IRF4 activation, is the combination of sgRNA-1 and sgRNA-4, which target -70 and -200 bp upstream relative to transcription start site. This result was consistent with previous observations that

CRISPRa method in which dCas9-VP64 protein was used was not capable of achieving high induction levels with single sgRNA expression (Cheng *et al.*, 2013). Due to this inefficiency problem, other novel CRISPR based activation methods like Suntag system, which includes VP64 epitope tagged dCas9 protein, and SAM activator systems which harbor multiple transcription activator domains coupled to dCas9, were generated (Aach *et al.*, 2014). CRISPR based activation should not be restricted to Mewo cells and other IRF4 expression-negative cell lines including non-melanoma cells should also be tested for the induction of its expression. For instance, IRF4 activation in immortalized melanocytes would be a powerful complementary tool to study the role of IRF4 in melanoma cells. Therefore, activation of endogenous IRF4 expression in IRF4-negative cells will be a valuable tool that can be later used in phenotypic assays.

After we validated the success of our CRISPR based knockout, knockdown and activation tools, we switched to the phenotypic assay part to characterize the role of IRF4 in melanoma cells. For this purpose, we decided to perform GFP competition assays since this assay is expected to give us an idea on whether IRF4 expression is critical for the competitive fitness and/or survival of melanoma cells. In this assay, we have a cell population, which is a mixture of GFP-marked sgRNA-expressing cells and untransduced cells that do not have sgRNA expression. After doxyxcycline treatment of this cell population, we followed the changes of GFP percentages by flow cytometer (See Appendix H). According to our results, when IRF4 is knocked out or knockdown in melanoma cells, GFP positive sgRNA expressing cells are somehow eliminated from the population while we did not observe such an effect in Mewo cells which are IRF4-expression-negative cells, suggesting that IRF4 expression is critical for the competitive fitness of melanoma cells. In previous studies, multiple myeloma and ABC-DLBCL cells were shown to have a similar effect where shRNA mediated knockdown resulted in decreases in GFP percentages in GFP competition assays. In these studies, it was proposed that multiple myeloma and ABC-DLBCL cells had non-oncogene addiction to IRF4 expression since these cells are “addicted” to IRF4 expression although these cells mostly do not have genetic aberrations in IRF4, but merely overexpress IRF4 (Shaffer *et al.*, 2008). According to our preliminary results, melanoma cells also have non-oncogene addiction to IRF4 expression similar to these lymphoma types. However, we need to replicate these experiments by using additional cell lines. Importantly, these results are

consistent with previous GFP competition assay results from our group performed by using shRNA-based knockdown of IRF4. In addition, in GFP competition assays performed by CRISPR-based knockout and knockdown methods, we observed a larger effect on decreases in GFP percentages, probably due to higher knockdown levels compared to shRNA. A future work for GFP competition assays should be a rescue experiment in which doxycycline removal reverses IRF4 knockdown. If IRF4 is critical for the competitive fitness of these cells, GFP percentages should come back to starting levels upon doxycycline treatment. However, this assay needs further optimization of reversible IRF4 knockdown by CRISPRi method and would be beneficial to study IRF4's role in melanoma cells.

In order to fully characterize IRF4's role in melanoma cell lines, we need to perform additional assays. Although we demonstrated that IRF4 is critical for the competitive fitness of these cells, the reason behind the decreases in GFP competition assays need to be answered in a more detailed manner. There may be multiple reasons that lead to this observation. One of the possible mechanisms of this observation is that IRF4 knockout or knockdown may affect cell cycle progression of melanoma cells and may lead to cell cycle arrest. Another explanation may be that IRF4 can affect proliferation and growth rates of the cells. Additionally, another possible reason can be that IRF4 knockout or knockdown may lead to cell senescence (Hanahan *et al.*, 2000). Therefore, we suggest that cell cycle progression, proliferation, viability and senescence assays should be performed as future work.

For the characterization of IRF4's role in melanoma cells, other hallmarks of cancer should also be investigated (Hanahan *et al.*, 2011). For instance, assays to analyze migration and invasion capabilities of melanoma cells in which IRF4 expression is manipulated by CRISPR based technologies can be performed as future work, and the results of these different experiments will be complementary to identify the role of IRF4 in melanoma. Results obtained from *in vitro* phenotypic assays can be also investigated *in vivo* experiments in the future.

REFERENCES

Aach, J., Stranges, P. B., Esvelt, K. M., Kosuri, S., Yang, L., & Church, G. M. (2014). NIH Public Access, *31*(9), 1–15. http://doi.org/10.1038/nbt.2675.CAS9, accessed at September 2016.

Beaumont, K. A., Mohana-kumaran, N., & Haass, N. K. (2014). Modeling Melanoma In Vitro and In Vivo, 27–46. http://doi.org/10.3390/healthcare2010027, accessed at September 2016.

Bikard, D., & Marraffini, L. A. (2013). Control of gene expression by CRISPR-Cas systems. *F1000Prime Reports*, *5*(November), 1–8. http://doi.org/10.12703/P5-47, accessed at September 2016.

Cheng, A. W., Wang, H., Yang, H., Shi, L., Katz, Y., Theunissen, T. W., … Jaenisch, R. (2013). Multiplexed activation of endogenous genes by CRISPR-on , an RNA-guided transcriptional activator system. *Nature Publishing Group*, *23*(10), 1163–1171. http://doi.org/10.1038/cr.2013.122, accessed at September 2016.

Cheon, D., & Orsulic, S. (2011). Mouse Models of Cancer. http://doi.org/10.1146/annurev.pathol.3.121806.154244, accessed at September 2016.

Cho, S. W., Kim, S., Kim, Y., Kweon, J., Kim, H. S., Bae, S., & Kim, J. S. (2014). Analysis of off-target effects of CRISPR/Cas-derived RNA-guided endonucleases and nickases. *Genome Research*, *24*(1), 132–141. http://doi.org/10.1101/gr.162339.113, accessed at September 2016.

De Silva, N. S., Simonetti, G., Heise, N., & Klein, U. (2012). The diverse roles of IRF4 in late germinal center B-cell differentiation. *Immunological Reviews*, *247*(1), 73–92.

http://doi.org/10.1111/j.1600-065X.2012.01113.x, accessed at September 2016.

Duffy, D. L., Iles, M. M., Glass, D., Zhu, G., Barrett, J. H., Höiom, V., … Montgomery, G. W. (2010). IRF4 variants have age-specific effects on nevus count and predispose to melanoma. *American Journal of Human Genetics*, *87*(1), 6–16. http://doi.org/10.1016/j.ajhg.2010.05.017, accessed at September 2016.

Gaj, T., Gersbach, C. A., & Iii, C. F. B. (2013). ZFN , TALEN , and CRISPR / Cas-based methods for genome engineering. *Trends in Biotechnology*, *31*(7), 397–405. http://doi.org/10.1016/j.tibtech.2013.04.004, accessed at September 2016.

Gilbert, L. A., Horlbeck, M. A., Adamson, B., Villalta, J. E., Chen, Y., Whitehead, E. H., … Weissman, J. S. (2014). Genome-Scale CRISPR-Mediated Control of Gene Repression and Activation. *Cell*, *159*(3), 647–661. http://doi.org/10.1016/j.cell.2014.09.029, accessed at September 2016.

Gilbert, L. A., Larson, M. H., Morsut, L., Liu, Z., Brar, G. A., Torres, S. E., … Qi, L. S. (2012). Resource CRISPR-Mediated Modular RNA-Guided Regulation of Transcription in Eukaryotes. *Cell*, *154*(2), 442–451. http://doi.org/10.1016/j.cell.2013.06.044, accessed at September 2016.

Hanahan, D., & Weinberg, R. A. (2011). Review Hallmarks of Cancer : The Next Generation. *Cell*, *144*(5), 646–674. http://doi.org/10.1016/j.cell.2011.02.013, accessed at September 2016.

Hanahan, D., Weinberg, R. A., & Francisco, S. (2000). The Hallmarks of Cancer Review University of California at San Francisco, *100*, 57–70.

Haurwitz, R. E., Jinek, M., Wiedenheft, B., & Zhou, K. (2010). Sequence- and structure-specific RNA processing by a CRISPR endonuclease, *329*(5997), 1355–1358.

Heckl, D., Kowalczyk, M. S., Yudovich, D., Belizaire, R., Rishi, V., Mcconkey, M. E., … Benjamin, L. (2015). Generation of mouse models of myeloid malignancy with combinatorial genetic lesions using CRISPR-Cas9 genome editing. *Nature Biotechnology*, *32*(9), 941–946. http://doi.org/10.1038/nbt.2951.Generation, accessed at September 2016.

Hsu, P. D., Lander, E. S., & Zhang, F. (2014). Development and applications of CRISPR-Cas9 for genome engineering. *Cell*, *157*(6), 1262–1278. http://doi.org/10.1016/j.cell.2014.05.010, accessed at September 2016.

Kearns, N. a, Genga, R. M. J., Enuameh, M. S., Garber, M., Wolfe, S. a, & Maehr, R. (2014). Cas9 effector-mediated regulation of transcription and differentiation in human pluripotent stem cells. *Development*, *141*(1), 219–23. http://doi.org/10.1242/dev.103341, accessed at September 2016.

Kim, H., & Kim, J. (2014). REVIEWS A guide to genome engineering with programmable nucleases. *Nature Publishing Group*, (April). http://doi.org/10.1038/nrg3686, accessed at September 2016.

Kit, A., Kit, M., Gnaq, O. U., & Vultur, A. (2013). SnapShot : Melanoma SnapShot : SnapShot : Melanoma. *CCELL*, *23*(5), 706–706.e1. http://doi.org/10.1016/j.ccr.2013.05.001, accessed at September 2016.

Klein, U., & Dalla-favera, R. (2008). Germinal centres : role in B - cell physiology and malignancy, *8*(january), 22–33. http://doi.org/10.1038/nri2217, accessed at September 2016.

Kuscu, C., Arslan, S., Singh, R., Thorpe, J., & Adli, M. (2014). Genome-wide analysis reveals characteristics of off-target sites bound by the Cas9 endonuclease. *Nat Biotechnol*, *32*(7), 677–683. http://doi.org/10.1038/nbt.2916, accessed at September 2016.

Larson, M. H., Gilbert, L. a, Wang, X., Lim, W. a, Weissman, J. S., & Qi, L. S. (2013). CRISPR interference (CRISPRi) for sequence-specific control of gene expression. *Nature Protocols*, *8*(11), 2180–96. http://doi.org/10.1038/nprot.2013.132, accessed at September 2016.

Li, K., Wang, G., Andersen, T., Zhou, P., & Pu, W. T. (2014). Optimization of Genome Engineering Approaches with the CRISPR / Cas9 System, *9*(8). http://doi.org/10.1371/journal.pone.0105779, accessed at September 2016.

Lin, G. G., & Scott, J. G. (2012). NIH Public Access, *100*(2), 130–134. http://doi.org/10.1016/j.pestbp.2011.02.012.Investigations, accessed at September 2016.

Lin, J. Y., & Fisher, D. E. (2007). Melanocyte biology and skin pigmentation, *445*(February), 843–850. http://doi.org/10.1038/nature05660, accessed at September 2016.

Lo, J. A., & Fisher, D. E. (2014). The melanoma revolution: from UV carcinogenesis to a new era in therapeutics. *Science (New York, N.Y.)*, *346*(6212), 945–9. http://doi.org/10.1126/science.1253735, accessed at September 2016.

Mitra, D., & Fisher, D. E. (2009). Transcriptional Regulation in Melanoma, *23*, 447–465. http://doi.org/10.1016/j.hoc.2009.03.003, accessed at September 2016.

Praetorius, C., Grill, C., Stacey, S. N., Metcalf, A. M., Gorkin, D. U., Robinson, K. C., …

Steingrimsson, E. (2013). XA polymorphism in IRF4 affects human pigmentation through a tyrosinase-dependent MITF/TFAP2A pathway. *Cell*, *155*(5), 1022–1033. http://doi.org/10.1016/j.cell.2013.10.022, accessed at September 2016.

Qi, L. S., Larson, M. H., Gilbert, L. A., Doudna, J. A., Weissman, J. S., Arkin, A. P., & Lim, W. A. (2013). Resource Repurposing CRISPR as an RNA-Guided Platform for Sequence-Specific Control of Gene Expression, *8*, 1173–1183.

Ran, F. A., Hsu, P. P. D., Wright, J., Agarwala, V., Scott, D. a, & Zhang, F. (2013). Genome engineering using the CRISPR-Cas9 system. *Nature Protocols*, *8*(11), 2281–308. http://doi.org/10.1038/nprot.2013.143, accessed at September 2016.

Sander, J. D., & Joung, J. K. (2014). CRISPR-Cas systems for editing, regulating and targeting genomes. *Nature Biotechnology*, *32*(4), 347–55. http://doi.org/10.1038/nbt.2842, accessed at September 2016.

Shaffer, A. L., Emre, N. C. T., Lamy, L., Ngo, V. N., Wright, G., Xiao, W., … Staudt, L. M. (2008). IRF4 addiction in multiple myeloma, *454*(July). http://doi.org/10.1038/nature07064, accessed at September 2016.

Shaffer, A. L., Emre, N. C. T., Romesser, P. B., & Staudt, L. M. (2009). IRF4 : Immunity.Malignancy ! Therapy ?, *15*(9), 2954–2961. http://doi.org/10.1158/1078-0432.CCR-08-1845, accessed at September 2016.

Shain, A. H., & Bastian, B. C. (2016). From melanocytes to melanomas. *Nat Rev Cancer*, *16*(6), 345–358. http://doi.org/10.1038/nrc.2016.37, accessed at September 2016.

Sorek, R., Lawrence, C. M., & Wiedenheft, B. (2013). CRISPR-mediated adaptive immune systems in bacteria and archaea. *Annu Rev Biochem*, *82*, 237–266. http://doi.org/10.1146/annurev-biochem-072911-172315, accessed at September

2016.

Stern, A., Keren, L., Wurtzel, O., Amitai, G., & Sorek, R. (2010). Self-targeting by CRIPR: gene regulation or autoimmunity? *Trends Genet.*, *26*, 335–340.

Tsai, S. Q., Wyvekens, N., Khayter, C., Foden, J. A., Thapar, V., Reyon, D., … Joung, J. K. (2014). Dimeric CRISPR RNA-guided FokI nucleases for highly specific genome editing. *Nature Biotechnology*, *32*(6), 569–576. http://doi.org/10.1038/nbt.2908, accessed at September 2016.

Tsao, H., Chin, L., Garraway, L. A., & Fisher, D. E. (2012). Melanoma: From mutations to medicine. *Genes and Development*, *26*(11), 1131–1155. http://doi.org/10.1101/gad.191999.112, accessed at September 2016.

Vogelstein, B., Vogelstein, B., Papadopoulos, N., Velculescu, V. E., Zhou, S., Jr, L. A. D., & Kinzler, K. W. (2013). Cancer Genome Landscapes, *1546*. http://doi.org/10.1126/science.1235122, accessed at September 2016.

Wang, T., Wei, J. J., Sabatini, D. M., & Lander, E. S. (2014). Genetic screens in human cells using the CRISPR-Cas9 system. *Science (New York, N.Y.)*, *343*(6166), 80–4. http://doi.org/10.1126/science.1246981, accessed at September 2016.

Wiedenheft, B., Sternberg, S. H., & Doudna, J. A. (2012). RNA-guided genetic silencing systems in bacteria and archaea, *46*, 44–46. http://doi.org/10.1038/nature10886, accessed at September 2016.

Wilkinson, R., & Wiedenheft, B. (2014). A CRISPR method for genome engineering. *F1000Prime Rep*, *6*(January), 3. http://doi.org/10.12703/P6-3, accessed at September 2016.

Wu, X., Scott, D. A., Kriz, A. J., Chiu, A. C., Hsu, P. D., Dadon, D. B., … Sharp, P. A. (2014). Genome-wide binding of the CRISPR endonuclease Cas9 in mammalian cells. *Nat Biotechnol*, *32*(7), 670–676. http://doi.org/10.1038/nbt.2889, accessed at September 2016.

Xiao, A., Cheng, Z., Kong, L., Zhu, Z., Lin, S., Gao, G., & Zhang, B. (2014). CasOT: a genome-wide Cas9/gRNA off-target searching tool. *Bioinformatics (Oxford, England)*, (ii), 1–3. http://doi.org/10.1093/bioinformatics/btt764, accessed at September 2016.

Yang, L., Esvelt, K. M., Aach, J., Guell, M., James, E., Norville, J. E., & Church, G. M. (2013). NIH Public Access, *339*(6121), 823–826. http://doi.org/10.1126/science.1232033, accessed at September 2016.

Yang, Y., Shaffer, A. L., Emre, N. C. T., Ceribelli, M., Zhang, M., Wright, G., … Staudt, L. M. (2012). Exploiting Synthetic Lethality for the Therapy of ABC Diffuse Large B Cell Lymphoma. *Cancer Cell*, *21*(6), 723–737. http://doi.org/10.1016/j.ccr.2012.05.024, accessed at September 2016.

APPENDIX A: VECTORS

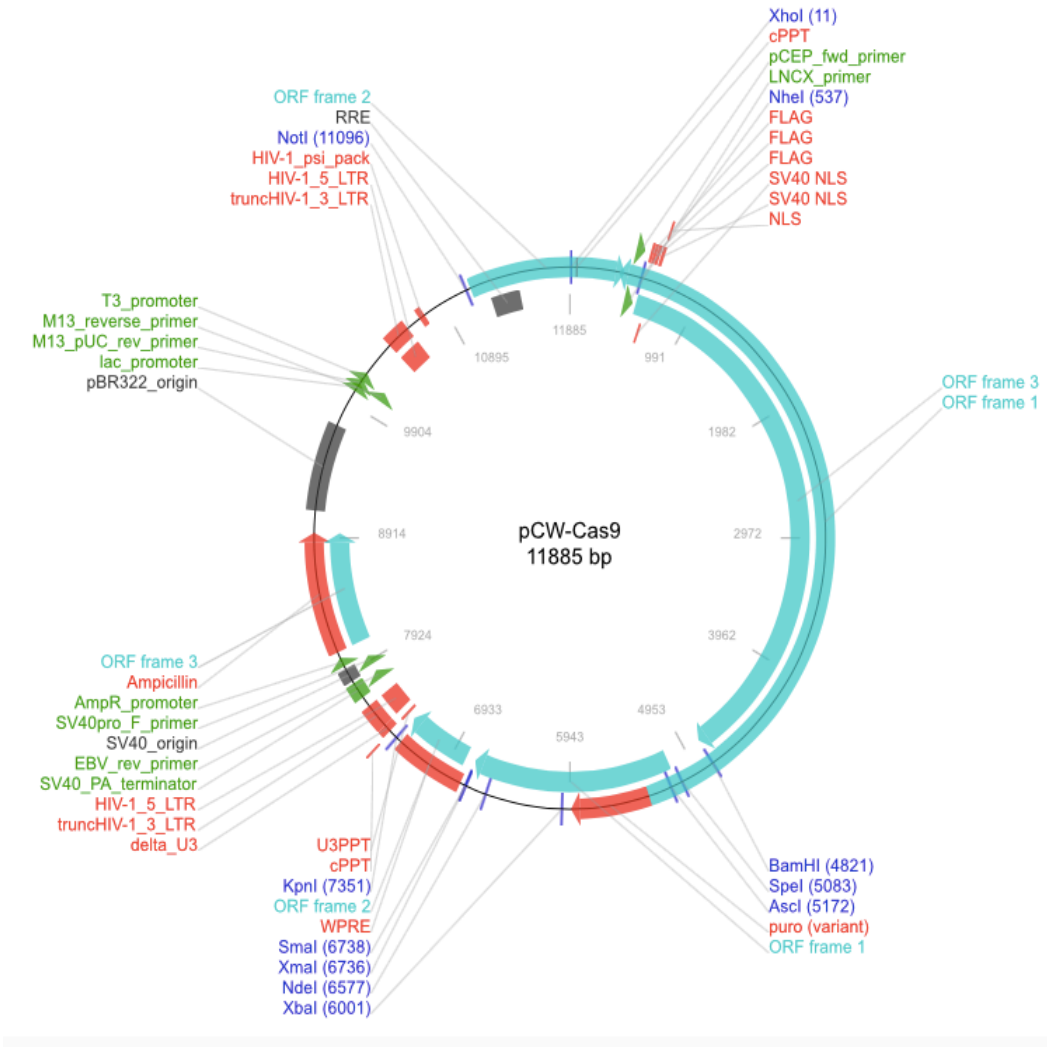

Figure A.1. Vector map of pCW-Cas9 (Addgene: 50661) plasmid that is used to generate Cas9 stable melanoma cell lines. (from Wang et al., 2014)

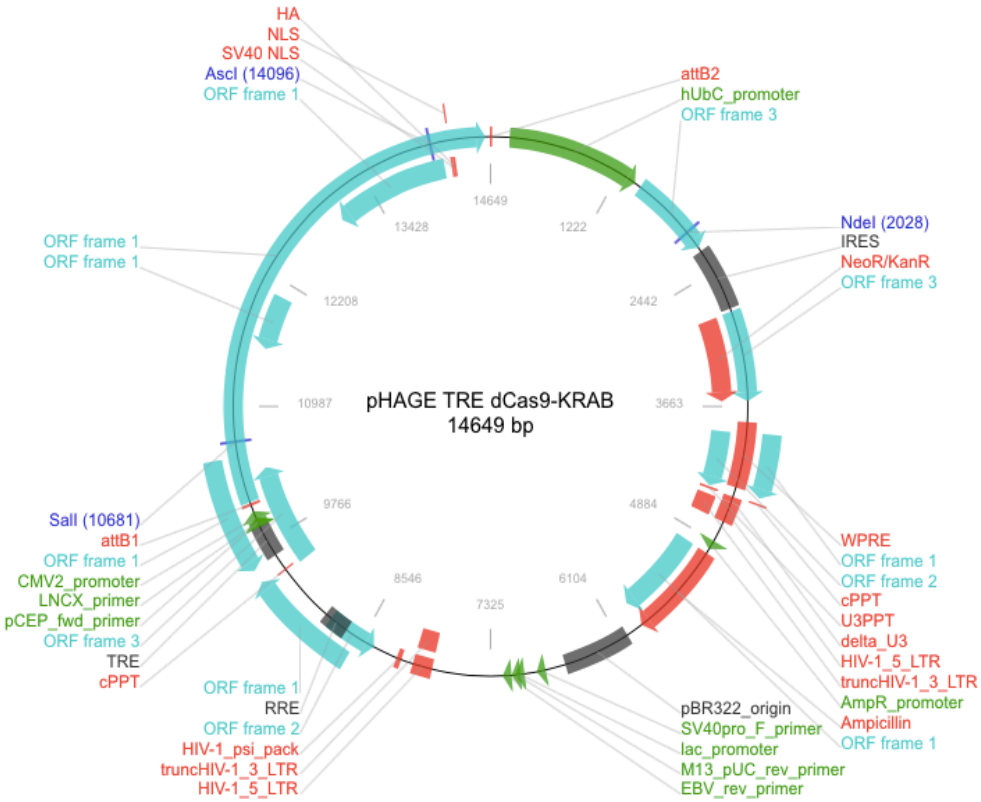

Figure A.2. Vector map of pHAGE TRE dCas9-KRAB plasmid (Addgene 50917) that is used to generate dCas9-KRAB stable melanoma cell lines (from Kearns et al., 2014)

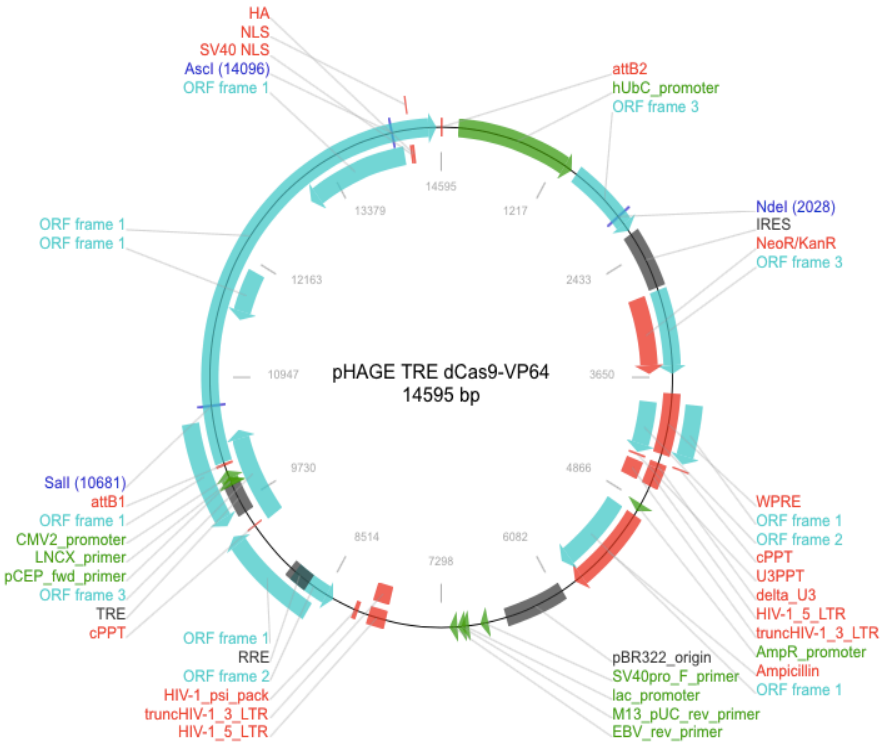

Figure A.3. Vector map of pHAGE-TRE-dCas9-VP64 plasmid (Addgene 50916) that is used to generate dCas9-VP64 stable melanoma cell lines (from Kearns et al., 2014)

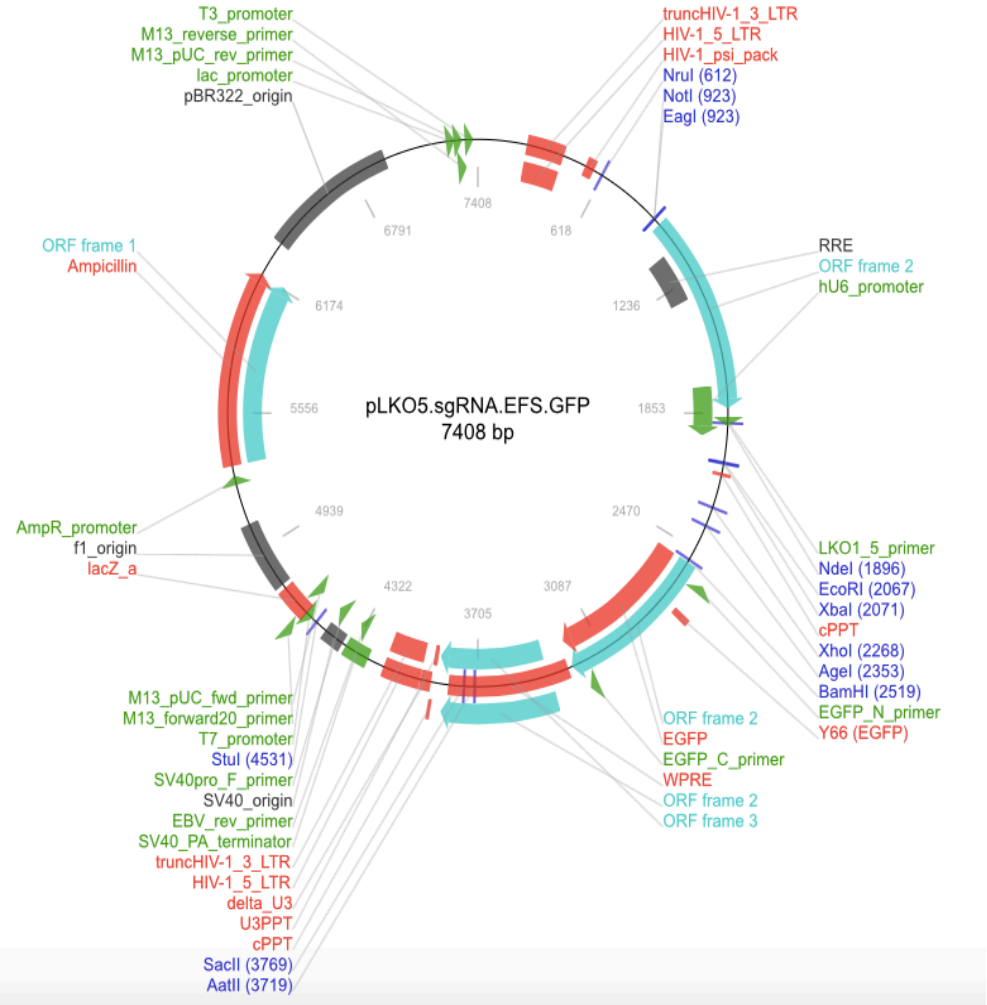

Figure A.4. Vector map of pLKO5.sgRNA.EFS.GFP plasmid (Addgene 57822) that is used to express sgRNAs in stable melanoma cell lines (from Heckl et al., 2015)

APPENDIX B: SANGER SEQUENCING RESULTS

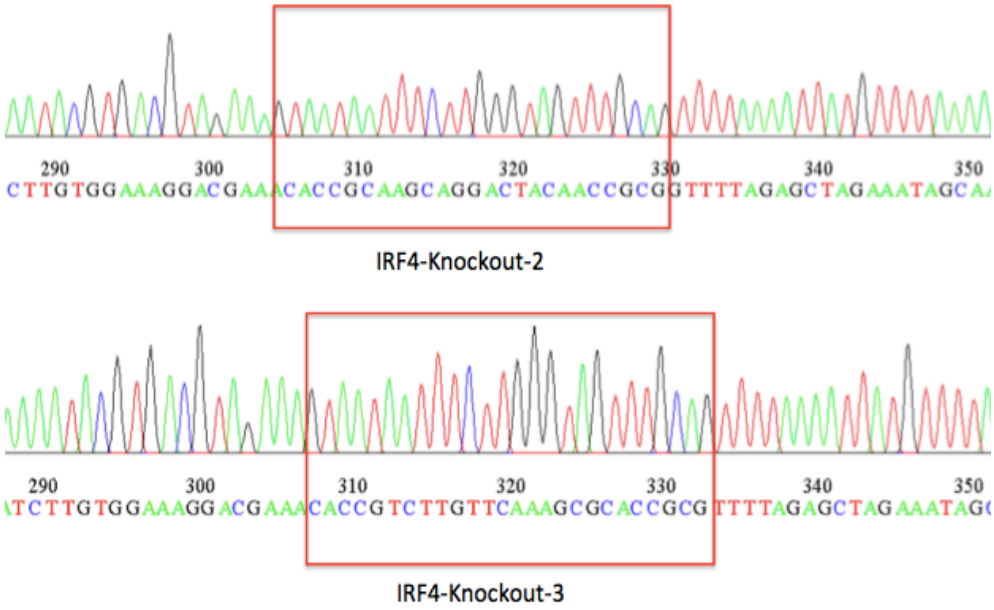

Figure B.1. Sanger sequencing result of IRF4-Knockout-2 and IRF4-KO-3 sgRNA constructs.

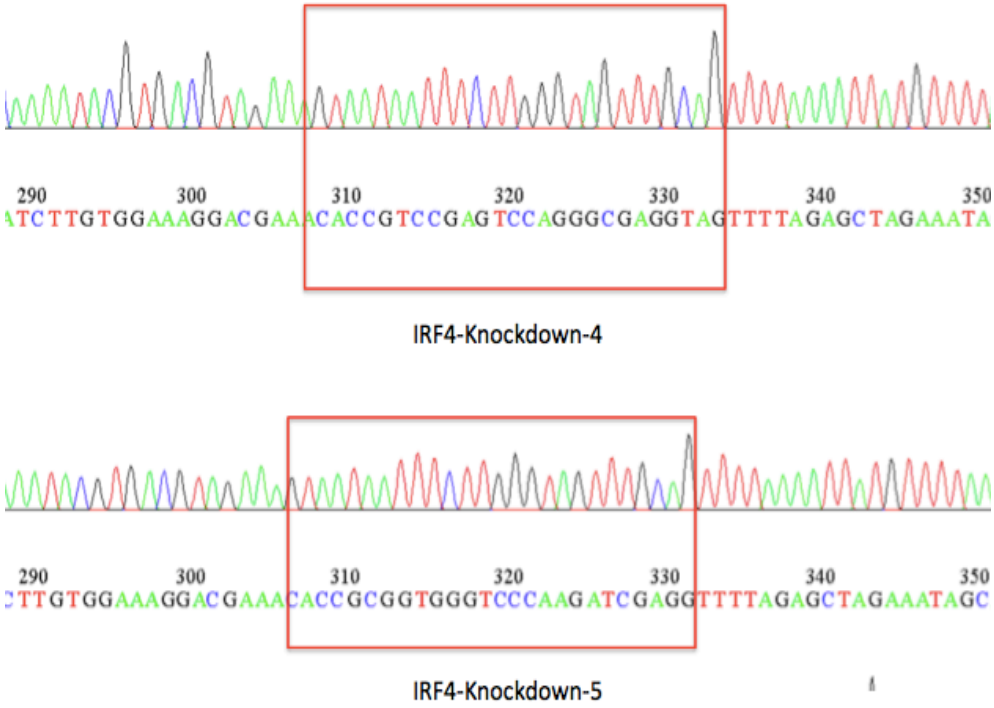

Figure B.2. Sanger sequencing result of IRF4-Knockdown-4 and IRF4-Knockdown-5 sgRNA constructs.

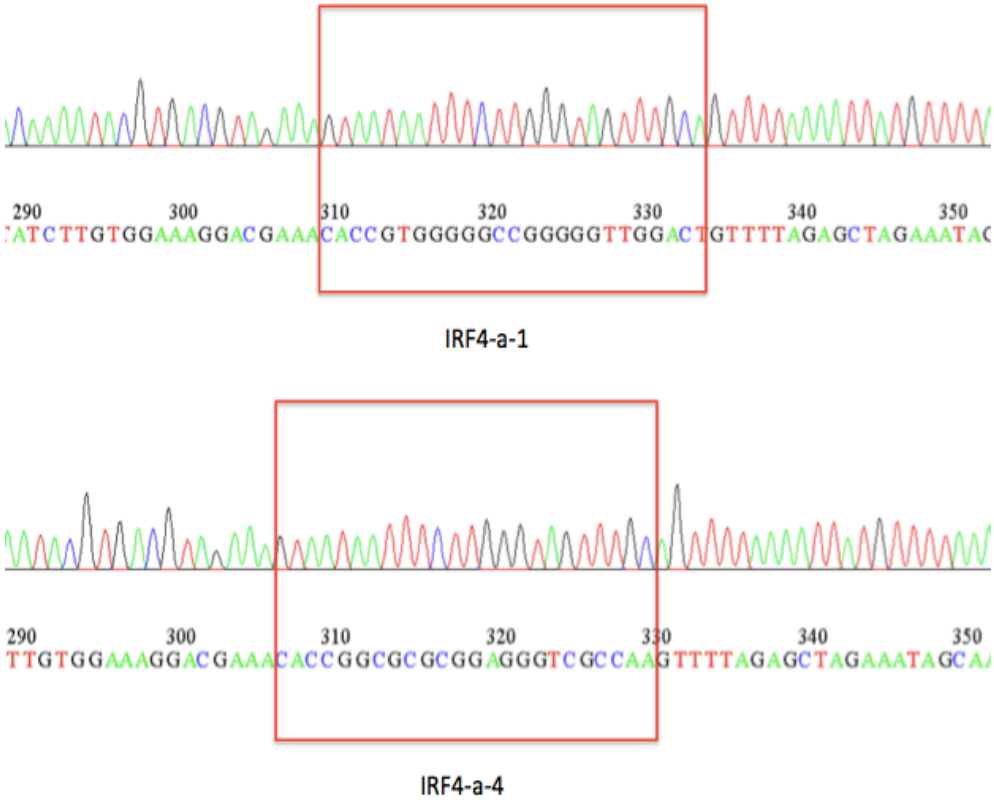

Figure B.3. Sanger sequencing result for IRF4-a-1 and IRF4-a-4 sgRNA constructs.

APPENDIX C: TARGET SITES

Table A.1 Target sites that are used in this study.

sgRNA Construct	Target Site	Score	Target Site Sequence (5'-3')
IRF4-Knockout-1	Exon-1	95%	GGTACTTGCCGCTGTCGATC
IRF4-Knockout-2	Exon-1	90%	CAAGCAGGACTACAACCGCG
IRF4-Knockout-3	Exon-2	89%	TCTTGTTCAAAGCGCACCGC
IRF4-Knockdown-1	TSS	67%	AGGAACTTTATAGAACTCTC
IRF4-Knockdown-2	TSS	94%	CAGTTTCACCGCTCGATCTT
IRF4-Knockdown-3	+150 bp	93%	GAACCTCTGGTTCGCGCTCC
IRF4-KD-4	+50 bp	88%	TCCGAGTCCAGGGCGAGGTA

Table A.1 Target sites that are used in this study (cont.)

IRF4-Knockdown-5	+30 bp	87%	CGGTGGGTCCCAAGATCGAG
IRF4-a-1	-70 bp	56%	TGGGGGCCGGGGGTTGGACT
IRF4-a-2	-120 bp	92%	ACTTTGCAAGCCGAGAGCCG
IRF4-a-3	-160 bp	81%	GAGCCTCAGGGCCGGCGTGA
IRF4-a-4	-200 bp	91%	GGCGCGCGGAGGGTCGCCAA
IRF4-a-5	-240 bp	95%	GCGAATCTCGCCTTTGCGCC
IRF4-a-6	-400 bp	90%	ATCACTAAACTGCAGCGATG

APPENDIX D: TRANSFECTION OF HEK293FT CELLS WITH sgRNA CONSTRUCTS

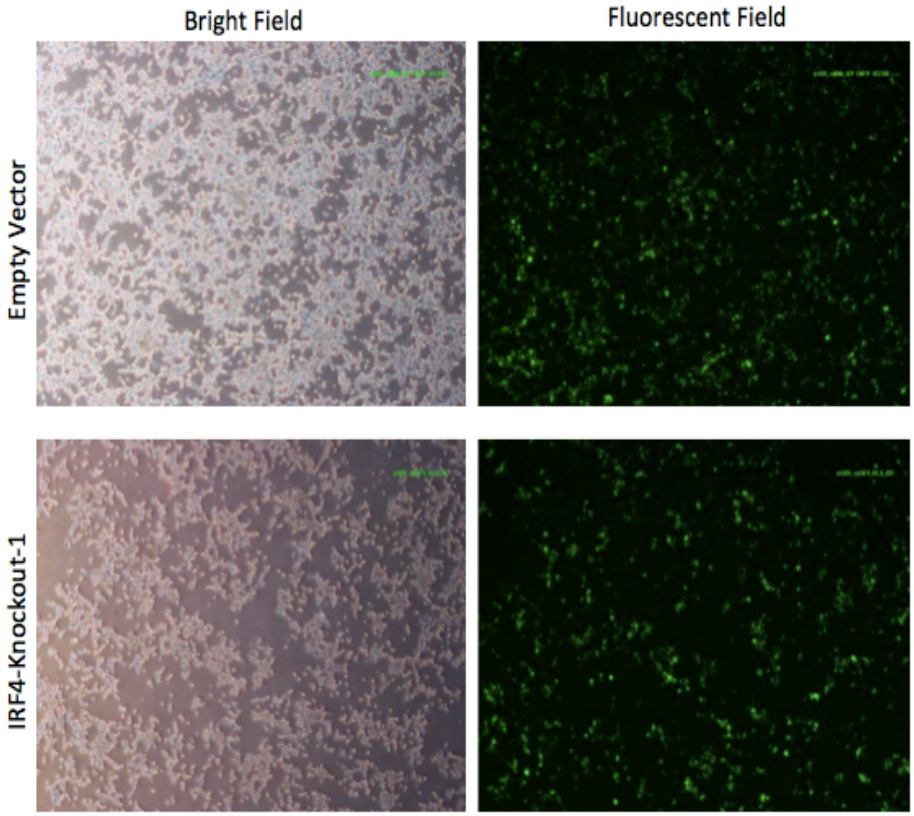

Figure D.1. Fluorescence microscopy images of HEK293FT cells that are transduced with empty vector and IRF4-Knockout-1 vectors along with helper plasmids. These results are representative. All transfections have similar results.

APPENDIX E: LENTIVIRAL TRANSDUCTION OF STABLE MELANOMA CELL LINES WITH sgRNA EXPRESSING LENTIVIRUSES

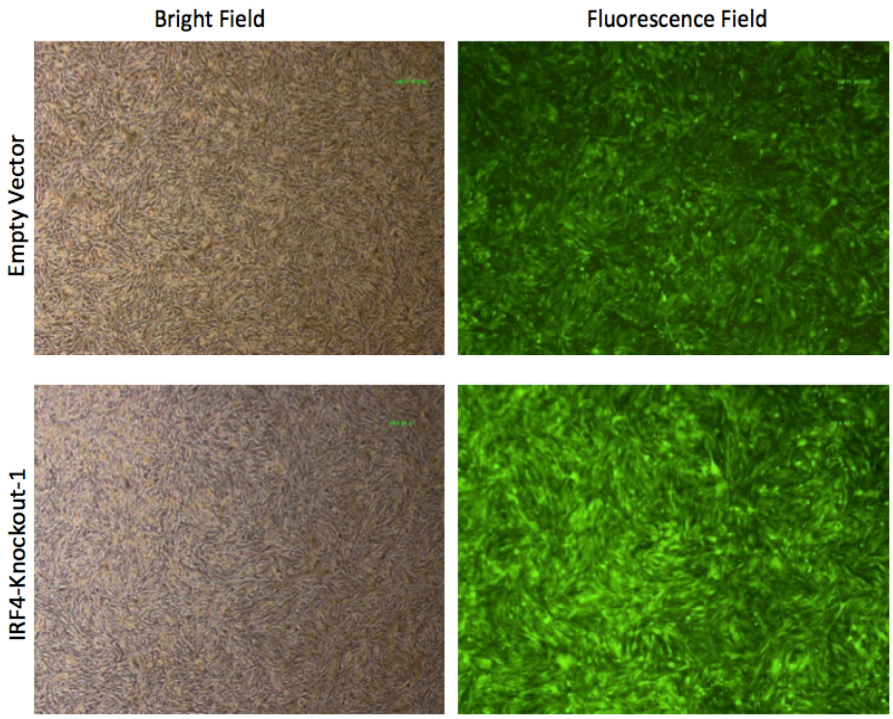

Figure E.1. Fluorescence microscopy images of SKMEL28-Cas9 stable cells, which were transduced with empty vector and IRF4-Knockout-1 sgRNA lentiviruses. These results are representative. All lentiviral transductions have similar results.

APPENDIX F: SANGER SEQUENCING RESULTS OF IRF4 KNOCKOUT CELLS FOR MUTATION VALIDATION

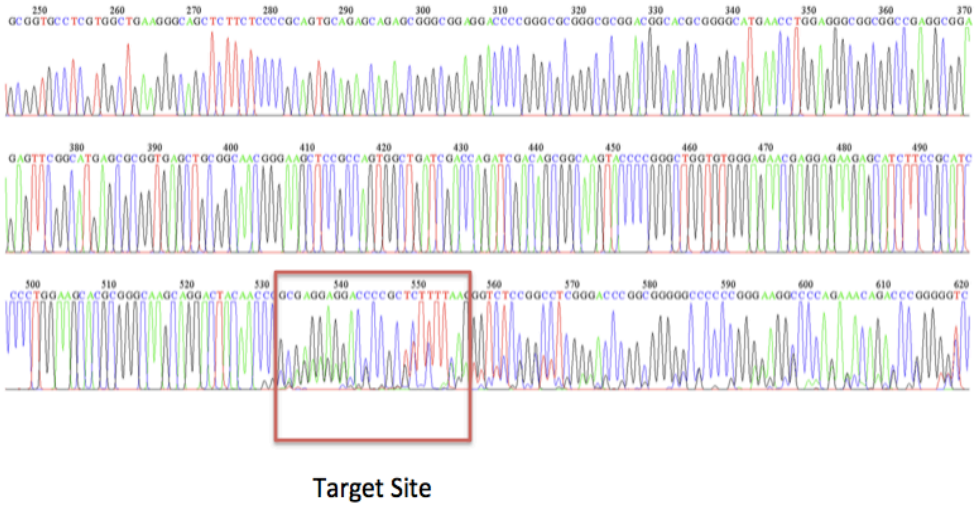

Figure F.1. Sanger sequencing validation of SKMEL-28 cells in which IRF4 is knocked out by using IRF4-Knockout-2 sgRNA construct. Target site is indicated in red box.

APPENDIX G: TIDE ANALYSIS OF KNOCKOUT EFFICIENCIES AT IRF4 TARGET SITES

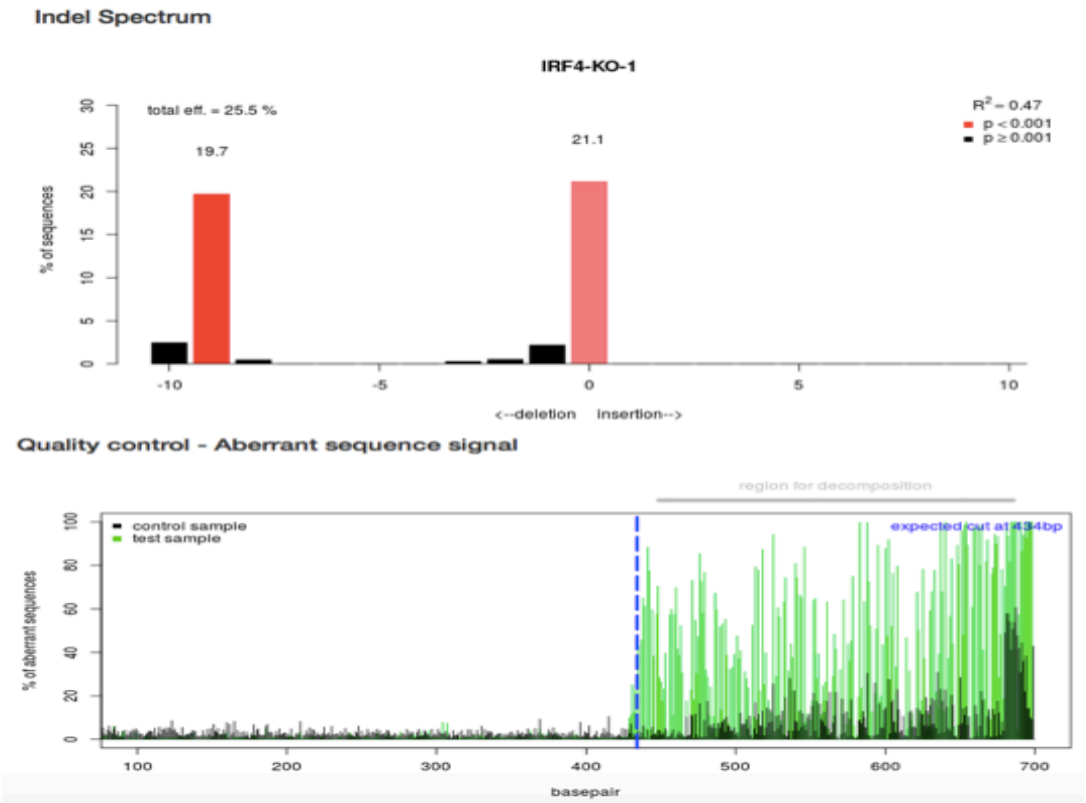

Figure G.1 Analysis of indel formation efficiencies by TIDE software at IRF4-Knockout-1 target site in SKMEL-28 cells

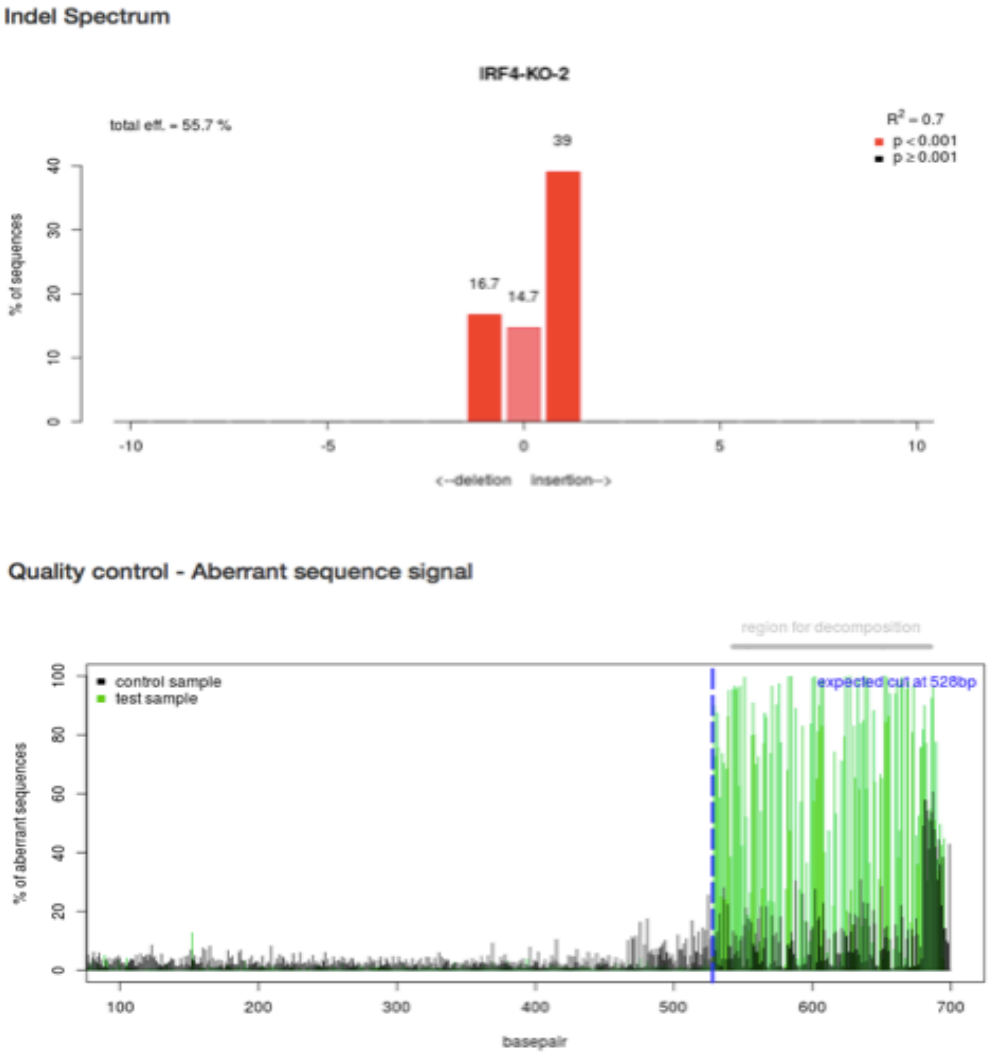

Figure G.2 Analysis of indel formation efficiencies by TIDE software at IRF4-Knockout-2 target site in SKMEL-28 cells

APPENDIX H: GFP COMPETITION ASSAY PROCEDURE

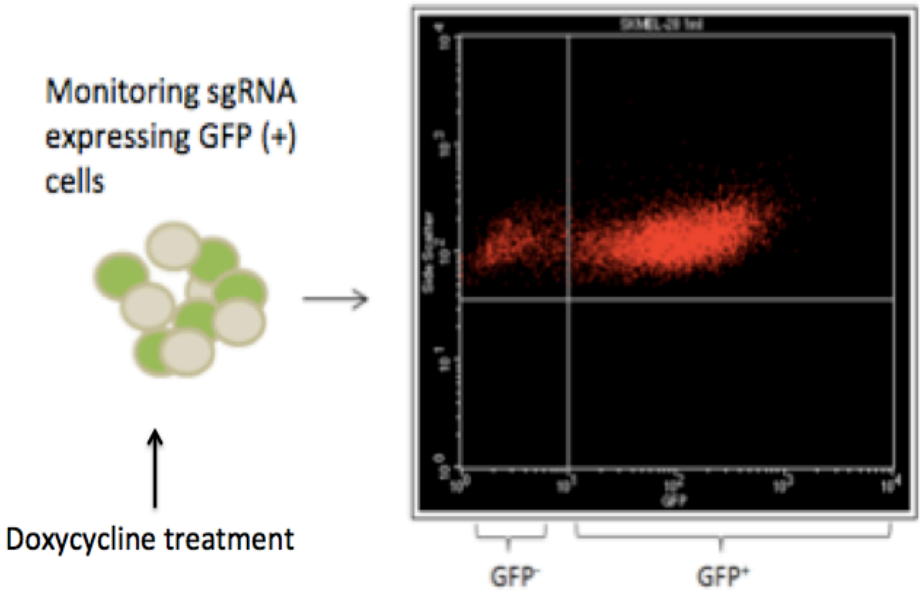

Figure H.1. Schematic view of GFP competition assay protocol (Adapted from Ayhan et al., 2014)

APPENDIX I: REPLICATION OF GFP COMPETITION ASSAY FOR MEWO CELLS WITH IRF4 KNOCKOUT

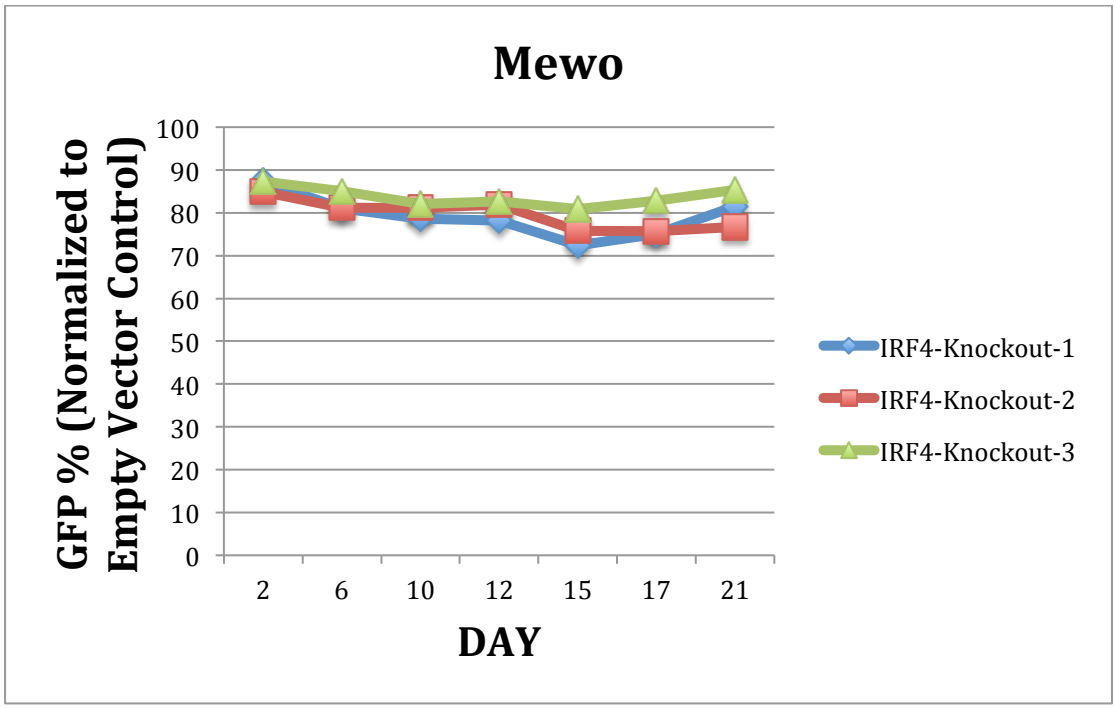

Figure I.1. Replication of GFP Competition Assay for Mewo cells with IRF4 knockout